ลักษณะสมบัติเชิงโมเลกุลของไอโซแอมีเลสจากหัวมัน
สำปะหลัง *Manihot esculenta* Crantz ‘KU50’

นางสาวภาวินี แป้นเพชร

วิทยานิพนธ์นี้เป็นส่วนหนึ่งของการศึกษาตามหลักสูตรปริญญาวิทยาศาสตรดุษฎีบัณฑิต
สาขาวิชาชีวเคมีและชีววิทยาโมเลกุล ภาควิชาชีวเคมี
คณะวิทยาศาสตร์ จุฬาลงกรณ์มหาวิทยาลัย
ปีการศึกษา 2559

MOLECULAR CHARACTERIZATION OF ISOAMYLASES FROM CASSAVA TUBER *Manihot esculenta* Crantz 'KU50'

Miss Pawinee Panpetch

A Dissertation Submitted in Partial Fulfillment of the Requirements
for the Degree of Doctor of Philosophy Program in Biochemistry and Molecular Biology
Department of Biochemistry
Faculty of Science
Chulalongkorn University
Academic Year 2016

Thesis Title	MOLECULAR CHARACTERIZATION OF ISOAMYLASES FROM CASSAVA TUBER *Manihot esculenta* Crantz 'KU50'
By	Miss Pawinee Panpetch
Field of Study	Biochemistry and Molecular Biology
Thesis Advisor	Associate Professor Tipaporn Limpaseni, Ph.D.
Thesis Co-Advisor	Professor Robert A. Field, Ph.D.

Accepted by the Faculty of Science, Chulalongkorn University in Partial Fulfillment of the Requirements for the Doctoral Degree

.....Dean of the Faculty of Science
(Associate Professor Polkit Sangvanich, Ph.D.)

THESIS COMMITTEE

.....Chairman
(Assistant Professor Manchumas Prousoontorn, Ph.D.)
.....Thesis Advisor
(Associate Professor Tipaporn Limpaseni, Ph.D.)
.....Thesis Co-Advisor
(Professor Robert A. Field, Ph.D.)
.....Examiner
(Assistant Professor Kanoktip Packdibamrung, Ph.D.)
.....Examiner
(Professor Aran Incharoensakdi, Ph.D.)
.....External Examiner
(Associate Professor Jarunya Narangajavana, Ph.D.)

ภาวินี แป้นเพชร : ลักษณะสมบัติเชิงโมเลกุลของไอโซแอมีเลสจากหัวมันสำปะหลัง *Manihot esculenta* Crantz 'KU50' (MOLECULAR CHARACTERIZATION OF ISOAMYLASES FROM CASSAVA TUBER *Manihot esculenta* Crantz 'KU50') อ.ที่ปรึกษาวิทยานิพนธ์หลัก: รศ. ดร. ทิพาพร ลิมปเสนีย์, อ.ที่ปรึกษาวิทยานิพนธ์ร่วม: ศ. ดร. โรเบิร์ต เอ ฟิลด์, 163 หน้า.

งานวิจัยนี้ศึกษายีนที่เกี่ยวข้องกับเอนไซม์ไอโซแอมีเลส (isoamylase: EC.3.2.1.68) ที่เร่งปฏิกิริยาการสลายพันธะไกลโคซิดิก α-1,6 ในแอมีโลเพคตินซึ่งเป็นองค์ประกอบของแป้งด้วยน้ำ ได้แยก RNA จากหัวมันสำปะหลังสายพันธุ์เกษตรศาสตร์ 50 และสังเคราะห์ cDNA ด้วยเทคนิค Reverse Transcription-PCR และวิเคราะห์ด้วย agarose gel electrophoresis พบว่ามีไอโซแอมีเลสยีน 3 ไอโซฟอร์ม ได้แก่ MeISA1, MeISA2 และ MeISA3 ยีน Me*ISA3* ที่มีความยาวเต็มนั้น ได้จากการทำ 5'RACE จากนั้นโคลนยีน Me*ISA1* และ Me*ISA2* เข้าสู่ pETDuet1 เพื่อทำการแสดงออกร่วม และโคลนยีน Me*ISA3* เข้าสู่ pET21b โดยตัดส่วน transit peptide ของยีนทั้งสามออก เมื่อตรวจสอบหาลำดับนิวคลีโอไทด์ โดยพบว่า ORFs ของยีนรีคอมบิแนนท์ที่สมบูรณ์เพื่อการแสดงออก Me*ISA1*, Me*ISA2* และ Me*ISA3* มีขนาด 2,292 เบส (763 กรดอะมิโน), 2,649 เบส (882 กรดอะมิโน) และ 2,127 เบส (781 กรดอะมิโน) ตามลำดับ โดยลำดับกรดอะมิโนของ rMeISA มีความเหมือนกับโปรตีน StISA1, StISA2 และ StISA3 ของมันฝรั่ง ในฐานข้อมูล NCBI 83.1%, 68.7% และ 80.9% ตามลำดับ เมื่อทำการแสดงออก rMeISA ทั้งสามใน *E. coli* SoluBL21(DE3) และทำให้เอนไซม์ให้บริสุทธิ์โดยคอลัมน์ Histrap™ จากการวิเคราะห์โดยวิธี SDS-PAGE และ Western blot พบว่า rMeISA1, rMeISA2 และ rMeISA3 มีขนาดประมาณ 87, 99 และ 80 kDa ตามลำดับ หลังการทำให้บริสุทธิ์ พบแอคติวิทีตัดกิ่งใน fraction ที่มี rMeSIA1 และ rMeISA2 อยู่ด้วย เท่านั้น ผลจากคอลัมน์ gel filtration และวิเคราะห์โดย Western blot ของ rMeISA1 และ rMeISA2 ที่ผลิตในช่วง 4-5 ชั่วโมงหลังการเหนี่ยวนำ พบว่าโปรตีนเชิงซ้อนมีขนาดประมาณ 259 ถึง 496 kDa ซึ่งสอดคล้องกับการรวมตัวกันของ ISA1 และ ISA2 ที่สัดส่วน 1:1 ถึง 4:1 rMeISA1/rMeISA2 และ rMeISA3 ที่บริสุทธิ์ สามารถเร่งปฏิกิริยาได้ดีที่ 37 องศาเซลเซียส ที่ pH 7.0 และ 6.0 ตามลำดับ ผลของ metal ion พบว่า การทำงานของ rMeISA1/rMeISA2 มีค่าสูงขึ้นโดยการกระตุ้นของ Co^{2+}, Mg^{2+} และ Ca^{2+}ตามลำดับ ขณะที่ Mn^{2+} และ Co^{2+} สามารถกระตุ้นการทำงานของ rMeISA3 ได้อย่างมีนัยสำคัญ อย่างไรก็ตามการทำงานของ rMeISA1/rMeISA2 และ rMeISA3 ถูกยับยั้งด้วย Cu^{2+} จากการวิเคราะห์ผลิตภัณฑ์ที่ได้จากการย่อยแอมีโลเพคตินด้วยไอโซแอมีเลสด้วย HPAEC-PAD พบพอลิเมอร์ของกลูโคสสายตรงขนาด DP 6 ถึง 20 โดยผลิตภัณฑ์หลักอยู่ในช่วง DP 10 ถึง 12 rMeISA1/rMeISA2 มีความจำเพาะต่อแอมีโลเพคติน ขณะที่ rMeISA3 จำเพาะต่อบีตา-ลิมิตเดกซ์ทรินมากที่สุด rMeISA1/rMeISA2 และ rMeISA3 ไม่สามารถย่อยพูลลูแลนได้ บ่งชี้ได้ว่าเอนไซม์เหล่านี้จัดอยู่ในกลุ่มไอโซแอมีเลส แอคติวิทีของไอโซแอมิเลสพบได้เมื่อ rMeISA1 และ rMeISA2 รวมตัวเป็นสารประกอบเชิงซ้อนเท่านั้น

ภาควิชา ชีวเคมี ลายมือชื่อนิสิต .....

สาขาวิชา ชีวเคมีและชีววิทยาโมเลกุล ลายมือชื่อ อ.ที่ปรึกษาหลัก .....

ปีการศึกษา 2559 ลายมือชื่อ อ.ที่ปรึกษาร่วม .....

5472875423 : MAJOR BIOCHEMISTRY AND MOLECULAR BIOLOGY
KEYWORDS: STARCH DEBRANCHING ENZYME/ ISOAMYLASE/ RECOMBINANT MEISA/ CASSAVA

PAWINEE PANPETCH: MOLECULAR CHARACTERIZATION OF ISOAMYLASES FROM CASSAVA TUBER *Manihot esculenta* Crantz 'KU50'. ADVISOR: ASSOC. PROF. TIPAPORN LIMPASENI, Ph.D., CO-ADVISOR: PROF. ROBERT A. FIELD, Ph.D., 163 pp.

Starch debranching enzyme or isoamylase (EC.3.2.1.68), an important enzyme in starch metabolism, catalyses the hydrolysis of α-1,6 glycosidic linkages of amylopectin. In this work, cassava isoamylase genes were isolated from cDNA generated from total RNA from tubers of *Manihot esculanta* Crantz cultivar KU50 by RT-PCR and analysed by agarose gel electrophoresis. Three putative isoamylase genes, Me*ISA1*, Me*ISA2* and Me*ISA3* were identified and amplified excluding the fragments encoding their transit peptides. Full length of Me*ISA3* gene was obtained by 5' Rapid Amplification of cDNA Ends (5' RACE). The mature Me*ISA1* and Me*ISA2* were successfully amplified and cloned into a pETDuet1 vector, while the mature Me*ISA3* was amplified and cloned into a pET21b and sequenced. The ORFs of mature recombinant Me*ISA1*, Me*ISA2* and Me*ISA3* genes were 2,292, 2,649 and 2,127 kb, encoding 763, 882 and 708 amino acid with substantial similarity to StISA1, StISA2 and StISA3 from potato at 84.4%, 68.9% and 80.9%, respectively. Then, rMeISA1 and rMeISA2 were coexpressed and rMeISA3 was single expressed in *Escherichia coli* SoluBL21(DE3) and purified by Histrap™ column. Analysis by SDS-PAGE and immunoblot showed approximate molecular weights of 87, 99, and 80 kDa, respectively. Debranching activity was only detectable in the fractions where both rMeISA1 and rMeISA2 were present. The heteromultimeric DBE from 4-5 h induced culture analysed by gel filtration chromatography and Western blot showed combinations of rMeISA1 and rMeISA2 at ratios of 1:1 to 1:4. Pooled fractions of rMeISA1/rMeISA2 with DBE activity and the purified rMeISA3 were used for enzyme characterisation. Both rMeISA1/rMeISA2 and rMeISA3 showed the optimum activity at 37ºC but their optimum pH were at 7.0 and 6.0, respectively. Enzyme activity of rMeISA1/rMeISA2 was enhanced by Co^{2+}, Mg^{2+} and Ca^{2+}, whereas rMeISA3 activity could be significantly activated by Mn^{2+} and Co^{2+}. Cu^{2+} was a strong inhibitor for both enzymes. Debranched amylopectin products analysed by HPACE-PAD showed chain length distributions typical of plant debranching enzymes with DP from 6 to 20 with major products around DP 10 to 12. rMeISA1/rMeISA2 were specific for amylopectin while rMeISA3 showed the highest activity on beta-limit dextrin. However, they could hardly hydrolyse pullulan at all, indicating their classification as isoamylase-type debranching enzyme. The debranching activity of rMeISA1 and rMeISA2 required their association as heteromeric complexes.

Department:	Biochemistry	Student's Signature .....
Field of Study:	Biochemistry and Molecular Biology	Advisor's Signature .....
		Co-Advisor's Signature .....
Academic Year:	2016	

ACKNOWLEDGEMENTS

I would like to express my deepest appreciation and gratitude to my advisor, Assoc. Prof. Dr.Tipaporn Limpaseni for her beautiful mind, kindness, instruction, guidance, encouragement, and support throughout this thesis.

My gratitude is also extended to Prof. Dr. Aran Incharoensakdi, Asst. Prof. Dr. Kanoktip Packdibamrung, Asst. Prof. Dr. Manchumas Prousoontorn and Assoc. Prof. Dr. Jarunya Narangajavana for serving as thesis committee. I am very thankful to Prof. Dr. Robert A. Field, my co-advisor, and also Prof. Dr. Alison M. Smith at John Innes Centre, for their suggestion, support and kindness.

I also wish to extend my gratitude to Asst. Prof. Dr. Rath Pichyangkura, Asst. Prof. Dr. Supa-art Sirikantaramas, Prof. Dr. Vichien Rimpanitchayakit and Prof. Dr. Anchalee Tassnakajon for their suggestion and support.

I would like to thank Mr. Prasert Thala from the National Research Centre of Millet and Corn (Suwan Farm) in Nakhon Ratchasima province for kindly providing cassava ‘KU50’ tubers.

My sincere thanks are extended to all members in Starch and Cyclodextrin Research Unit and friends in the Department of Biochemistry, Faculty of Science, Chulalongkorn University for their assistance and friendship and I would like to give special thanks to Mr. Karan Wangpaiboon for his assistance and suggestion.

Finally, I wish to express my deepest gratitude to my family, especially my mother for all their continuous support, helpful and understanding. Thanks to Mumu, my beloved dog, for boosting my spirit whenever I need.

The thesis is supported by research grant from The Royal Golden Jubilee Ph.D. Program, Thailand Research Fund and Chulalongkorn University, the 90TH Anniversary of Ratchadaphiseksomphot Endowment Fund of Chulalongkorn University, the IIAC of the CU Centenary Academic Development Project and Thailand Research Fund. Studies at the John Innes Centre are supported by the UK BBSRC Institute Strategic Program on Understanding and Exploiting Metabolism (MET) [BB/J004561/1] and the John Innes Foundation.

CONTENTS

Page

Page

Page

Page

Page

LIST OF TABLES

LIST OF FIGURES

LIST OF ABBREVIATIONS

A	absorbance
BSA	bovine serum albumin
°C	degree celcius
CLD	chain length distribution
cm	centimetre
Da	Dalton
D-enzyme	Disproportionating enzyme
DP	Degree of Polymerisation
et al.	Et Alii (latin), and others
g	gram
GH	Glycoside Hydrolase
h	hour
IPTG	Isopropylthiogalactoside
ISA	isoamylase
Kb	kilobase
m	milli
M	molar
mA	milliampere
mg	milligram
min	minute
ml	milliliter
mol	mole
MW	molecular weight
OD	optical density

PAGE	polyacrylamide gel electrophoresis
PCR	polymerase chain reaction
rpm	revolution per minute
SDS	sodium dodecyl sulfate
V	volt
U	unit

CHAPTER I

INTRODUCTION

1.1 Cassava

Cassava (*Manihot esculenta* Crantz) is a root crop which belongs to the flowering plant (spurge) family, Euphorbiaceae (Jos 1969). It is a major staple food crop of the tropical and subtropical areas such as Africa, South America and Asia (Munyikwa et al. 1997). Cassava, commonly called manioc, yuca and Brazilian arrowroot (Allem 1994; Govaerts et al. 2000; McGuffin 2000; Olsen and Schaal 2001; Rogers and Appan 1973), in the form of powdery extract is called tapioca. Dislike other major crops, cassava is definitely able to be cultivated under extreme stress conditions such as drought and low nutrient availability which reasonable high yields can be obtained (Tonukari 2004). Although cassava leaves provide relatively high protein and can also be consumed, the main part is the swollen tuber (Figure 1). Its edible starchy tubers serve as the third largest sources of dietary energy, after rice and maize (Fargette et al. 1990), consumed by approximately over 500 million people in the world especially in the tropics. In addition, cassava ranks fourth as a crop in the developing countries, after rice, maize and wheat as a cheap source of carbohydrate energy according to the United Nations Food and Agriculture Organization (FAO). Thailand is one of the major sources of cassava production, ranking second among the world major producers (Figure 2).

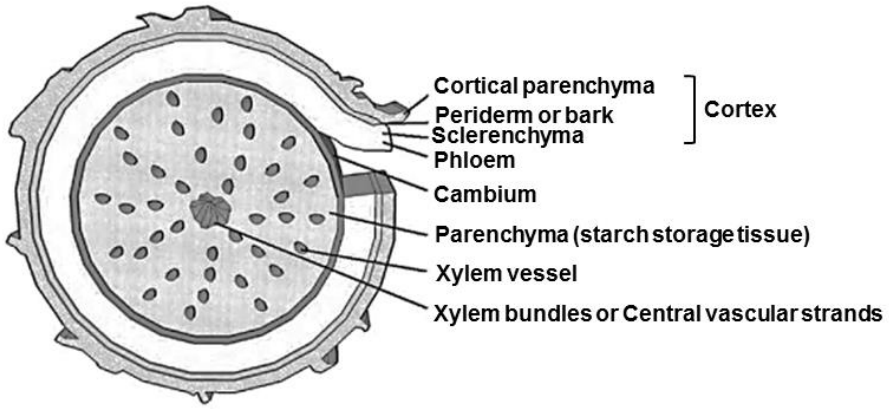

Figure 1 Drawing of cross-section of cassava tuber showing the different components (BeMiller and Whistler 2009).

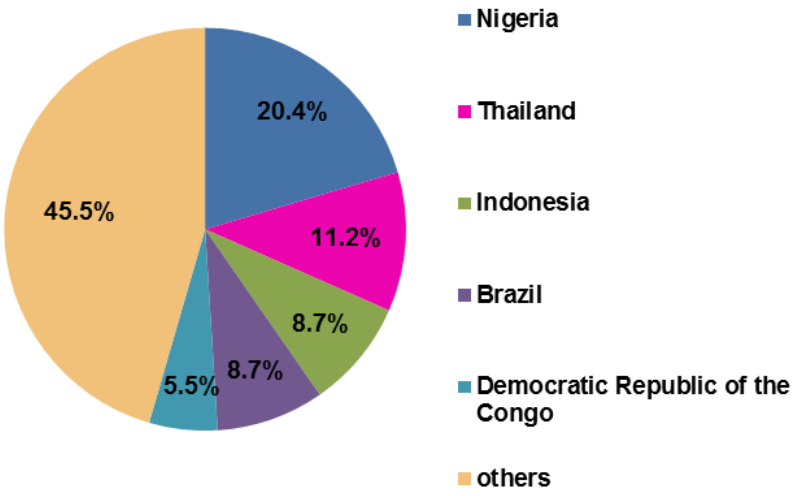

Figure 2 Percentages of global cassava production of around 270 million tonnes produced in 2014 (UN Food and Agriculture Organization Corporate Statistical Database (FAOSTAT)).

Cassava provides quantitatively high starch content of about 74 to 85% of its total root dry weight (Figure 3, (Baguma 2004)). The composition of cassava tuber is moisture (46 to 85%), total carbohydrate (25 to 36%), protein (0.3 to 3.5%), dietary fiber (0.1 to 3.7%), and other substances including vitamins and minerals (3%) (Bradbury and Holloway 1988; Favier 1977; Woot-Tsuen et al. 1968). From the high level of cassava starch production and its unique properties, cassava starch has been utilised in food and non-food applications such as in pharmaceutical and food industries. Although cassava starch itself harbours high potential, it is still under-exploited. So, improvement of starch quality and quantity for the desired properties are necessarily needed.

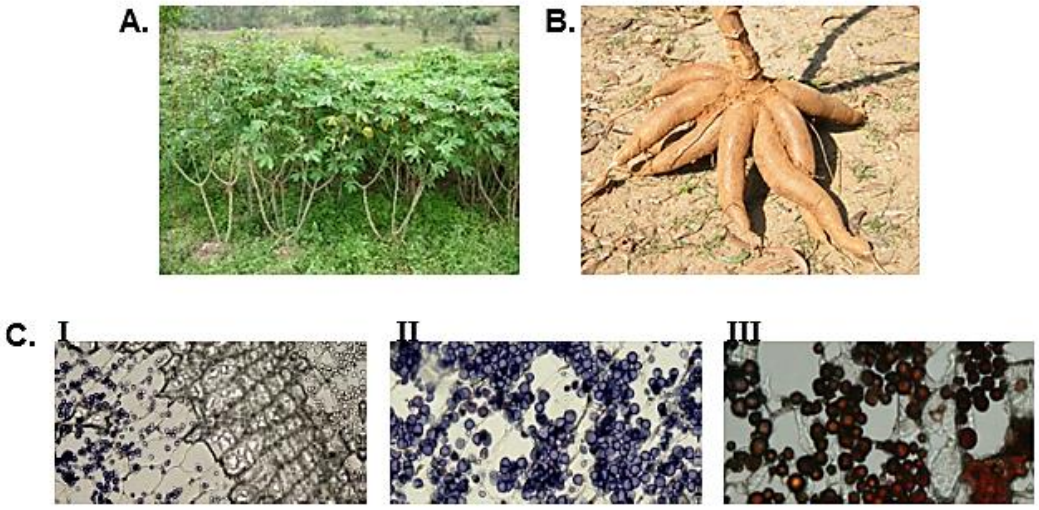

Figure 3 (A) Cassava plants **(B)** Cassava tubers **(C)** Images of iodine-staining of amylose (dark blue stained) and amylopectin (reddish-brown stained) showing its cellular distribution. **(CI)**, **(CII)**, and **(CIII)** represent periderm region, cortical parenchyma region, and parenchyma region, respectively (Baguma 2004).

1.2 Starch

Starch is a principal reserve carbohydrate of higher plants and algae (Ball and Morell 2003). Starch is synthesised in the plastids including chroloplasts in leaves (stored as transitory starch, the primary product of photosynthesis) and in amyloplasts (stored as storage strach) such as in seeds and tubers (Ball et al. 1996). It made up of two different types of α-linked polyglucans. Several thousands of these polymers are arranged tightly into a three dimentional structure called semicrystalline structure of starch granule. Starch can be fractionated by chemical treatment into two types of glucose polymers called amylose and amylopectin molecules.

1.2.1 Amylose

Amylose, a smaller molecule, is mainly a linear chain of glucose units linked by α-1,4 glucosidic bonds. The number of repeated glucose subunits (n) is normally in the range of 300 to 3000 however it can be up to many thousands (Figure 4A). Amylose usually consists of less than 1% of α-1,6 branch points (approximately 1 branch per 100 glucose residues) (Ball and Morell 2003; Buléon et al. 1998), and constitutes around 15 to 35% of starch contents. However, the amount of amylose in starch is variable depends on the plant species and variety (Denyer et al. 2001). Moreover, Shannon and Garwood (1984) found that the plant organs, the developmental stage of the organ, and the growth conditions of the plant also affected the amylose content in the starch as well. Because of the long linear chains of amylose, once after extraction and in the solution, hydrogen bonding is readily formed between the chains, resulting in rigid gels forming.

1.2.2 Amylopectin

The other component, which is generally the main component (about 65 to 85% of starch) and is much larger than amylose, is amylopectin. This molecule is highly branched glucose polymers which the main linear chains are linked by α-1,4 glucosidic linkages while the branch points are interlinked by α-1,6 linkages as shown in Figure 4B (Ball et al. 1996; Ball and Morell 2003). Amylopectin is formed by 2,000 to 200,000 glucose residues. The branching points occur at every 24 to 30 glucose units, resulting in a soluble molecule (Green et al. 1975). Amylopectin can be quickly degraded as it has many exposed non-reducing ends onto which enzymes can attach. The branches are clustered and arranged in a well-organised structure (Figure 5C). The unbranched chains which typically contain about 15 glucose residues called A chain. The chains of about 15 to 45 glucose units with branching are called B chains while C chain is a single chain with a reducing end of one amylopectin molecule. An average length and width of amylopectin molecule is around 200 to 400 nm (20 to 40 clusters) and 15 nm, respectively (Kainuma 1988; Smith and Martin 1993). In addition, most starches are phosphorylated by some phosphates are covalently linked to glucose residues. For instance, potato starch contains one phosphate per three hundred glucose units (Takeda and Hizukuri 1982). In solution, dissolved amylopectin has less hydrogen bonding between the molecules than amylose due to its highly branching pattern and has a lower trend of gelling (retrogradation) during cooling. So, the waxy starches (almost 100% amylopectin by weight) are used mainly as a thickener or stabilizer in various applications.

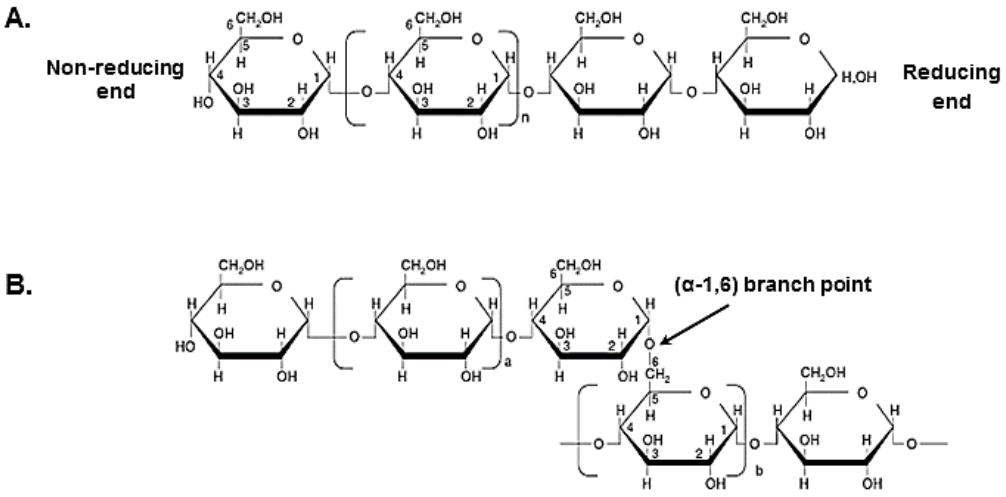

Figure 4 Structure of amylose and amylopectin (Tester et al. 2004). **(A)** Short segment of linear polyglucan, amylose, linked by α-1,4 linkages **(B)** Branch point of amylopectin linked by α-1,6 linkages

Interior structure of the starch granule (Figure 5B), which the sizes are varied from 2 to 100 μm, shows the radial arrangement of amylopectin molecules (Figure 5C). The adjacent branches in the cluster may form double helices and packed regularly, resulting in crystallinity of the starch granule. Nevertheless, the starch granule is not a uniform crystalline structure because it also contains amorphous (shapeless) regions. Starch granules from leaves and storage organs have macrostructurally difference. The storage starch shows internal growth rings, the alternating of the amorphous and the crystalline regions, that is sensitive to chemical and enzymatic attack (Figure 5B and C). Conversely, the granules of transitory starch in leaves are generally smaller than those of the storage organs and are thought to have a crystalline core and amorphous outer mantle, comprising less branching glucan polymers (Beck 1985; Steup et al. 1983)

Moreover, the ratios of amylose: amylopectin are varied among the plant species (as shown in Table 1). On the other hand, generally, amylopectin is similar to glycogen by comprising the same monomer unit of glucose. However, they differ structurally in the ratio of α-1,6 to α-1,4 which amylopectin contains fewer branching than glycogen (Ball et al. 1996).

Table 1: Approximate contents of amylose and amylopectin in some sources of starch

Starch source	Amylose (%)	Amylopectin (%)	Reference
Barley	28	72	(Bertoft et al. 2008)
Potato	14	86	(Vermeylen et al. 2006)
Rice	20	80	(Bertoft et al. 2008)
Sweet potato	20	80	(Srichuwong et al. 2005)
Tapioca	18	82	(Srichuwong et al. 2005)
Waxy maize	1	99	(Vermeylen et al. 2006)
Wheat	33	67	(Kalinga et al. 2013)

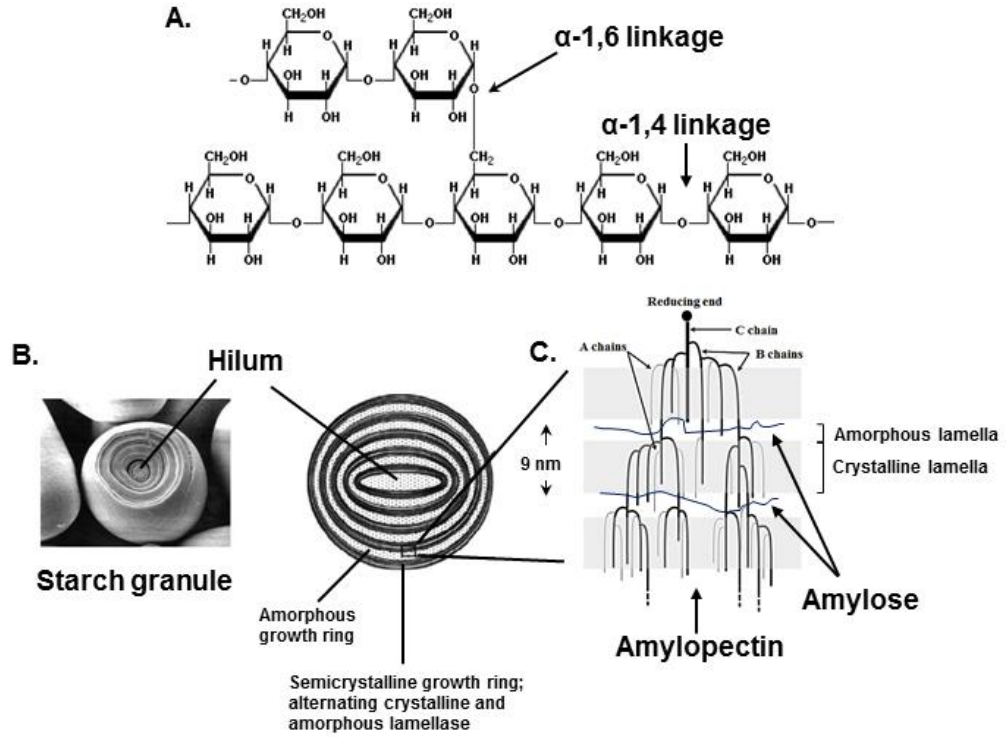

Figure 5 Illustration of starch granule structure. **(A)** Glucose polymer linked by α-1,4 and α-1,6 bonds. **(B)** Insight structure of starch granule from storage tissue showing alternating of semicrystalline and amorphous regions (growth rings). The semicrystalline growth rings comprise alternating of crystalline and amorphous lamellae. **(C)** Semicrystalline structure consisting of alternating of amorphous lamella (containing branches of amylopectin and amylose) with crystalline lamella (containing well-organised double helices).

1.2.3 Starch applications

At the present time, many enzymatic starch manipulation processes have been reported for producing starch derivatives with desired properties. For instance, in saccharification process, isoamylases are used to enhance the efficiency and the quality of syrup production (Ghosh and Ray 2010). High amylose starches or resistant starch (RS) is one of the most valuable starch derivatives. The resistant starch in functional foods provides health benefits for individuals because it escapes from the digestion in stomach and small intestine then reach colon where the fermentation takes place and the short-chain fatty acids are produced and colonic bacterial cell mass is increased (Topping and Clifton 2001). There are several processes to obtain the resistant starch such as an enzymatic treatment with/without a physical treatment. For example, α-amylase together with pullulanase were utilised in corn starch treatment and the RS level was increased about 13.9% when measured by using the Goni method (Zhang and Jin 2011). In addition, Hickman et al. (2009) prepared enzyme-modified starches by using beta-amylolysis of wheat and corn starches after autoclaving. The RS content of the corn starch was increased by 18.5%, and by 14% for the wheat starch, whereas the RS level was increased only less than 2% by using autoclave treatment alone. Finally, understanding of the characteristics and the role of enzymes in starch metabolism possibly leads to the future uses of these enzymes in the starch modification processes.

1.3 Beta-limit dextrin

Beta-limit dextrin is the remaining branched glucose polymers produced by hydrolysis of amylopectin by β-amylase which catalyses the hydrolysis of α-1,4 linkages of amylopectin, then the successive maltose units were removed from the non-reducing ends of the chains of polymers (Figure 6).

1.4 Pullulan

Pullulan is a polysaccharide polymer which consists of maltotriose units (Leathers 2003). Three glucose residues in maltotriose linked by α-1,4 bonds whereas consecutive maltotriose units are linked to each other by α-1,6 linkages (Figure 7). The unique linkage pattern of pullulan leads it to distinctive physical traits. For example, from its adhesive properties, the pullulan can be used to form a strong and oxygen barrier films.

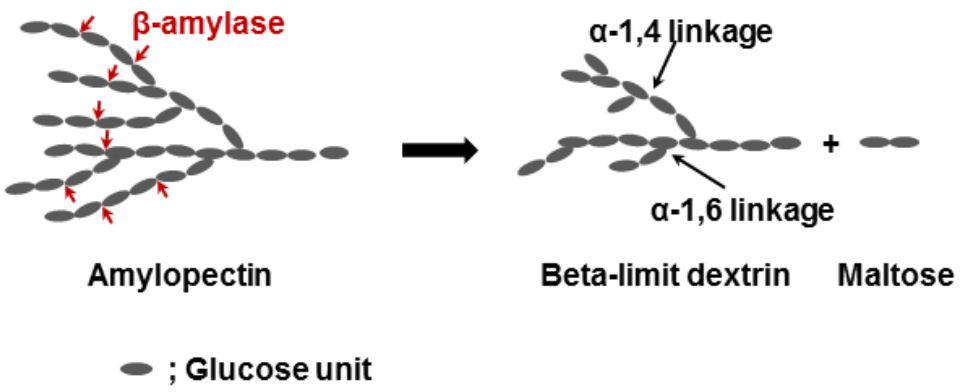

Figure 6 Schematic illustration of structure of beta-limit dextrin with α-1,4 and α-1,6 glucosidic bonds, the remaining product from β-amylolysis of amylopectin

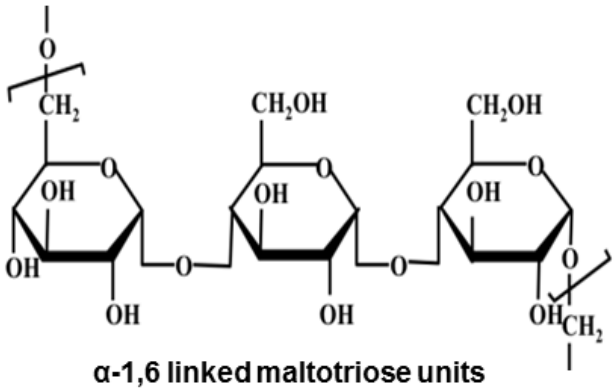

Figure 7 Structure of pullulan (Catley and Whelan 1971)

1.5 Starch metabolism and the enzymes involved

1.5.1 The overall pathway

Starch, the essential carbohydrate reserve in plants, is produced in both non-photosynthetic and photosynthetic tissues. Transitory starch is a type of starch which is temporarily stored in chloroplasts in leaves or other photosynthetic tissues. Another type belongs to storage starch found in non-photosynthetic organs such as roots, seeds and tubers. The transitory starch is synthesised in chloroplasts via carbon fixation in photosynthesis during the day time. The following night, the starch in leaves is then degraded and exported as sucrose to the plastid, especially amyloplasts, of the storage organs and stored as storage starch.

Starch biosynthesis pathway is still unclear. However, many reports proposed that the pathway started from the conversion of most of cytosolic sucrose molecules into nucleotide diphosphate glucose and then converted into amylose and amylopectin by action of several enzymes; chloroplastic isoforms of phosphoglucoisomerase (PGI) and phosphoglucomutase (PGM) catalyse the conversion of fructose-6-phosphate into glucose-1-phosphate, ADP-glucose pyrophosphorylase (AGPase) generates ADP-glucose, which functions as glucosyl donor, and pyrophosphate from glucose-1-phosphate and ATP (Zeeman et al. 2007). Starch synthases (SS) catalyse the synthesis of amylose from ADP-glucose. Starch branching enzyme (SBE) catalyses the branching at every 15 to 20 glucose units of linear α-polyglucan at C-6 of glucosyl residue (Munyikwa et al. 1997) and starch debranching enzymes (DBE) catalyse the hydrolysis of α-1,6 glucosidic linkages of both too short chains and incorrect branch points to facilitate the forming of starch granules (Zeeman et al. 2007).

On the other hand, the starch degradation, starch granules are degraded by two main types of hydrolytic enzymes; β-amylases and the debranching enzyme isoamylase3 (ISA3). The action of these enzymes is enhanced by the phosphorylation of the starch granule to disrupt the granular surface by glucan water dikinases (GWD and PWD). Following this, the phosphorylated starch granule is dephosphorylated by glucan phosphate phosphatases (SEX4 and LSF2) to allow complete hydrolysis of the starch polymers (Blennow and Engelsen 2010; Edner et al. 2007; Tabata et al. 1978; Takeda and Hizukuri 1981). Maltose, the major product of hydrolysis, is then exported from the chloroplast into the cytosol via the maltose transporter (MEX1). The starch hydrolysis also produces minor maltotriose products, which is disproportionated by disproportionating enzyme1 (DPE1) to produce longer chains that are suitable to be further hydrolysed by β-amylases and glucose which is exported into the cytosol. Maltose and glucose, exported from the chloroplast, in the cytosol are then further transformed into hexose phosphates and used in cellular metabolism or converted into sucrose for export to the target organs of plant (Smith 2012). Sucrose is transformed into UDP-glucose and fructose by the action of Sucrose synthase (SuSy) and the two sugars are then converted into hexose phosphates. The hexose phosphates are then directly imported into amyloplasts via hexose phosphate transporters otherwise they are converted into ADP-glucose in the cytosol before being uptaken into amyloplasts via ADP-glucose transporters (Figure 8).

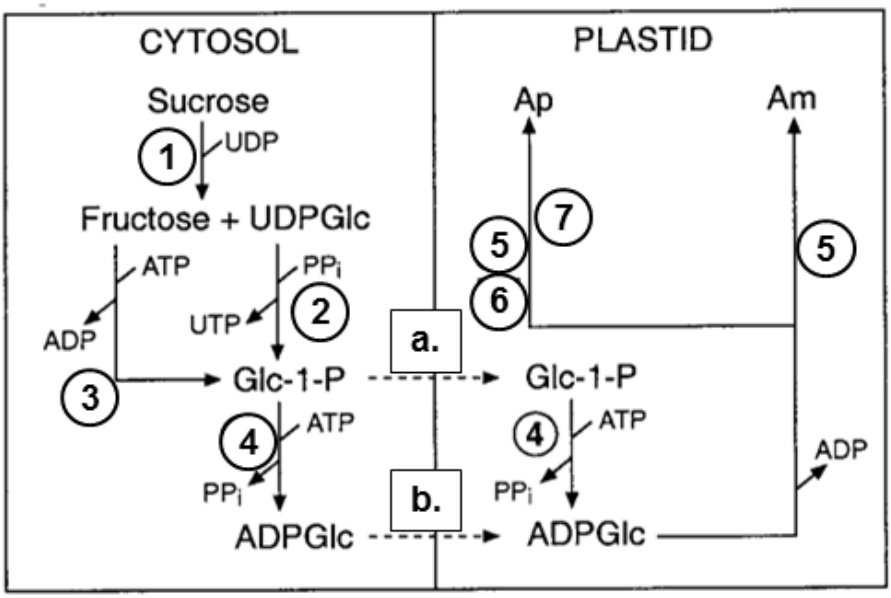

Figure 8 The major metabolites and enzymes involved in the starch biosynthesis pathway in storage organs beginning with sucrose from photosynthesis. Carbon molecules as hexose phosphates and ADP-glucose (ADPGlc) are shown to enter the plastid via hexose transporter **(a.)** and ADP-glucose transporter **(b.)**, respectively. Enzyme activities are as follows; **(1)** Sucrose synthase, **(2)** UDP-glucose pyrophosphorylase, **(3)** phosphoglucomutase, **(4)** ADP-glucose pyrophosphorylase, **(5)** starch synthase (GBSSI), **(6)** starch branching enzyme and **(7)** starch debranching enzymes (ISA1 and ISA2). PPi is an inorganic pyrophosphate.

1.5.2 Important enzymes participated in starch metabolism

1.5.2.1 The synthesis of ADP-glucose through ADP-Glucose pyrophosphorylase (AGPase)

ADP-glucose pyrophosphorylase catalyses the synthesis of ADP-glucose, α-glucan reserved, in glycogen and starch biosynthesis (Smith et al. 1995). The prokaryotic and plants AGPases share similar size (~220 kDa), catalytic property and allosteric regulation but differ in protein structure. The prokaryotic AGPase (glgC) is a homotetrameric enzyme, whereas plant AGPase is a heterotetrameric enzyme ($\alpha_2\beta_2$) consisting of a pair of small (S) and a pair of large (L) subunits, encoded by different genes (Cross et al. 2004; Hwang et al. 2005; Müller-Röber et al. 1990; Salamone et al. 2002; Singh et al. 2002). According to the multiple forms of S and L subunits in plants, the encoding genes are more complex and diverse than those of prokaryotes. The Bacterial AGPase is activated by intermediates of glycolysis (e.g. pyruvate, fructose-6-phosphate, fructose-1,6 bisphosphate) and inhibited by AMP. While, algae and higher plants AGPases are activated by 3-phosphoglyceric acid and inhibited by Pi which are the key intermediates in CO_2 assimilation by the C_3 pathway. The primary sequences analysis indicates that the S subunits are highly conserved between species, whereas those of the L subunits are less conserved even within species (Smith-White and Preiss 1992), suggesting its different function. Importantly, the S subunit is essential for catalytic activity whereas the large subunit is important for enzyme regulation. In addition, the S subunit by itself is able to form a catalytically active homotetrameric enzyme with deficiency of allosteric properties when it was expressed singly in *E. coli* (Ballicora et al. 1995; Hwang et al. 2005). In opposition to the L subunit, which is unable to form an active enzyme without the S subunit. This suggests that the S subunit

contains the catalytic ability while the L subunit simply enhances the allosteric properties of the enzyme (Gómez-Casati and Iglesias 2002).

From phylogenetic studies, plants AGPase is distinctively localised into different targets such as leaf, root and endosperm. Moreover, AGPase is further classified into two groups based on subcellular localisation, i.e. plastidial and cytosolic forms (Denyer et al. 1996; Okita 1992; Thorbjørnsen et al. 1996). In cereal endosperms, AGPase dually prepsent in both plastid and cytocol, whereas in other organs and non-cereal plants, AGPase activity is totally found in plastid. The cytosolic AGPase in cereals plays a crucial role in serving ADP-glucose for starch synthesis. Mutants lacking of cytosolic AGPase but has normal plastidial AGPase activity, the starch contents decreased (Denyer et al. 1996; Johnson et al. 2003). This shows that plastidial AGPase alone cannot compensate the normal starch synthesis rates in cereal endosperm. The role of cytosolic and plastidial AGPase in starch biosynthesis has been revealed from mutants studies in maize, Shrunken-2 and Brittle-2 (Denyer et al. 1996; Giroux et al. 1996; Hannah and Nelson 1976) and barley, Risø 16 (Johnson et al. 2003). In barley, Risø 16 lacking of cytosolic AGPase but has normal plastidial AGPase activity results in the reduction of starch content however the plastidial AGPase by itself is enough for normal starch synthesis. Conversely, in maize endosperm, plastidial activity alone is not sufficient for normal rates of starch accumulation (Thorbjørnsen et al. 1996).

In the photosynthetic tissue, triose phosphates are accumulated in the chloroplast during the light cycle. On the other hand, in sink storage tissue, 3-PGA, an intermediate of glycolysis pathway, is produced in low level, while Pi peaks during starch accumulation. This showed that inhibitory effect of Pi which probably is the key

modulator may dominate over 3-PGA activation of AGPase activity in sink tissue. Tissues that contain no activity of an extraplastidial AGPase, glucose-1-phosphate (Glc-1-P) is transported into the amyloplast via hexose transporter (Figure 8).

1.5.2.2 The synthesis of amylose by granule bound starch synthase I (GBSSI)

GBSSI is one of the starch synthases. All members share the similar basic structure, comprising a glass domain (substrate-binding domain), a typical transit peptide (Keeling and Myers 2010), and eight motifs (Cao et al. 1999; Vrinten and Nakamura 2000). The starch synthases are divided into three distinct classes based on the localisation in the plastids; granular-bound starch synthases (GBSS), entirely bind to the starch granule, starch synthases (SS), whole or nearly whole active in the soluble phase, and one presents in both the granule-bound and soluble phases. Furthermore, based on cDNA and peptide sequences, these fractions are further subdivided into four subclasses consisting of GBSSI (60 kDa), SSI (57 kDa), SSII (77 kDa) and SSIII (110-140 kDa). Recently, Edwards and co-workers (2002) further subdivided GBSSI into GBSSIa and GBSSIb isoforms in pea. Likewise, in monocots, SSII was also suggested to further subdivided into two subdivisions, SSIIa and SSIIb (Imparl-Radosevich et al. 1999).

The synthesis of amylose was firstly attributed to the granule-bound starch synthase I (GBSSI) (Leloir et al. 1961). Then, the discovery has been supported by several studies involving in waxy-phenotypic mutants with a defective *gbssI* gene product. Various mutants have been identified in different species such as in rice (Murata et al. 1965), maize (Weatherwax 1922), wheat (Nakamura et al. 1995), barley

(Ishikawa et al. 1994), potato (Hovenkamp-Hermelink et al. 1987) and pea (Denyer et al. 1995). Amylose content markedly decreased in *gbssI* mutant in potato (Visser et al. 1991). Although GBSSI is considered to be the sole enzyme involving in amylose synthesis, normal starch granules in tissues such as leaf, stem and root was observed in graminea waxy mutants, indicating that another gene(s) might involve in amylose formation. Moreover, for example, the leaves and stem of waxy rice and the leaves of waxy maize contained amylose. Recently, these were supported by the isolation of a second isoform of GBSSI, from waxy wheat (Nakamura et al. 1998) and pea leaves (Edwards et al. 2002) designated as GBSSII and GBSSIb, respectively, which they were demonstrated to play role in the synthesis of amylose.

1.5.2.3 The synthesis of amylopectin by the soluble starch synthases (SS)

Several studies have revealed that SSI, SSII and SSIII are involved in amylopectin synthesis (Figure 9) although the role of SSI and SSIIb remains unclear. Craig and collegues (1998) suggested that *rug5* mutant, which is closely allied with a defect in *ssII* gene, showed altered amylopectin branching pattern with decreasing of intermediate-sized glucans (DP 15 - 25), while short-chain glucans (DP < 10) were increased in pea (Craig et al. 1998; Fontaine et al. 1993). In potato tubers, single antisense inhibition of SSII and SSIII (Edwards et al. 1999; Lloyd et al. 1999) or combination (Lloyd et al. 1999) resulted in higher producing of short chains rather than long chains. The present knowledges indicate that loss of SSII (in dicots) or SSIIa (in monocots) leads to decreasing of starch content, changing of chain length distribution of amylopectin and physicochemical properties of starch, and perturbing crystallisation. The SS is considered to contribute to amylopectin branch length distribution as

observed in various mutant studies such as *dull1* of maize (Gao et al. 1998), *STA3* mutant in *Chlamydomonas reinhardtii* (Fontaine et al. 1993) and transgenic potato carrying antisense SSIII construct (Edwards et al. 1999).

1.5.2.4 The role of starch branching enzymes (SBE or Q-enzyme)

Starch branching enzymes (SBE) participate in amylopectin synthesis (Figure 9). They catalyse the hydrolysis of α-1,4 linkage and subsequent formation of α-1,6 glucosidic linkage between the cleaved chain and a hydroxyl group on C6 of a glucosyl moiety of an α-1,4 glucan template. They are a member of the α-amylase family structurally characterised by a catalytic $(\beta/\alpha)_8$-barrel domain (Jespersen et al. 1993; Svensson 1994). The domain encompasses specific active sites that arise from the inter-connecting β-loops providing for substrate binding and catalytic activity. Two classes of SBE have been identified, designated as A (SBEII) and B (SBEI), based on amino acid sequences and *in vitro* catalytic activities of purified enzymes (Burton et al. 1995). In monocots, SBEII have been subdivided into SBEIIa and SBEIIb depending on their specific catalytic properties, lengths of amino acid in N-terminal domain and polyglutamic acid repeats in C-terminal (Jobling et al. 1999). SBEI has been identified in maize (Baba et al. 1991), rice (Kawasaki et al. 1993), pea (Burton et al. 1995), cassava (Salehuzzaman et al. 1992), and wheat (Morell et al. 1997). Furthermore, SBEII has been isolated in pea (Bhattacharyya et al. 1990), maize (Gao et al. 1997), rice (Mizuno et al. 1993), barley (Sun et al. 1998), wheat (Nair et al. 1997), cassava (Baguma et al. 2003) and sorghum (Mutisya et al. 2003). Remarkably, SBEI and SBEII provide different substrate specificity. SBEII isoforms have lower affinity on amylose than SBEI, implying that SBEI isoforms prefers longer glucan chains than SBEII (Guan

and Preiss 1993). In addition, they structurally differ in architectural features. For instance, SBEII possess an extended serine rich in N-terminal domain, whereas SBEI have a prolonged C-terminus of around 100 amino acid residues. Interestingly, several studies showed that SBE isoforms are expressed differentially and independently during organ/tissue development and within the amyloplast. Moreover, genes encoding SBEI are constitutively expressed in photosynthetic tissues but those of SBEII are preferentially expressed in starch storage organs. For example, in potato, SBEII is predominantly expressed in leaves with very low level, while in the tuber SBEI is the major isoform (Jobling et al. 1999). Furthermore, in monocots, such as in barley (Sun et al. 1998), maize (Gao et al. 1997), wheat (Nair et al. 1997), and rice (Mizuno et al. 1993), the maximum expression level of sbeII is reached in kernel maturation. Conversely, SBEI is highly expressed in the second half of embryo development in barley (Mutisya et al. 2003), maize (Gao et al. 1997), and wheat (Morell et al. 1997), whereas SBEIIa in maize is more highly expressed in leaves rather than in endosperm. In potato, SBEI is apparently present in soluble fraction more than SBEII, whereas both isoforms in pea embryo are found with comparable level in the soluble fraction (Jobling et al. 1999). Although SBEIIa and SBEIIb share similar role, expression profile and distribution between the granule and stroma, amylose-excessed phenotype was observed only in sbeIIb mutants in cereal grains. The functions of different isoforms were questioned.

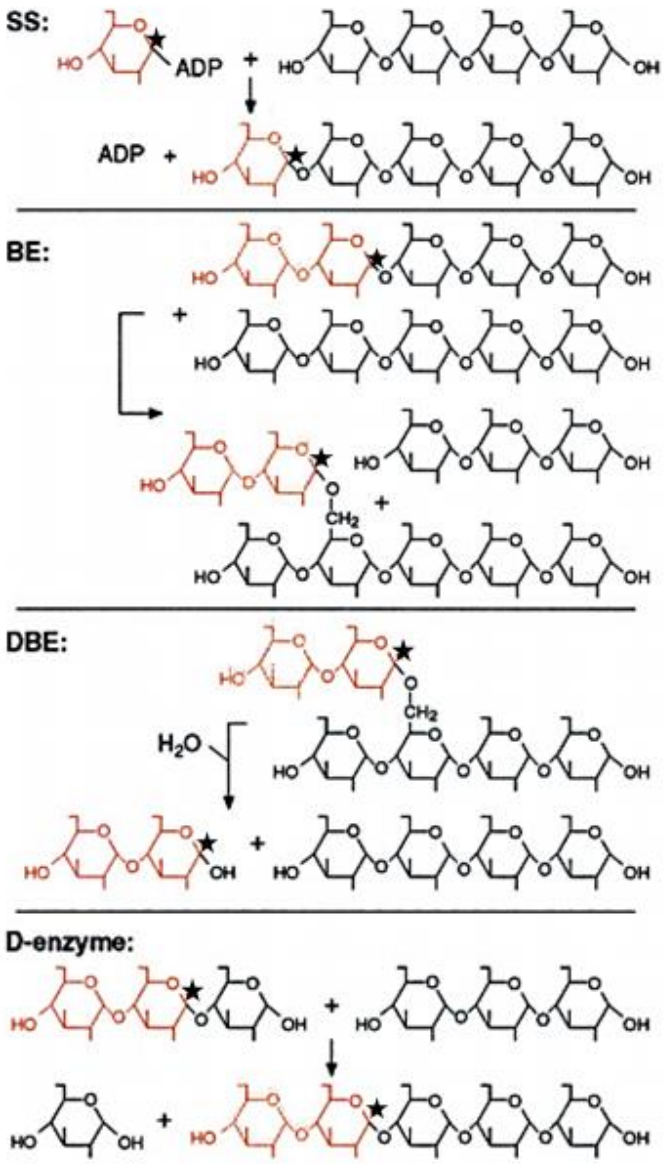

Figure 9 Enzymatic steps in amylopectin synthesis (Myers et al. 2000). The transferred glucosyl units are represent in red, and black stars indicate reducing carbons.

Analysis of starches obtained from *sbe* mutant lines was used to elucidate the function of different SBE isoforms. In both monocots and dicots, *sbeI* mutant resulted in minimal effects on starch synthesis and composition in leaves, endosperm and tubers (Ball and Morell 2003; Blauth et al. 2002; Satoh et al. 2003; Seo et al. 2002). Nevertheless, loss of SBEI in rice caused significant changes in the fine structure of amylopectin and physicochemical properties of the starch in rice endosperm (Satoh et al. 2003). On the other hand, single elimination of potato SBEII led to increased level of amylose (Jobling et al. 1999) although the increasing of amylose content of starch was observed in double suppression of both SBEI and SBEII (Schwall et al. 2000). This suggested that the function of SBEI in starch synthesis might overlap to that of SBEIIs (SBEIIa and SBEIIb). However, the function of each isoform remains unclear. Noticeably, substrate specificities of each isoform, configuration of the substrate molecules (helical structure or interchain) and enzyme complexes occur during starch synthesis required to be further studied.

1.5.2.5 The role of debranching enzymes (DBE)

Starch debranching enzymes are a member of the α-amylase family (Jespersen et al. 1993). They catalyse the hydrolysis of the α-1,6 glucosidic linkages of branched α-polyglucans such as amylopectin. Due to similarity of peptide sequence and substrate specificity, DBE is subdivided into two groups; pullulanase-type or R-enzyme (EC: 3.2.1.41) and isoamylase-type (EC: 3.2.1.68) debranching enzyme (Doehlert and Knutson 1991; Ishizaki et al. 1983). Pullulanase capable of debranching pullulan and amylopectin but not glycogen, while isoamylase is able to hydrolyse both glycogen and amylopectin (Nakamura et al. 1996) but not pullulan. Furthermore, pullulanase

produces maltotriosyl groups, whereas isoamylase generates maltotriosyls and oligosaccharides. Pullulanase is protein product encoded by one gene, but three genes encoding three isoamylase proteins (ISA1 to ISA3) were conserved in higher plants. We herein focused on the isoamylase-type debranching enzymes (ISA). In monocots, such as cereals, isoamylases are multimeric enzymes consisting of one larger type of homomeric enzyme (ISA1 homomer) and two smaller types of heteromers (ISA1/ISA2 heteromers) (Burton et al. 1995). Conversely, in dicots such as potato, two distinct subunits were present in heteromultimeric enzymes (ISA1/ISA2) (Ishizaki et al. 1983). However, no evidence of multimeric form of ISA3. Interestingly, ISAs are proposed to play an essential role in both starch biosynthesis and degradation. Several studies, for example in Arabidopsis and potato (Bustos et al. 2004; Hussain et al. 2003), ISA1 and ISA2 were shown as subunits of heteromeric isoamylase complex and played a crucial role in starch biosynthesis involving in mature amylopectin formation. Although the real mechanism of ISA in amylopectin synthesis of starch granule formation is still unclear, several models have been proposed based on mutagenesis analyses. For instance, the *sugary1* (*su1*) mutant, lacking of DBE activity, in maize and rice showed the high accumulation of not only starch but also highly-branched, water soluble glucan so-called phytoglycogen (Doehlert et al. 1993; Fujita et al. 2003; James et al. 1995; Kubo et al. 1999; Nakamura et al. 1997; Nakamura et al. 1996). Further support for the participation of ISA in amylopectin synthesis, phytoglycogen-accumulating phenotypes in ISA-deficient mutants has been reported in *Chlamydomonas reinhardtii* (*sta7*) (Dauvillée et al. 2001; Mouille et al. 1996) and Arabidopsis (*dbe1*) (Zeeman et al. 1998).

Ball et al. (1996) proposed a classical model of trimming the shape of amylopectin clusters and hence this model is called “the glucan trimming model” (Figure 10). They suggested the sequential course of events which excess branches of highly-branched glucan polymers synthesised by SS and SBE is cleared off by DBE, especially ISA, otherwise the crystallisation will be obstructed. However, the trimming model has some limits as observed in *dbe1* mutants in Arabidopsis, which accumulate both starch and phytoglycogen. This suggested that the accumulation of phytoglycogen in wild-type is perhaps resulted from concert action of several glucan-degrading enzymes.

Alternatively, Zeeman and co-workers (1998) discovered the phytoglycogen-accumulated phenotype in mutant lines (*dbe1*) of Arabidopsis. However, the normal starch was apparently accumulated to the normal level (Zeeman et al. 1998) leading to the proposal of indirect role of DBE in amylopectin synthesis called soluble glucan clearing model (Figure 11). They suggested that not only DBE but other starch-metabolising enzymes play scavenging function in stroma by removing of any soluble glucans produced by SS and SBE from small soluble malto-oligosaccharides. In DBE-deficient mutant, highly-branched, water soluble glucans or phytoglycogen will be accumulated from the actions of SS and SBE.

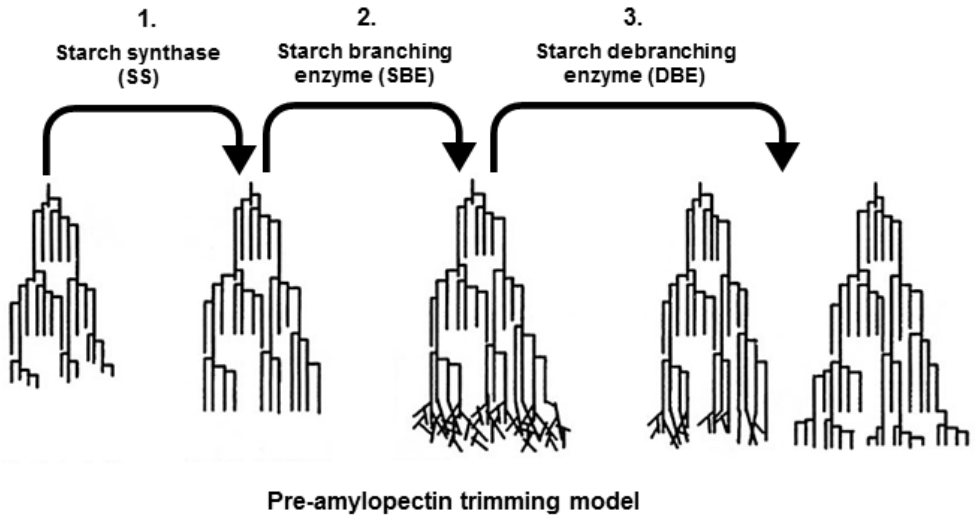

Figure 10 Model to explain the involvement of DBE (ISA1 and ISA2) in starch biosynthesis (Myers et al. 2000). The trimming model proposed by Ball et al. (1996) suggested a direct involvement of DBE in mature amylopectin formation. The amylopectin clusters are created at the surface of the starch granule with a sequence of synthetic events as follows; **(1)** chain elongation by SS, **(2)** chain branching by SBE, highly branched-amylopectin is formed, **(3)** selective trimming of this highly branched-structure by DBE (mainly ISA1 and ISA2) providing a bed of short chains which the next round of synthesis can occur. The highly branched, soluble glucans will be accumulated when the DBE activity is decreased or eliminated as found in the *su1*, *sta7* and *dbe1* mutants.

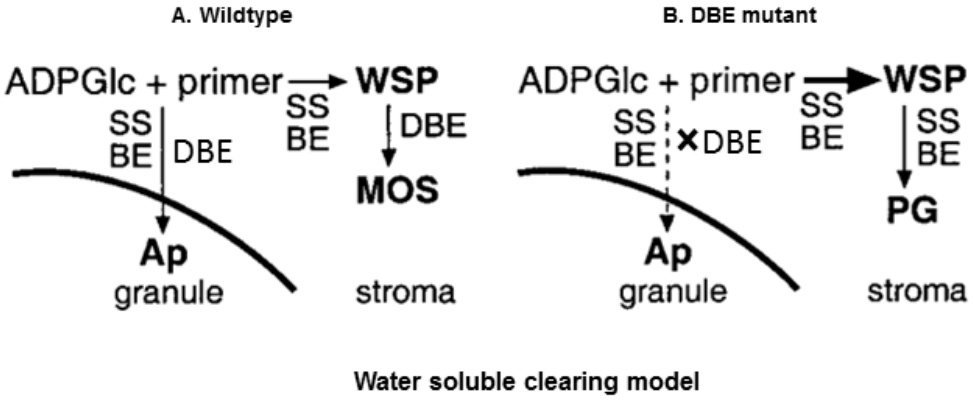

Figure 11 Model to explain the involvement of DBE (ISA1 and ISA2) in starch biosynthesis (Myers et al. 2000). The DBE was proposed with indirect involvement in starch synthesis (Zeeman et al. 1998). Amylopectin synthesis requires SS and SBE. **(A)** water soluble glucan synthesised in plastid stroma by SS and SBE is sequentially hydrolysed by DBE to produce competent amylopectin. The glucosyl and maltosyl units are presumably returned to the beginning step. **(B)** In the absence of DBE activity, water soluble polysaccharides produced by SS and SBE are further modified and transformed into phytoglycogen by the two enzymes.

Despite these fascinating models, it remains unresolved whether glucan trimming, WSP clearing or some other mechanisms would clearly explain the mode of action of DBE in amylopectin synthesis because it is extremely difficult to test in direct way.

On the other hand, ISA3 is presumably might be essential for starch degradation. During mobilisation of transitory starch, both starch biosynthesis and degradation occur simultaneously, ISA3 is required for hydrolysing branched-glucans arisen during starch degradation, mainly from β-amylolysis.

1.5.2.6 The function of disproportionating enzyme (D-enzyme)

D-enzyme was firstly reported in potato tuber (Peat et al. 1956). After that, it was discovered in beans, peas, carrot, tomato, spinach, and Arabidopsis (Lin and Preiss 1988; Manners and Rowe 1969; Okita et al. 1979). It catalyses disproportionating of small soluble oligosaccharides of at least maltotriosyl units or amylopectin into maltooligosaccharides (Colleoni et al. 1999; Lin and Preiss 1988; Takaha et al. 1998). In addition, analysis of D-enzyme in potato *in vitro* showed its ability of transferring branched glucans and producing of cyclic glucans (Colleoni et al. 1999; Takaha et al. 1998). Mutation studies, to understand role of D-enzyme in starch biosynthesis, in *Chlamydomonas* and Arabidopsis showed divergent functions. Mutation in Chlamydomonas, significant reduction in total glucopolysaccharide, abnormal starch granules, and atypical chain-length distribution of amylopectin were observed compared to the wild type. On the contrary, starch-excessed phenotype was detected in Arabidopsis mutants (Critchley et al. 2001). However, transgenic lines of potato tubers transformed with antisense D-enzyme constructs showed no changing of starch

synthesis and its fine structure (Takaha et al. 1998). These findings implicate that additional researches for clearly understanding of the function of D-enzyme in starch synthesis are required.

1.5.2.7 The role of β-amylase

The quantitatively most noticeable exo-hydrolases are β-amylases (Glycoside Hydrolase family 14; GH14), which typically hydrolyse maltosyl residues from the non-reducing end of α-glucan chain following an inverting (i.e. single displacement) mechanism. Hence, the anomeric carbon (C1) is converted from α to β-configuration and β-maltose is released. Subsequently, the same α-glucan chain may be further hydrolysed when either the reducing end or a branching point is reached. Additional reactions have been reported for activity of β-amylase (Fazekas et al. 2013; Mikami et al. 1994) however production of β-maltose seems to be their main activity. This related to the starch-excess phenotype of potato mutant line lacking of plastidial β-amylase (Scheidig et al. 2002). Plants typically harbour a relatively high numbers of β-amylases which differ in kinetic properties and *in vivo* functions based on their subcellular localisations (Fettke et al. 2012). Since β-amylases from plants act on single helices, hydrosoluble glucans are more preferable than highly ordered and insoluble glucans (Edner et al. 2007; Hejazi et al. 2008).

1.5.2.8 Endo-hydrolases (α-amylases)

The second large group of starch-hydrolysing enzymes is α-amylases (GH13). Unlike β-amylases, α-amylases hydrolyse internal α-1,4 interglucose linkages and either linear or branched α-glucans are released. For branched substrates, α-amylase

acts on either site of the α-1,6 glucosidic linkages. Furthermore, α-amylases use the retaining (double displacement) mechanism, following hydrolytic cleavage of the target bond accounting for α-configuration of the free C1 position of the glucan released. Similar to β-amylases, extra activities of α-amylase have also been reported (Kim et al. 1999; Qian et al. 2001), but endo-hydrolase activity appears to be the major catalytic activity which preferentially act on single helical and soluble glucans.

1.5.2.9 Other factors and evidence implicating their involvement

From mutation studies of reduced starch degradation rates revealed that degradation of starch granule requires not only starch-hydrolysing enzymes but also enzymes that play roles in phosphorylation and dephosphorylation of glucan polymers. In potato, transgenic plants are deficient in a protein associated with starch granule (R1) showed reduction rates of starch degradation (Lorberth et al. 1998). In addition, the starch-excess phenotype Arabidopsis (*sex1* mutant) lacking of R1 protein is deficient in starch phosphate and has high accumulation of leaf starch (Yu et al. 2001). The R1 protein was shown to be a glucan water dikinase (GWD). The two phosphorylating enzymes consisting of GWD and PWD (phosphoglucan water dikinase) are essential for normal starch degradation by catalysing attachment of phosphate group to C3- and C6-positions of glucose in amylopectin (Ritte et al. 2006). For instance, starch degrading acitivity of recombinant BAM and ISA3 is greatly enhanced by the presence of GWD and ATP in *in vitro* experiments (Edner et al. 2007).

On the other hand, two enzymes (SEX4 and LSF2), catalysing dephosphorylation of phosphorylated glucans in starch granule, are also required for normal rates of starch degradation. In degradation of phosphorylated starch granules,

the degradation rates of BAM and ISA3 is significantly enhanced by addition of SEX4 (Kötting et al. 2009).

These results indicate that both phosphorylation and dephosphorylation are important for complete starch degradation by increasing accessibility of important starch-degrading enzymes such as BAM and ISA3 (Tabata et al. 1978; Takeda and Hizukuri 1981).

To date, it is still not clear of roles of several enzymes in starch metabolism in cassava. However, several enzymes in cassava starch metabolism have been reported; the granule-bound starch synthase (Salehuzzaman et al. 1992), catalysing the elongation of α-1,4-linked linear polyglucans, three isoforms of starch branching enzymes (Yaiyen 2009), involving in formation of α-1,6 linkages in amylose and especially amylopectin. Recently, the molecular characteristics of 4-α-glucanotransferase or D-enzyme, catalysing the transfer of maltosyl unit of (1,4)-α-D-glucose to produce longer chain oligosaccharides, have been reported (Tantanarat et al. 2014). In this study, we focused on the molecular characteristics of the cassava isoamylase-type debranching enzymes.

1.6 Objectives

Cassava starch comprises different glucan chains, amylose and amylopectin. Distinct ratio of amylose and amylopectin in cassava starch gives unique physicochemical properties of the starch. At present, the industrial applications of starch, both unmodified (native) starch and modified starch, are significantly increased. Hence, it might be of value to produce cassava starch with high quality and desired properties which benefits for industrial uses and the commercial price of cassava can

particularly be raised. These can be achieved by modifying the levels and properties of the starch-metabolising enzymes. To be able to manipulate starch in term of its beneficial properties, it is necessary to understand all enzymes involving in starch metabolism. In our laboratory, starch synthase, starch branching enzymes and disproportionating enzyme have been studied. In this research, we aimed at molecular characterisation of another important enzyme in cassava starch metabolism, the cassava isoamylases.

Objectives of this research

1. Isolation and expression of isoamylase genes from cassava *Manihot esculenta* Crantz 'KU50' tuber
2. Functional characterisation of the cassava isoamylases

CHAPTER II

MATERIALS AND METHODS

2.1 Plant materials

Cassava cultivar KU50 tubers (*Manihot esculenta* Crantz) were harvested from the National Research Centre of Millet and Corn (Suwan Farm), Nakhon Ratchasima, Thailand.

2.2 Equipments

Autoclave: Model H-88LL, Kokusan Emsinki Co., Ltd., Japan

Autopipette: Pipetteman Gilson, France

Centrifuge, refrigerated centrifuge: Model J2-21, Beckman Instrument, Inc., U.S.A. and Sorvall Legend XTR, ThermoFisher Scientific, Inc., Germany

Centrifuge, microcentrifuge: Model 5430, Eppendorf Co., Ltd., Germany

Dark Reader blue transilluminators, Dark Reader^{R}, Clare Chemical Research, Inc., U.S.A.

Electrophoresis unit:

- Mini protein, Bio-Rad, U.S.A.
- Mini Horizontal Gel Electrophoresis System, Major Science, U.S.A.
- Submarine agarose gel electrophoresis unit, Bio-Rad, U.S.A.

Eppendorf Biospectrometer® basic: Eppendorf, Germany

Fraction collector: Frac-920, GE Healthcare Bio-Sciences AB, Sweden

Gene Pulser®/ *E. coli* Pulser^{TM} cuvette: Bio-Rad, U.S.A.

Gel Document: SYNGEND, England

Incubator, shaker: Innova^{TM} 4000 and 4080, New Burnwick Scientific, U.S.A.

Incubator, waterbath: Model M20S, Lauda, Germany and Biochiller 2000, FOTODYNE Inc., U.S.A. and ISOTEMP 210, Fisher Scientific, U.S.A.

Laminar flow: HT123, ISSCO, U.S.A. and Streamline^{R} Vertical Laminar Flow Cabinet Model SCV- 4A1, Gibthai Co., Ltd., Singapore.

Magnetic stirrer: Model Fisherbrand, Fisher Scientific, U.S.A.

Magnetic spinbar: Teflon® PTFE, Scienceware®, Capitol Scientific, Inc., U.S.A.

Membrane filter: Cellulose nitrate, pore size 0.45 µm, Whatman, England and Polyethersulfone (PES) Syringe filter, pore size 0.45µm, Stratlab, England

Microplate reader: Synergy^{TM} H1, Biotek Instruments, Inc., U.S.A.

MicroPulser^{TM} electroporator: Bio-Rad, U.S.A.

pH meter: Model MP220, Mettler-Toledo International, Inc., U.S.A.

Spectrophotometer: Model G10S UV-Vis, ThermoFisher Scientific, Inc., U.S.A.

Thermal Cycler Block: Type 5020, ThermoFisher Scientific, Inc., Finland

Vortex: Model G560E, Scientific Industries, Inc., U.S.A.

Water bath: Charles Hearson Co.Ltd., England

2.3 Chemicals

Absolute ethanol (Merck)

Acrylamide (AppliChem PanReac)

Agarose (Vivantis)

Ammonium hydroxide (Sigma-Aldrich)

Ammonium persulfate (AppliChem)

Ampicillin (Affymetrix)

Amylopectin from maize (Sigma-Aldrich)

Beta-limit dextrin (Sigma-Aldrich)

Beta-mercaptoethanol (Bio Basic)

Boric acid (Univar)

5-bromo-4-chloro-3'-indolyphosphate p-toluidine salt (BCIP) (Thermo Scientific)

Citric acid (Univar)

Cobalt (II) chloride (Merck)

Copper (II) sulphate (Sigma-Aldrich)

Deoxynucleotides (dNTPs) (Thermo Scientific)

Dipotassium phosphate (Univar)

Ethylenediaminetetraacetic acid (EDTA) (AppliChem)

Formaldehyde (Carlo Erba)

Glacial acetic acid (Merck)

Glucose (Univar)

Glycerol (Univar)

Glycine (Norgen Biotek)

Glycogen (Sigma-Aldrich)

Calcium (II) chloride (Univar)

Chloroform (Carlo Erba)

Dinitrosalisylic acid (Sigma-Aldrich)

6x-His Epitope Tag Antibody (HIS.H8) (ThermoFisher Scientific)

Hydrochloric acid (Labscan)

Imidazole (Acros)

Iron (III) chloride (Univar)

iScript™ Reverse Transcription Supermix for RT-qPCR (Biorad)

Isopropyl β-D-1-thiogalactopyranoside (IPTG) (ThermoFisher Scientific)

Isopropanol (Merck)

Magnesium (II) chloride (Univar)

Magnesium chloride hexahydrate (USB)

Manganese (II) chloride (Univar)

Methanol (Honeywell)

Nickel (II) sulphate (M&B)

Nitro-blue tetrazolium chloride (NBT) (Thermo Scientific)

Pierce® Goat Anti-Mouse IgG, (H+L), Alkaline Phosphatase Conjugated (ThermoFisher Scientific)

Potato starch (Sigma-Aldrich)

Potato amylopectin (Sigma-Aldrich)

Potassium chloride (Univar)

Potassium dihydrogen phosphate (Univar)

Phenol (Merck)

Precision Plus Protein™ Standards (BioRad)

PureLink® Plant RNA Reagent (ThermoFisher Scientific)

Pullulan (Megazyme)

Skim milk (ThermoFisher Scientific)

SMARTer® RACE 5’/3’ kit (Takara)

Sodium chloride (Univar)

Sodium citrate (Univar)

Sodium azide (Merck)

Sodium dodecyl sulphate (SDS)

Sodium hydroxide (Lab-Scan)

Sodium potassium tartrate (Univar)

Tetramethylethylenediamine (TEMED) (ThermoFisher Scientific)

TriColor Broad Protein Ladder (Biotechrabbit)

Tris-HCl (Vivantis)

Tryptone type-I (Himedia)

Tween-20 (Sigma)

Yeast extract (Schalau)

Zinc (II) sulphate (Univar)

2.4 Enzymes and Restriction enzymes

Pfu DNA polymerase (Promega)

Taq DNA polymerase (Invitrogen)

T4 DNA Ligase (Thermo Scientific)

FastDigest *Sac*I (ThermoFisher Scientific)

FastDigest *Not*I (ThermoFisher Scientific)

FastDigest *Eco*RV (ThermoFisher Scientific)

FastDigest *Xho*I (ThermoFisher Scientific)

FastDigest *Nde*I (ThermoFisher Scientific)

FastDigest *Sal*I (ThermoFisher Scientific)

PrimeSTAR DNA polymerase (Takara)

DNaseI

Pseudomonas amyloderamosa isoamylase (Sigma)

2.5 Bacterial strains and plasmids

***Escherichia coli* TOP10** (Invitrogen™, Thermo Scientific), genotype: F^- *mcrA* Δ(*mrr*-*hsd*RMS-*mcr*BC) φ80*lac*ZΔM15 Δ*lac*X74 *rec*A1 *ara*D139 Δ(*araleu*)7697 *gal*U *gal*K *rps*L (StrR) *end*A1 *nup*G, was used as a host for plasmid propagation.

***Escherichia coli* SoluBL21™ (DE3)** (Amsio), genotype: F^- *ompT hsd*S_B (r_B^- m_B^-) *gal dcm* (DE3), was used as an expression host for protein production.

pJET1.2/blunt (Thermo Scientific) was used as a cloning vector.

pET21b (Novagen) was used as an expression vector.

2.6 General techniques for molecular cloning and gene expression

2.6.1 Plasmid preparation

Cells harbouring plasmid were cultured in 5 ml of LB broth containing appropriate antibiotics at 37 ºC with shaking at 250 rpm for overnight. Then, cells were harvested by centrifuging at 13,000 rpm 30 sec at room temperature and used for plasmid extraction using Presto™ Mini Plasmid Kit from Geneaid.

2.6.2 Electrocompetent cell preparation (Sambrook et al. 1989)

The procedures were slightly modified from Sambrook et al. (1989). *E. coli* TOP10 or *E. coli* SoluBL21 (DE3) cells were grown in LB broth at 37 ºC with shaking at 250 rpm for overnight as starter culture. The culture was transferred into fresh LB media (1:50) and grown at 37 ºC with rotary shaking at 250 rpm until optical density measured at a wavelength of 600 nm (OD_{600}) reached 0.3 to 0.4. The culture was chilled on ice about 10 to 15 min and centrifuged at 3,000 x g at 4 ºC for 10 min to fractionate

the cell pellet. The cells were washed with 300 ml of cold ultra-pure water twice followed by 300 ml of cold 10% (v/v) glycerol. After centrifugation, the cells were suspended in the final volume of 600 µl of cold 10% (v/v) glycerol, mixed gently by pipetting. Finally, aliquots of 40 µl of the cell suspension were kept at -80 ºC until used.

2.6.3 Transformation of recombinant plasmid into *E. coli* host cell

(Sambrook et al. 1989)

The recombinant plasmids were transformed into *E. coli* competent cells by electroporation. The 1 to 3 µl of recombinant plasmids or 3 to 5 µl of ligation mixture was mixed with the competent cells on ice. The mixture was then transferred to a chilled 0.2 cm-gap sterile electroporation cuvette and electroporated by using 25 µF, 200 Ω of the pulse controller unit and 250 kV time constant 4.6 - 4.8 msec. After that, for cells recovery, the cells were grown in a new nuclease-free microcentrifuge tube containing 600 µl of LB broth and incubated at 37 ºC with rotary shaking for 45 min. The cell culture was plated on LB agar plate containing 100 µg/ml of ampicillin and incubated at 37 ºC for overnight.

2.6.4 Colony PCR technique

The cells grown on the ampicillin-containing plate were analysed. Each single colony was picked by sterile toothpick and suspended in 10 µl of nuclease-free water. Two microlitres of the suspension culture was used as template for PCR by using *Taq* DNA polymerase. The temperature profiles are as follows: 1 round of 95 ºC 3min followed by 25 cycles of 94 ºC 30 sec, 55 ºC 30 sec,72 ºC 3 min and 1 round of final extension at 72 ºC 5 min. Then, the PCR products were analysed by agarose gel electrophoresis. The cell suspension of positives clones kept at 4 ºC were inoculated

into LB broth containing ampicillin and cultured at 37 ºC with shaking for overnight for plasmid extraction and nucleotide sequencing by 1st BASE.

2.6.5 Agarose gel electrophoresis

The 0.8 g of agarose powder was added to 100 ml of TBE electrophoresis buffer (Appendix D) in an Erlenmeyer flask and heated in microwave oven to get complete solubilisation. The MaestroSafe™ pre-stained dye was added into the agarose solution (with 1:50000 dilution rate) and mixed. Then, the agarose solution was cooled down to 60 °C to 70 °C and the gel was cast. After the gel was completely set, the DNA/RNA sample was mixed with one-fifth volume of gel loading buffer (30% (v/v) glycerol, 0.25% (w/v) bromophenol blue and 0.25% (w/v) xylene cyanol FF) and the mixture was slowly loaded into the wells. Electrophoresis was performed at constant voltage of 100 volts until the front (bromophenol blue) reached at about 2 cm above the bottom of the gel. The DNA/RNA was visualized under UV light and photographed by using Gel Document device.

2.7 General techniques for protein characterisation

2.7.1 Sodium Dodecyl Sulphate-Polyacrylamide Gel Electrophoresis (SDS-PAGE) (Bollag et al. 1996)

The slab gel of 8% (w/v) of separating gel and 5% (w/v) of stacking gel containing 0.1% (w/v) of SDS was set. The protein samples to be analysed were combined with 5X sample buffer. Then, the sample was slowly introduced into wells of the gel and the electrophoresis was run in electrophoresis buffer pH 8.3 containing

0.1% (w/v) of SDS at constant voltage of 150 V at room temperature. The protein bands on the gel were visualised by Coomassie staining or Silver staining.

2.7.2 Silver-staining of SDS-PAGE (Bollag et al. 1996)

After electrophoresis, the gel was soaked in 50% (v/v) methanol/10% (v/v) acetic acid for 1 h with 2 changes. Then, the gel was rinsed in ultrapure water for 20 min with 2 changes. In the meantime, solution C was prepared by dropwise adding solution A to solution B and ultrapure water was added to the final volume of 50 ml. After that, the gel was soaked in the solution C for 15 min on rocking shaker and then rinsed several times in ultrapure water. The final step is to develop the gel by washing in solution D. When the bands were appeared, the gel development was stopped by adding 1% (v/v) acetic acid. (See Appendix D for components of solution A, B and C)

2.7.3 Native-Polyacrylamide Gel Electrophoresis (Native-PAGE) (Bollag et al. 1996)

The slab gel of 6% (w/v) of separating gel containing 0.15% (w/v) of substrate and 5% (w/v) of stacking gel were set. The protein samples to be analysed were combined with 6X native buffer and slowly introduced into wells of the gel. The electrophoresis was run in cold electrophoresis buffer pH 8.3 at constant current of 15 mA per gel at 4 ^{o}C by using Mini-Gel electrophoresis unit. The protein bands on the gel were visualised by Coomassie staining while debranching activity was analysed by I_2 staining after soaking the gel in 50 mM phosphate buffer pH 7.2 at room temperature for overnight.

2.7.4 Western blot

After SDS-PAGE, the proteins were transferred onto nitrocellulose membrane under constant electric current, 350 mA, for 25 min 30 sec in 1X Tris-Glycine buffer

pH 8.3. Then, the membrane was incubated in blocking buffer, 10% (w/v) of skim milk in 1X Tris-buffered saline - tween, for overnight at room temperature on the rocking shaker. The membrane was then washed twice in TBS-tween buffer for 10 min meanwhile antibody buffer (1% (w/v) of skim milk in 1X TBS-tween buffer) was prepared. The membrane was incubated in primary Ab solution (4 µl of 6X-His tag Ab in 10 ml of antibody buffer) for 2 h at room temperature with shaking. Then, the membrane was washed in 1X TBS-tween buffer for 30 min. After that, the membrane was incubated in secondary Ab solution (3 µl of alkaline phosphatase-attached goat anti-mouse IgG in 10 ml of antibody buffer) for 1 h at room temperature with shaking. The membrane was washed in 1X TBS-tween buffer for 20 min and quickly washed in 1X TBS buffer. The last step was the colorimetric detection of alkaline phosphatase activity on the membrane. Substrates of alkaline phosphatase were prepared by mixing 66 µl of 50 mg/ml of NBT and 33 µl of 50 mg/ml of BCIP in alkaline phosphatase buffer. The protein bands were visualised by incubating membrane with the prepared substrates and the substrates were removed immediately after the bands were apparently appeared. (See Appendix B)

2.7.5 Modified Dinitrosalicylic acid assay (DNS assay) for debranching enzyme activity assay (DBE activity) (Miller 1959)

The enzymatic reaction was terminated by adding of equal volume of 3, 5-dinitrosalicylic acid and boiled for 10 min. The increasing of reducing sugar produced in the reaction was determined by measuring of A_{540}. The amount of reducing sugar produced in the reaction was calculated from the equation of glucose standard as follows;

$$Y = 0.9228X + 0.0411$$

where Y stands for A_{540} value while X represents µMole of reducing sugar produced.

2.8 Cloning of cassava isoamylase genes (Me*ISA*)

2.8.1 Total RNA extraction from cassava tubers

Nine-month old cassava tubers were kindly provided by the National Research Centre of Millet and Corn (Suwan Farm). To extract total RNA, cortex of the tuber was sliced and ground in liquid nitrogen using precooled mortar and pestle. Then, 500 µl of cold Plant RNA Reagent was added into 50 - 100 mg of frozen ground tissue, mixed by brief vortexing, and incubated at room temperature for 5 min. The supernatant was fractionated by centrifuging at 13,000 x g for 2 min. After that, 100 µl of 5M NaCl and 300 µl of chloroform was added sequentially to the clarified extract and mixed thoroughly by inversion. The sample was centrifuged at 13,000 x g at 4 °C for 10 min then the top aqueous phase was transferred to an RNAse-free tube. After that, repeat this following step twice by adding equal volume of phenol-chloroform to the aqueous solution and mixed by vortexing briefly. The solution was centrifuged at 13,000 x g at 4 °C for 10 min then the top aqueous phase was transferred to an RNAse-free tube. To obtain total RNA, equal volume of isopropyl alcohol was added to the aqueous phase and the sample was mixed and incubated at room temperature for 10 min. RNA pellet was collected by centrifuging at 13,000 x g at 4 °C for 10 min. The pellet was washed by adding 1 ml of 75% (v/v) ethanol and the liquid was discarded by centrifuging at 13,000 x g at room temperature for 1 min. The RNA pellet was dried at room temperature and stored at -80 °C. The pellet was dissolved by adding 30 – 50 µl of 10 mM Tris-HCl (pH 8.5). The concentration of this total RNA solution in µg/ml equals A_{260} x dilution factor x 40, measured by UV-Vis spectrophotometer. The purity of the

total RNA was monitored by the ratio of A_{260}/A_{280} values and by agarose gel electrophoresis (described in section 2.6.5).

2.8.2 DNase treatment of the RNA prior to Reverse Transcription-Polymerase Chain Reaction (RT-PCR)

DNA contaminant in the RNA solution was removed by RQ1 RNase-free DNase. The reaction was performed by mixing 5 µg of RNA with 1 µl of RQ1 RNase-free DNase 10x buffer, RQ1 RNase-free DNase 5 µl (1 unit/µl) and nuclease-free water to a final volume of 10 µl and incubated at 37 °C for 30 min. Then, 1 µl of RQ1 DNase Stop Solution was added to stop the reaction by incubating at 65 °C for 10 min. Finally, a portion of DNase-treated RNA was taken to the reverse transcription reaction to construct cDNA.

2.8.3 Construction of cDNA by reverse transcription technique for Me*ISA1* and Me*ISA2* gene

The cDNA was constructed by using iScript™ Reverse Transcription Supermix for RT-qPCR. A 4 µl of DNase-treated RNA was added to the reverse transcription reaction containing 4 µl of 5X iScript reverse transcription supermix and nuclease-free water to a final volume of 20 µl. The reaction was performed with the temperature profile described in Table 2.

Table 2: Cycling profile of cDNA construction of Me*ISA1* and Me*ISA2* using reverse transcription technique

	Temperature	**Time**
Priming	25 °C	5 min
Reverse transcription	42 °C	30 min
RT inactivation*	85 °C	5 min

*After RT inactivation, cDNA was kept at -80 °C for long term storage.

2.8.4 5'Rapid Amplification of cDNA End (5'RACE) of Me*ISA3* gene

Due to the incomplete sequence of Me*ISA3* reported in both NCBI and Phytozome databases, so the 5'RACE was performed by using SMARTer® RACE 5'/3' kit. The RNA reaction mixture was prepared on ice by mixing 1 µg of total RNA with 1 µl of 5'-CDS Primer A, nuclease-free H_2O to the volume of 11 µl and 1 µl of the SMARTer II A Oligonucleotide. The Master Mix was prepared by mixing the following reagents: 4 µl of 5X First-Strand Buffer, 0.5 µl of 100 mM DTT, 1 µl of 20 mM of dNTPs, 0.5 µl of RNase Inhibitor (40 U/µl) and 2 µl of SMARTScribe Reverse Transcriptase (100 U). Then, the Master Mix was added into the RNA reaction mixture, mixed by gently pipetting and the tube was spin briefly. The reaction was incubated at 42 °C for 90 min and terminated by heating at 70 °C for 10 min.

2.8.5 Amplification of cassava isoamylase genes (Me*ISA*) using PCR technique

Three cassava isoamylase genes (Me*ISA* genes) have been reported in NCBI and Phytozome databases. The full length sequences of Me*ISA1* and Me*ISA2* genes

were amplified by using gene specific primers shown in Table 3. The purified PCR products of these putative genes were cloned into pJET1.2/blunt cloning vector and sequenced. Then, new set of the gene-specific primers for each gene was designed for gene amplification without their signal peptide sequences. The *Sac*I and *Not*I restriction sites were incorporated with a pair of primers for Me*ISA1* gene whereas *Eco*RV and *Xho*I sites were introduced in the primers of Me*ISA2* (Table 4). The mature recombinant Me*ISA1* and Me*ISA2* genes (rMe*ISA1* and rMe*ISA2*) were amplified and directly cloned into expression vector, a pETDuet1. For the Me*ISA3*, full length gene was amplified by using 10X Universal Primer A Mix (10X UPM) provided in the SMARTer® RACE 5'/3' kit as forward primer and R1_pET21b (Table 4). The purified PCR product was cloned into pJET1.2/blunt cloning vector and sequenced.

To subclone the rMe*ISA3* gene into a pET21b expression vector, the mature gene was amplified by using gene specific forward primer named F1full_pET21b (shown in Table 4). This primer contained *Nde*I restriction site which was designed after the full length sequence was obtained. The gene amplification was performed by using Q5® Hi-Fidelity DNA polymerase for rMe*ISA1* and rMe*ISA2* whereas PrimeSTAR DNA polymerase was used for rMe*ISA3* amplification with the cycling profiles as shown in Table 5A and B.

Table 3: Primers for full length Me*ISA* genes amplification

Gene	Primers name; oligonucleotide sequence
Me*ISA1*	F-FLisa1; 5’-ATGGACTTAATTCAATCTTCTGCTTCTCGC-3’
	R-FLisa1; 5’-AGCAATTTCATCAGGAGAAAGGATTAAG-3’
Me*ISA2*	F-FLisa2; 5’-ATGGCAACACTTCTTCCTTCCTTTGC-3’
	R-FLisa2; 5’-ACCACCAAGGCTAGTGGCTTCAAACAGAG-3’
Me*ISA3*	10X UPM; 5’-CTAATACGACTCACTATAGGGCAAGCAGTGGTATCAACGCAGAGT-3’
	R1_pET21b; 5’-CCTGGTCGACTGTCAGTTTCGCTTCAAG-3’

Table 4: Primers for mature Me*ISA* genes amplification

Gene	Primer name; oligonucleotide sequence	Restriction site*
Me*ISA1*	F_DUisa1; 5’-CCGTGAGCTCGATGGCCACCAGAAGAGATGG-3’	*Sac*I
	R_DUisa1; 5’-ATAAGCCTGCGGCCGCAGCAATTTCATCAGGAGAAAGG-3’	*Not*I
Me*ISA2*	F_DUisa2; 5’-GTCCGATATCGATGTGTGGAGCTGTGGAGTC-3’	*Eco*RV
	R_DUisa2; 5’-ACTCGCTCGAGACCACCAAGGCTAGTGGC-3’	*Xho*I
Me*ISA3*	F1full_pET21b; 5’-GGAGTCCATATGCTAATGTCGGAAACCAGCCC-3’	*Nde*I
	R1_pET21b; 5’-CCTGGTCGACTGTCAGTTTCGCTTCAAG-3’	*Sal*I

*The restriction sites are underlined.

Table 5: Temperature profiles of Me*ISA* genes amplification by PCR technique

A. Using Q5® Hi-Fidelity DNA polymerase for Me*ISA1* and Me*ISA2*

Cycles	**Temperature**	**Time**
1	98 ºC	30 sec
30-35	98 ºC 61 ºC 72 ºC	10 sec 10 sec 1 min 50 sec
1	72 ºC	2 min

B. Using PrimeSTAR DNA polymerase for Me*ISA3*

Cycles	**Temperature**	**Time**
1	98 ºC	10 sec
30	98 ºC 60 ºC 72 ºC	10 sec 10 sec 3 min
1	72 ºC	7 min

After final extension, PCR products were kept at 4 ºC

2.8.6 Construction of recombinant plasmids

Me*ISA1* and Me*ISA2* were cloned into a pETDuet1 vector as expression vector step by step. The PCR products of Me*ISA1* and Me*ISA2* were double excised with *Sac*I and *Not*I restriction enzymes and *Eco*RV and *Xho*I restriction enzymes, respectively. The multiple cloning sites (MCS) I and II of a pETDuet1 vector were also double digested with the restriction enzymes as used as in digestion of the PCR product of Me*ISA1* and Me*ISA2*, respectively. Generally, the excised PCR products and linearised vectors were cleaned up after gel electrophoresis using genepHlow™ Gel/PCR kit (Geneaid) prior to ligating. Firstly, the pETDuet1MeISA1 was constructed by ligating the Me*ISA1* PCR product with the vector by mixing the follows; 100 ng of purified *Sac*I-*Not*I-digested pETDuet1, purified *Sac*I-*Not*I-digested Me*ISA1* PCR product (molar ratio over vector of 5:1), 10X T4 DNA Ligase buffer 2 µl, T4 DNA Ligase 1 Wiess unit (5 Weiss unit/µl) and nuclease-free water to the final volume of 20 µl. The ligation reaction was incubated at 22 ºC for 10 min. Then, the ligation mixture was cleaned up by adding of equal volume of chloroform, mixing by vortex and then centrifuged at 13,000 x g at room temperature for 5 min. The upper phase was transferred to new nuclease-free microcentrifuge tube and kept at -20 ºC which 5 µl of the ligation was transformed into *E. coli* TOP10 competent cells by electroporation. The colonies grown on the ampicillin-containing plate were analysed by colony PCR technique and positive clones were subjected to nucleotide sequencing.

Secondly, the pETDuet1MeISA1-2 was constructed after nucleotide sequence of pETDuet1MeISA1 was analysed. The ligation reaction, transformation, and nucleotide sequencing were carried out as described above which *Eco*RV-*Xho*I-

digested pETDuet1MeISA1 and Me*ISA2* PCR product were used instead of *Sac*I-*Not*I-digested pETDuet1 and Me*ISA1* PCR product.

For Me*ISA3,* PCR product was cloned into pJET1.2/blunt vector by mixing 10X reaction buffer 2 µl with pJET1.2/blunt Cloning Vector (50 ng/µl) 1 µl, purified PCR product 8 µl (5:1 molar ratio), T4 DNA Ligase 1 µl and nuclease-free water to the final volume of 20 µl. The ligation reaction was done by incubating at 22 ºC for 10 min. After that, the ligation reaction was cleaned by adding equal volume of chloroform, vortexing briefly and centrifuged at 13,000 x g at room temperature for 5 min. The upper phase was transferred to new nuclease-free microcentrifuge tube and kept at -20 ºC which 5 µl of the ligation was transformed into *E. coli* TOP10 competent cells by electroporation. The colonies grown on the plate containing ampicillin were analysed by colony PCR technique and positive clones were subjected to nucleotide sequencing. Afterwards, to construct the pET21bMeISA3, the PCR was performed by using new designed gene specific forward primer to obtain mature Me*ISA3*. The PCR product and pET21b vector were excised with *Nde*I and *Sal*I restriction enzymes and purified. The ligation to the nucleotide sequencing was carried out by following the procedures of Me*ISA1* and Me*ISA2* as described above. Finally, recombinant plasmids of the positive clones of each Me*ISA* gene were transformed into *E. coli* SoluBL21 (DE3) for expression.

2.9 Expression of recombinant Me*ISA* genes (rMe*ISA* genes) and production of recombinant isoamylases (rMeISAs) in *E. coli* SoluBL21 (DE3)

2.9.1 Co-expression of rMe*ISA1* and rMe*ISA2*

The cells harbouring pETDuet1MeISA1-2 were grown in LB broth containing ampicillin at 37 ºC with shaking 250 rpm for overnight as a starter culture. The overnight culture was transferred into new ampicillin-containing LB broth (1:50) and grown at 37 °C with shaking 250 rpm until OD_{600} reached 0.4 to 0.5. Then, cells were continuously grown under induction of various concentrations of Isopropyl β-D-1-thiogalactopyranoside (IPTG) at 20 °C with shaking 200 rpm for various time points. The cells were harvested by centrifuging at 3,000 x g at 4 °C for 15 min, suspended in binding buffer (25 mM potassium phosphate buffer, 0.1 M NaCl and 40 mM imidazole, pH 7.2) and then lysed by ultrasonication. The lysate was fractionated by centrifuging at 10,000 x g at 4 °C for 30 min. The crude extract was primarily analysed by Western 2blot and modified DNS assay. The induction time of 4 – 5 h was selected for further protein purification and characterisation. Nevertheless, the cultures of the 1st and 20th hr after induction were also used for purification of each single rMeISA2 and rMeISA1, respectively. Importantly, the purified proteins from these three indicated time points were compared in terms of the activity of single or combination of enzymes as well.

2.9.2 Expression of rMe*ISA3*

The cells harbouring pET21bMeISA3 were grown in ampicillin-containing LB broth at 37 ºC with shaking 250 rpm for overnight as a starter culture. The overnight culture was transferred into new ampicillin-containing LB broth (1:50) and grown at 37 °C with shaking at 250 rpm until OD_{600} reached 0.4 to 0.5. Then, cells were continuously grown under induction of various concentrations of IPTG at 16 °C with

shaking 250 rpm for various indicated time points. The cells were harvested by centrifuging at 3,000 x g at 4 °C for 15 min, suspended in binding buffer and lysed by ultrasonication. The insoluble fraction was removed by centrifuging at 10,000 x g at 4 °C for 30 min. The intracellular extract was primarily analysed by Western blot and modified DNS assay and kept at 4 ºC for purification and characterisation.

2.10 Purification of rMeISAs

2.10.1 Purification of rMeISA1 and rMeISA2 using Nickel affinity column (Histrap™ column)

The intracellular proteins of the culture at induction time 4 – 5 h was applied to Histrap™ column equilibrated with binding buffer. The rMeISA1 and rMeISA2 were eluted by elution buffer (25 mM potassium phosphate buffer and 0.1 M NaCl, pH 7.2), using an imidazole gradient (100 to 200 mM imidazole). The pooled activity fractions (rMeISA1/rMeISA2) was dialysed against 50 mM potassium phosphate buffer pH 7.2. The relative amount of the purified rMeISA1 and rMeISA2 was detected by Bradford (1976) method by measuring the absorbance at 595 nanometres (A_{595}). Twenty five microliters of protein sample was mixed with 250 µl of Bradford working solution containing Coomassie blue G-250 in 96-well microplate. Bovine Serum Albumin was used as a protein standard. The purity of rMeISA1 and rMeISA2 was analysed by Silver-staining of SDS-PAGE (described in Section 2.7.2). In addition, the presence of these two rMeISAs was analysed by Western blot and the debranching activity was tested by modified DNS method.

Moreover, the intracellular fractions of the cultures of 1 and 20 h after induction, represented for the rMeISA2 and rMeISA1 respectively, were also purified singly. The

crude proteins were applied to Histrap™ column equilibrated with binding buffer. The rMeISA1 and rMeISA2 were eluted by elution buffer (25 mM potassium phosphate buffer and 0.1 M NaCl, pH 7.2), using an imidazole gradient (100 to 150 mM imidazole). The purified fraction of each isoform was dialysed against 50 mM potassium phosphate buffer pH 7.2. The purified recombinant enzymes were analysed on SDS-PAGE by silver-staining. The activity was tested by modified DNS assay.

2.10.2 Purification of rMeISA1/rMeISA2 complex using gel filtration column

To analyse the complexity of these two isoamylases, the crude extract of 4 – 5 h of induction period was purified by gel filtration column. The crude protein was concentrated by using Aquacide II absorption prior to loading onto the column. The Sephacryl S-300 HR was packed in a glass column (1.25 cm. x 120 cm.) and equilibrated with gel filtration buffer (25 mM potassium phosphate buffer and 50 mM NaCl, pH 7.2) with the flow rate of 0.23 ml/min. Fraction sizes of one millilitre were collected. Proteins were detected at A_{280} and by Western blot and the activity was measured by modified DNS assay.

2.10.3 Purification of rMeISA3 using Histrap™ column

The crude extract of overnight culture was subjected to Histrap™ column equilibrated with binding buffer. The rMeISA3 was eluted by elution buffer (25 mM potassium phosphate buffer and 0.1 M NaCl, pH 7.2), using an imidazole gradient (100 to 200 mM imidazole). The pooled fractions was dialysed against 50 mM potassium phosphate buffer pH 7.2. The relative amount of purified rMeISA3 was detected by Bradford method and it was analysed by Coomassie-staining of SDS-PAGE and Western blot. The debranching activity was measured by modified DNS method.

2.11 Characterisation of rMeISAs

The substrate specificity and the effect of pH, temperature and divalent ions and chemicals were studied. The characterisation was done by the measuring of relative debranching activity of the purified enzymes determined by modified DNS method as described in Section 2.7.5

2.11.1 The purified rMeISA1 and rMeISA2 by Histrap™ column

Enzymatic assay for debranching activity of rMeISA1 and rMeISA2

The enzymatic reaction containing 0.75% (w/v) maize amylopectin and 50 mM phosphate buffer pH 7.2 was incubated with 53 mU of purified enzymes at 37 °C for 3 h in the reaction volume of 200 µl. The activity of enzymes was measured by modified DNA assay. One unit of ISA activity was defined as the amount of the enzymes that releases 1 µmole of reducing sugar per minute at pH 7.2 and 37 °C using maize amylopectin as substrate.

2.11.1.1 Optimum pH

The purified enzymes were incubated with 0.75% (w/v) maize amylopectin at 37 °C in 50 mM buffer at various pH values [sodium citrate buffer (pH 4.0, 5.0, 6.0), potassium phosphate buffer (pH 6.0, 7.0, 8.0) and glycine-NaOH (pH 8.0, 9.0)] at 37 °C for 3 h.

2.11.1.2 Optimum temperature

The purified enzymes were incubated with 0.75% (w/v) maize amylopectin in 50 mM phosphate buffer pH 7.2 in the range of temperature (25 - 60 °C) for 3 h.

2.11.1.3 Effect of metal ions and some chemicals

The reaction was carried out by incubating of the purified enzymes in 50 mM phosphate buffer pH 7.0 at 37 °C for 3 h containing metal ions/chemicals (with final concentration of 1 mM of Ca^{2+}, Co^{2+}, Cu^{2+}, Fe^{3+}, Mg^{2+}, Mn^{2+}, Zn^{2+}, EDTA, and 0.04% (w/v) SDS).

2.11.1.4 Substrate specificity

The purified enzymes were incubated with various substrates as follows; potato starch, potato amylopectin, maize amylopectin, glycogen, beta-limit dextrin, and pullulan. The enzymatic reaction containing 50 mM potassium phosphate buffer pH 7.0 and 0.75% (w/v) substrate was incubated with 2 mU of purified enzymes at 37 °C for 3 h.

2.11.1.5 Activity of each single purified rMeISA1 and rMeISA2 and their mixtures *in vitro*

The activities of purified rMeISA1 and rMeISA2 from 20th h and 1st induction times were tested. Each isoform was individually incubated with 0.75% (w/v) maize amylopectin in 50 mM potassium phosphate buffer pH 7.2 at 37 ºC for 3 h. Moreover, these two isoforms were also mixed *in vitro* with the molar ratio of rMeISA1: rMeISA2 of 1:3 to 3:1 and incubated with the similar enzymatic condition to that of activity testing of each enzyme. The activities were measured by modified DNA assay.

2.11.2 The purified rMeISA3 by Histrap^{TM} column

Enzymatic assay for debranching activity of rMeISA3

The enzymatic reaction containing 0.75% (w/v) beta-limit dextrin and 50 mM sodium acetate buffer pH 6.0 was incubated with 10 U of purified enzyme at 37 °C for

15 min in the reaction volume of 200 µl. The activity of enzymes was measured by modified DNA assay. One unit of ISA activity was defined as the amount of the enzymes that releases 1 µmole of reducing sugar per minute at pH 6.0 and 37 °C using beta-limit dextrin as substrate.

2.11.2.1 Optimum pH

The enzymatic reaction was performed by incubating the purified enzyme with 0.75% (w/v) beta-limit dextrin at 37 °C in 50 mM buffer at various pH values [sodium citrate buffer (pH 4.0, 5.0, 6.0), potassium phosphate buffer (pH 6.0, 7.0, 8.0) and glycine-NaOH (pH 8.0, 9.0)] at 37 °C for 15 min.

2.11.2.2 Optimum temperature

The purified enzyme was incubated with 0.75% (w/v) beta-limit dextrin in 50 mM sodium acetate buffer pH 6.0 in the range of temperature (25 – 60 °C) for 15 min.

2.11.2.3 Effect of metal ions and some chemicals

The reaction was carried out by incubating of the purified enzymes in 50 mM sodium acetate buffer pH 6.0 at 37 °C for 15 min containing divalent ions/chemicals (with final concentration of 1 mM of Ca^{2+}, Co^{2+}, Cu^{2+}, Fe^{3+}, Mg^{2+}, Mn^{2+}, Zn^{2+}, EDTA, and 0.04% (w/v) SDS).

2.11.2.4 Substrate specificity

The purified enzyme was incubated with various substrates as follows; potato starch, potato amylopectin, maize amylopectin, glycogen, beta-limit dextrin, and pullulan. The enzymatic reaction containing 50 mM sodium acetate buffer pH 6.0 and 0.75% (w/v) substrate was incubated with 10 U of purified enzyme at 37 °C for 15 min.

2.11.2.5 Debranching activity of purified rMeISA3 on Native-PAGE

The activity of purified rMeISA3 on Native-PAGE was carried out as described in Section 2.7.3 by using beta-limit dextrin as substrate.

2.11.3 Determination of molecular weight of enzyme complexes of rMeISA1 and rMeISA2 by gel filtration chromatography

The sizes of multimeric complexes of rMeISA1 and rMeISA2 were analysed by using gel filtration chromatography. The molecular weights of protein complexes were determined by comparing of the partition coefficient (K_{av}) from calibration curve and the molecular weights of gel filtration standards; thyroglobulin (bovine) 670 kDa, γ-globulin (bovine) 158 kDa, ovalbumin (chicken) 44 kDa, myoglobin (horse) 17 kDa. Blue dextran and potassium chromate were used for determination of the void volume (V_0) and total bed volume (V_t), respectively. K_{av} values of protein standards were calculated from the following formula;

$$K_{av} = \frac{V_e - V_0}{V_t - V_0}$$

V_e equals the volume for elution of a component (elution volume).

2.11.4 Determination of ratio of rMeISA1 and rMeISA2 in hetero-multimeric complexes

After separation by gel filtration, the partially purified proteins were further analysed by SDS-PAGE and Western blot. Protein amounts were detected by Bradford method and the activity was measured by modified DNS assay. The rMeISA1: rMeISA2 ratio in the complexes was calculated from the molecular weights of the protein detected from the fractions with debranching activity (peak-to-peak) of the chromatogram and from using Quantity One-4.6.6 program by calculating the intensity of protein bands present on Western blot membrane

2.11.5 Chain Length Distribution (CLD) analysis of debranched amylopectin

2.11.5.1 Debranching activity of rMeISA1/rMeISA2

After Histrap^{TM} purification and dialysis, the debranching reaction was carried out by mixing of 0.75% (w/v) maize amylopectin and 50 mM phosphate buffer pH 7.2 and incubated with 4 mU of purified rMeISA1/rMeISA2 from the pooled activity fractions at 37 °C for 1 h. After that, the reaction was directly passed through the 0.22 μM nylon syringe filter prior to submission to High-Performance Anion-Exchange Chomatography-Pulsed Amperometric Detection (HPAEC-PAD). The CL analysis was performed on Dionex equipped with a CarboPac PA100 (4 mm. i.d. x 250 mm. length). The elution was performed with a linear gradient of sodium acetate (0 to 400 mM) in 150 mM NaOH. The CLD pattern of the purified rMeISA1/rMeISA2 was compared to that of 4 mU of commercial *Pseudomonas amyloderamosa* isoamylase (PaISA), which incubated with the same substrate under the same reaction condition.

2.11.5.2 Debranching activity of rMeISA3

After Histrap™ purification and dialysis, the debranching reaction was carried out by mixing of 0.75% (w/v) maize amylopectin and 50 mM acetate buffer pH 6.0 and incubated with 10 mU of purified rMeISA3 at 37 °C for 21 hr. After that, the reaction was passed through the 0.22 μM nylon syringe filter prior to submission to HPAEC-PAD. The CL analysis was performed on Dionex equipped with a CarboPac PA100 (4 mm. i.d. x 250 mm. length) and the elution was performed with the same condition of rMeISA1/rMeISA2 as described above. The CLD pattern of the purified rMeISA3 was compared to that of 10 mU of commercial PaISA, which incubated with the same substrate under the same reaction condition.

2.11.6 Prediction of N- and O-glycosylation in MeISAs

The deduced amino acid sequences of each isoform translated from the full length genes (Section 2.8.5) were submitted to NetNGlyc 1.0 and NetOGlyc 4.0 servers for the prediction the possible positions of N- and O-glycosylation, respectively.

CHAPTER III

RESULTS

3.1 Cloning of cassava isoamylase genes (Me*ISA* genes)

3.1.1 Total RNA extraction from cassava tuber and cDNA construction

Total RNA of 9 months old cassava tuber was isolated as described in section 2.8.1. The integrity of RNA was observed on 0.8% (w/v) agarose gel electrophoresis. The 18S rRNA (small subunit) and 25S rRNA (large subunit) were present as two major bands. Messenger RNA (mRNA) was present as a smear whereas tRNA was present as faint band at the bottom of the gel (Fig 12). Furthermore, the value of A_{260}/A_{280} measured by UV-Vis spectrophotometer was greater than 2.0 which mean that RNA was obtained with high purity. So, these results showed that the RNA was suitable for using as template for cDNA construction.

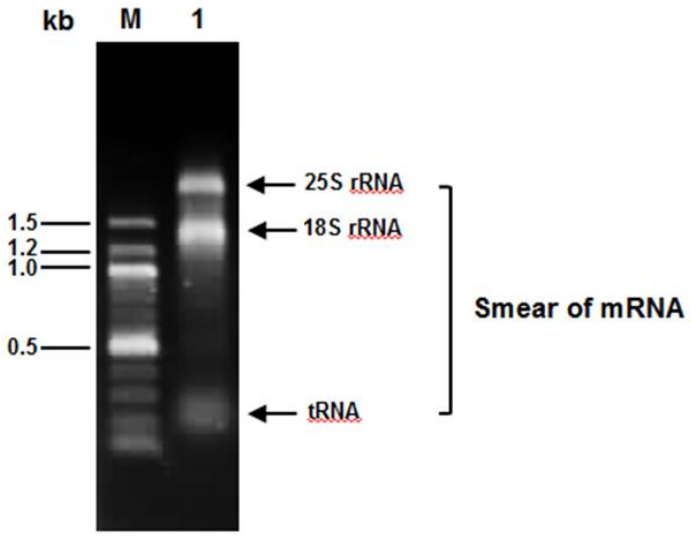

Figure 12 Total RNA from cassava tubers analysed on 0.8% (w/v) agarose gel electrophoresis

Lane M: Gene Ruler 1 kb DNA Ladder

Lane 1: Total RNA

3.1.2 Me*ISA* genes amplification and recombinant plasmid construction

Full length of Me*ISA1* and Me*ISA2* were amplified by using PCR as described in section 2.8.5. The PCR products of about 2.4 kb and 2.6 kb of putative Me*ISA1* and Me*ISA2*, respectively, were obtained. In addition, full length gene of around 2.3 kb of Me*ISA3* was obtained after the 5' RACE. However, 159 bp of Me*ISA1*, 48 bp of Me*ISA2* and 267 bp of Me*ISA3*, which encoded their signal peptides at 5' ends, were ignored for the following step of mature gene amplification (shown by underline in Fig. 13, 14 and 15, respectively).

ATGGACTTAATTCAATCTTCTGCTTCTCGCTTCCTCTCTCTTCCCTTTCACATTCCTCCTCGAAACAA
GGATGCCGCTGAATTTCTCATTTTCCGCCAAAGGAAATGCTTCTCCCATTCTCAATCATTATCAACTG
TTAGGACTTCTCCGTTGATTGAAGCCACCAGAAGAGATGGAGGATCAGAGTTGGAGACTGCGGTGGTT
GTCGACAAGCCTAGATTGGGAAAATATCAGGTGTCTGAGGGCCATCCGGCGCCGTTTGGGGCTACTGT
TAGGGATGGTGGAGTTAATTTCTCTGTCTATTCTGCCAATGCCGTTTCTGCTTCTCTCTGTTTGATTT
CTCTCGATGATTTAGCTGAGAATAGAGTGACTGAGGAGATCCCCCTAGATCCTCTCGCTAATAAGACT
GGATATATTTGGCATGTATTTCTTAAAGGAGAGTTTAGAGATGTATTATATGGCTACAGATTTGATGG
AAAATTTTCTCGTGGGGAAGGACATTACTTTGATTCTTCTAAGATAGTGTTGGATCCTTATGCAAAAG
CAGTTATAAGCAGAGGGGAATTTGGTGTTCTAGGACCTGATGATAATTGCTGGCCCCAAATGGCTGGT
ATGATACCGGCTGCTCAAGATAAGTTTGACTGGCAAGGAGATCTACCATTGAGATATTCTCAGAAAGA
TCTAGTGATATATGAGATGCATGTTCGAGGTTTTACACGGCATGAATCAAGCAGAACTGAATTCCCTG
GGACATATCTTGGTATTGTGGAAAAGCTTGATCACTTGAAGGAACTTGGTGTCAATTGCATAGAGTTA
ATGCCATGCCATGAGTTCAATGAGCTTGAGTACTTCAGTTACAATTCTGTCTTGGGCGACCACAGGAT
GAACTTTTGGGGATATTCTACTGTCAATTACTTTTCACCTATGACAAGATATTCTTCTGCTGGGACAC
GTAACTGTGGCCGTGATGCAATTAATGAGTTCAAGTTTCTTGTTAGAGAAGCTCATAAACGAGGAATT
GAGGTGATCATGGATGTTGTTTTCAATCACACAGCTGAAGGAAATGAGAAAGGCCCCATCTTATCTTT
TAGAGGAATAGATAACAGTGTCTATTATATGCTTGCTCCCAAGGGAGAGTTCTATAACTATTCGGGTT
GTGGGAACACATTCAATTGCAACCATCCTGTTGTGCGCCAACTTATATTAGACTGTTTAAGATATTGG
GTAATAGAAATGCATGTGGATGGCTTCCGCTTTGATCTTGCTTCTATTATGACCAGGGGTAGCAGTCT
ATGGGATCCAGTTAATGTATTTGGGAAACCAATAGAAGGTGATTTGTTAACGACTGGTTCTCCTCTTG
GGAGCCCTCCATTGATTGACATGATAAGTAATGATCCAATACTTCGTGAAGTAAAGCTCATTGCTGAA
GCATGGGATGCGGGAGGCTTGTATCAAGTGGGTACATTTCCTCATTGGCAAATATGGTCGGAGTGGAA
TGGGAAGTTTCGTGACATTGTGAGGCAGTTCATCAAGGGTACAGATGGCTTTGCTGGGGCTTTCGCTG
AATGCCTGTGTGGTAGCCCTAATCTATACCAGGAAGGAGGAAGGAAACCATGGAACAGCATCAACTTT
GTATGTGCTCATGATGGTTTTACTTTGGCTGATTTGGTGACCTATAATAACAAAAATAACTTGGCAAA
TGGGGAAGACAACAATGATGGAGAGAATCATAACAATAGCTGGAACTGTGGACAGGAAGGAGAGTTTG
CAAGCATCTTAGTGAAGAAGTTAAGGAAACGGCAAATGCGAAATTTCTTTGTTTGTCTTATGGTTTCA
CAAGGTATTCCAATGATATATATGGGGGATGAATATGGTCACACAAAAGGGGGCAATAACAATACATA
TTGCCATGACAACTATATCAATTACTTTCGATGGGATAAGAAGGAAGAGTCATCATCAGACTTCTATA
GATTTTGCTGCCAGATGACCAAGTTCCGCCATGAGTGCAAGTCCCTTGGTTTGAATGATTTCCCAACA
GCAGAGAGGTTACAGTGGCATGGTCATTACCCTTGTGTGCCAGATTGGTCTGAGACAAGCCGATTTGT
TGCCTTTACACAGATTGACTCAGCAAAGGGAGAGATATATGTTGCGTTCAATGCTAATCATTTGCCTG
TTACCGTCACACTGCCTGAACGGCCGGGATACAGATGGGAGCCTCTGGTAGACACTGGGAAGCCGGCA
CCATATGATTTCCTTTACAGCGACGTCCCTGAAAGAGATGCCGCTGTTAAACAGTATGGTCACTTCCT
GGATGCAAATTTTTACCCCATGCATAGTTACTCTTCTATCATCTTAATCCTTTCTCCTGATGAAATTG
CTTAG

Figure 13 Full length Me*ISA1* gene. The gene consisted of 2,385 bp with the ATG start and TAG stop codons highlighted. The 159 nucleotides at 5' terminus which encoded signal peptide predicted by ChloroP1.1 were underlined.

ATGGCAACACTTCTTCCTTCCTTTGCAATAAGTCGTTGCTGCTATAGCTGTGGAGCTGTGGAGTCATCAAAATTG
ACACTCACCACGCGTTACACATCTGGCAAAAAAATGGAGCTAGGGTTTGGGAGAACGGATGTAGAAAAAAGGCTC
TTGGTTGGTGAAGTTGCACAAAATGTCAGAAGTACTCTGCATTGGAATCATAATTCAGGAGTATTTGCTGCTGCA
AGGGTCCCAGTTCAGGAAACTGAACAAATATTATCTACAATCACTGAAGTTGATGAACTTCAAAAGGTATCAAGT
TATCTGTTTAGGACACAAATTGGTGGTAATGTTAAAGTTTCTGTTAGAAAGAAAAATGCCAAATATGCAGTTTAC
ATTGAGGTTTCATCCCTGGAACTGGGTAATAGTGACTACCGACTGGTGCTTGCTTGGGGAATATATCGATCTGAT
TCATCATGTTTCATGCCTCTAGATTCTCAACGTTTAGACCCAGTTGCCAGGACCATGGAAACTCCATTTGTACAA
AATGCTTTTGCTATATTTTCACTTGAATTGGAGTTTGAAGCAAAACAAACTCCCTTCTCTCTCTCATTTCTACTG
AAATCTATGTTTAATACCGATTCAAGTGGCTCAGAGATCAGGAACCATAAGAAGGCTAATTTTTCTGTGCCAATT
GGTTTTAGTTCGGGTTATCCAGATCCACTGGGCCTTTCCTTTTCAACTGATGGCTCCATGAATTTTGCATTTTTT
TCAAGAAATGCAGAAGGTGTGGTTCTGTGCTTGTATGATGACTCTACAACAGACAAACCTGCTTTAGAGCTTGAT
CTCGATCCATATGTTAATCGATCAGGCGATGTCTGGCACGCCTCACTGGAAGGGGCGTGCACATTTTCAAGCTAT
GGTTACCGGTGCATGGGAGGTATTCTTCAGGGAGAAACAGGTAAAGATTATGTAGAGCGTGTTCTTTTGGATCCC
TATGCTAGAATCATTGTTAATTTCACAGCAGATCATGGATCTCATTCGTCACTGAAGTATCTTGGACGATTATGC
AAGGAGCCTGCTTTTGAGTGGAGTGATGAAGTTTATCCAAATTTGGACATGGAGAAACTAGTTGTCTATCGATTG
AATGTGAAGCGTTTCACTGAGCACAAGTCTAGTCAGCTCTATAGTGATATAGCGGGCACCTTTGCTGGTTTGACT
GAGAAGTTGAACCATATAAAAAATCTTGGTGTAAATGCAGTCTTATTAGAGCCAATATTTCCATTTGATGAAGAA
AAAGGGCCGTTTTTTCCACGGCACTTCTTTTCACCATCAAATATATATGGGCCTTCTGGTGGCTCTATTTCTGCT
ATTACCTCAATGAAGGAGATGGTGAAGCAATTTCATGCCAATGGGATTGAGGTTTTACTTGAAGTTGTTTTCACC
CATACTGCTGAAGGCGGATCACTGCAAGGAATTGATGACTTCTCTTATTATTATGCAAATAGAGCTGTAGAGTTG
GAATCTAGAAATGCTTTGAATTGTAATTATCCTATTGTTCAAAGGATGATTCTAGATAGTCTTCGGCACTGGGTG
ACCGAGTATCACATTGATGGTTTCTGTTTTATAAATGCTTCATTTCTGCAGAGAGGCTTTCATGGTGAAATTCTA
TCTCGCCCTCCCTTGGTTGAAGCAATTGCCTTTGATCCACTGCTCTCAAAGACCAAGATCATTGCTGACTGCTGG
GATCCAGAAGACGTGATACCAAAGGACACCTGCTTCCCTCATTGGAAAAGATGGGCAGAGATGAATGCAAAATTT
TGTTTTGATGTCAGAAATTTTTTGAGAGGTGAAAGTCTTCTTAGTGACCTTGCAACACGGCTTTGTGGGAGTGGA
GACATCTTTTCAAGTGGACGAGGGCCAGCTTTTTCTTTCAATTATGTTGCCAGGAACTCCGGACTTCCTCTAGTG
GACTTAGTCAGCTTCAGTAGCAGTGAGCTAGCCTCAGAATTAAGCTGGAATTGTGGAGAAGAAGGAGCAACAAAC
AAAACCCCTGTCCTTGAAAGGAGACTTAAACAAATTCGTAACTATCTCTTCATTCTTTATGTTTCTTTGGGTGTA
CCTGTTCTCAATATGGGAGATGAGTGTGGCCAATCTTCAAATGGTTCCACTTCATATGGTGATAGAAAACCTTTT
GATTGGAATGCTTTGTCAATGGGTTTTGGTATTCAAATGACACGGTTCATCTCATTCATGAGTTCATTAAGAAGG
AGGCGAAGTGATGTCCTCCAAAAGAGGAACTTCATGAAGGAAGAAAATATTGATTGGCATGGAAGTGGTCAGTCT
CCACCAAGATGGGAAGATCGATCCTGCAAATTCCTGGCCATGACATTGAAGACCGAGAAAACAGAGAACAAGTTG
AGCCCTGAATCTTCCAACATAAAGGGTGACCTATTCATGGCTTTCAATGCATATCCCCATTCAGAGAGCGTTATT
CTACCACCAGTTCCTGAAGGAATGACATGGCATCGGCTGGTTGACACCTCTCTTCCATTTCCAGGGTTCTTTTCC
GAAGATGGTGAACCAGTTTTTGAACAGATGGCAGGGTTAATTGCTTACGAAATGAAATCTCACAGCTGCACTCTG
TTTGAAGCCACTAGCCTTGGTGGTTAG

Figure 14 Full length Me*ISA2* gene. The gene consisted of 2,652 bp with the ATG start and TAG stop codons highlighted. The 48 nucleotides at 5' terminus which encoded signal peptide predicted by ChloroP1.1 were underlined.

ATGCTTCGGCCATTACTTCCCTGTGATTCCACTTCCGCTGCTAAAATGCGTCTCTTTGCTTCACCATT
TTCTAATAACTACACCATCGCTATTGTCCCTTCTTCTGCTGGACATTCTCATGTTCTGGACATGGGAT
TGAAGTTGAGTAAACAAGCTTCGAGTAGCAGTGGGCTTCGAATTTTTAGTCAGGGTCGTGATAAGCAC
AGAACGCCCAGTGTTTATGGTCGTGGTGCTCGAGAACGGGTGCTTGAGGAGAAGGAAGCGTCTCTAAT
GTCGGAAACCAGCCCGTCTTTTAAAATTTTCCCTGGTCAGGCATCTCCGTTGGGCGTATCTGAAGTTG
ATAAGGGAATCAATTTTGCTATTTTTTCACAGCATGCCACTTCTGTCACCCTTTGCCTATCTCTTCCT
CAAAGGGGAGTACATGAAAGGCTAGTTGGTAACGTGATTGAGCTGGCCTTGGATCCTCATGTGAATAA
AACAGGAGACATTTGGCATATCTGTATAGAGGATTTGCCTCGTAGCAATGTGCTTTATGGTTATCGGG
TAGATGGTCCTCAAAATTGGAATCAGGGGCATCGGTTTGACAGTAATATCATACTTGTAGATCCTTAT
GCTAAGCTAGTTGAAGGTCGTCGATATTTTGGAGATGCTAGCCTTAAGTTGTCTAAATTTCTTGGAAC
TTATGATTTTGATAGCTCGCTTTTTGACTGGGGAGATAACTACAAGCTTCCAAATATACCAGAGAAAG
ATCTTGTTATCTATGAAATGAATGTTCGTGCATTTACGGCTGATAAATCTAGCGGCTTAGATCCAAAA
ATACGTGGGAGTTACCTTGGTGTAATTGAAAAGATCCCACACCTTCTGGAGCTGGGTGTCAATGCAGT
TGAGTTGCTGCCTGTGTTTGAATTTGATGAATTTGAGTTTCAGAGACGCCCAAACCCCAGAGATCACA
TGATAAATACATGGGGTTATTCAACAATAAACTTCTTTGCTCCTATGAGTCGCTATGCTAGTGGTGGT
GGAGGACCTTGTAATGCATCTCGAGAATTCAAAGAAATGGTTAAAGCCTTGCATGGTGCCGGCATTGA
GGTTATTTTAGATGTCGTCTATAATCATACAAATGAAGCAGATGACCAAAATCCTTATACCACTTCAT
TTCGTGGAATAGATAATAAGGTTTATTACATGTTAGACCCGAACAGTGGCCAGTTGCTGAACTTTTCT
GGATGCGGGAATACATTAAACTGTAATCATCCTGTGGTCATGGAGCTCATCCTTGACAGCCTAAGACA
CTGGGTCACTGAATACCATGTAGATGGATTTCGATTTGACTTGGCTAGTGTACTTTGTCGTGGAACAG
ATGGCACTCCACTTAGTGCTCCCCCAGTTATTAGGGCAATTGCCAAAGAACCTATCCTATCAAGATGT
AAAATTATTTCAGAACCTTGGGATTGCGGAGGCCTTTATTTGGTTGGAAAATTTCCTAACTGGGACAG
ATGGGCCGAGTGGAACGGGAAGTACCGTGATGACATGAGAAGATTTATTAAGGGTGATTCTGGTATGA
AAGGGAGTTTTGCAACCCGTGTTGCTGGATCTGCTGACCTGTACAGCGCGAATAAGCGCAAACCTTGT
CATAGCATTAATTTTGTAATAGCACACGATGGATTCACACTGTATGATCTCGTTTCTTACAATTTTAA
GCACAATGATGCCAATGGAGAAGGTGGAAATGATGGAAGCAATGACAATTTTAGTTGGAATTGTGGCT
TTGAAGGAGAAACTGATGATCCTTCTATTAAAGCTTTACGCTCCCGCCAAATGAAAAATTTCCATCTG
GCATTAATGATATCTCAGGGAACACCAATGATGCTAATGGGGGATGAATACGGGCATACTCGCTATGG
TAATAACAATAGTTATGGGCATGACACTTCTATTAACAATTTCCAGTGGGGATTTTTGGATAAACAAA
GGAGCAGTCACTTCAGGTTCTTCTCTGAGGTGATAAAGTTTCGACTAATGCACCAAGTATTTCGTCAT
GAAAATTTTCTCAGCAATAATGAAGTGACATGGCATGAAGACAACTGGGACAATTATGAAAGCAAATT
CCTTGCATTTACGCTTCATGACAGTATTGGAGCAGATATCTATTTGGCATTTAATGCTCATAACTACT
ATGTTAAAGTTTCGATACCCCCTCCACCATCAAAGAGGCGTTGGTTTCGTGTGGCGGACACCAATCTT
GCATCTCCAGACGACTTTGTTCCTGAAGGTGTCCCAGGCATTGAGAATTCCTATAATGTGGCTCCATA
CTCCTCGATTCTTCTTGAAGCGAAACTGACATGA

Figure 15 Full length Me*ISA3* gene. The gene consisted of 2,346 bp with the ATG start and TGA stop codons highlighted. The 267 nucleotides at 5' terminus which encoded signal peptide predicted by ChloroP1.1 were underlined.

Then, new gene specific forward and reverse primers were designed. The *Sac*I and *Not*I sites were introduced into the primers of Me*ISA1* while *Eco*RV and *Xho*I sites were incorporated to that of Me*ISA2*. The PCR was performed as described in section 2.8.5. The PCR products of about 2.2 kb of rMe*ISA1* and 2.6 kb of rMe*ISA2* were amplified and analysed on 0.8% (w/v) agarose gel electrophoresis (Fig. 16, lanes 1 and 2 respectively). After that, the purified PCR products of these 2 genes were excised with the same pair of restriction enzymes used in cutting of MCSI and MCSII, and subsequently ligated into a pETDuet1 expression vector. The pETDuet1MeISA1-2 (Fig. 17) was transformed into *E. coli* TOP10 and sequenced. The nucleotide sequences showed the open reading frame (ORF) of rMe*ISA1* and rMe*ISA2* of 2,292 bp and 2,649 bp encoded 763 and 882 amino acid residues, respectively. Eighteen nucleotides encoded 6x histidine residues were detected at 5' and 3' termini of rMe*ISA1* and rMe*ISA2*, respectively (as shown in boxes in Fig. 18 and 19). The pETDuet1MeISA1-2 was transformed into *E. coli* SoluBL21 (DE3) for expression.

After 5'RACE of Me*ISA3* was successful, the new gene specific forward primer harbouring *Nde*I site for mature Me*ISA3* amplification was designed. The PCR was carried out as described in section 2.8.6. The PCR products of about 2.1 kb of rMe*ISA3* was amplified and analysed on 0.8% (w/v) agarose gel electrophoresis (lane 3 in Fig. 16). The purified PCR product was digested with *Nde*I and *Sal*I restriction enzymes and ligated into pET21b expression vector. The recombinant pET21bMeISA3 was transformed into *E. coli* TOP10 and sequenced. After the nucleotide sequence was analysed, the pET21bMeISA3 was transformed into *E. coli* SoluBL21 (DE3) expressing host. The sequencing results showed that the ORF of rMe*ISA3* comprised

2,127 bp encoded 708 amino acid residues, which 18 of nucleotides encoded 6x histidine residues were present at 3’ terminus (Fig. 20).

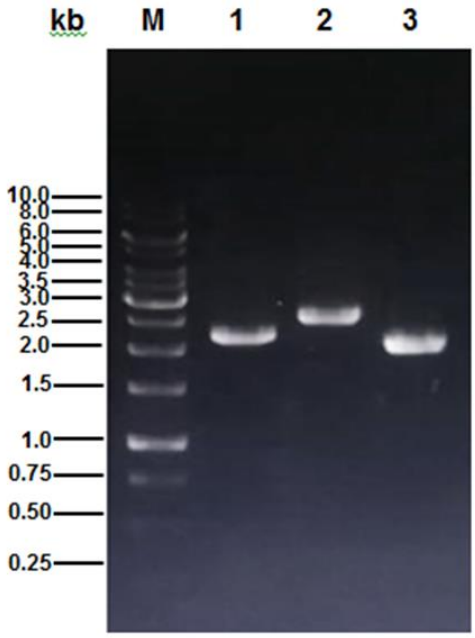

Figure 16 PCR products of 3 mature rMe*ISA* genes analysed on 0.8% (w/v) agarose gel electrophoresis

Lane M: GeneRuler 1 kb DNA Ladder

Lane 1: 2.2 kb of rMe*ISA1*

Lane 2: 2.6 kb of rMe*ISA2*

Lane 3: 2.1 kb of rMe*ISA3*

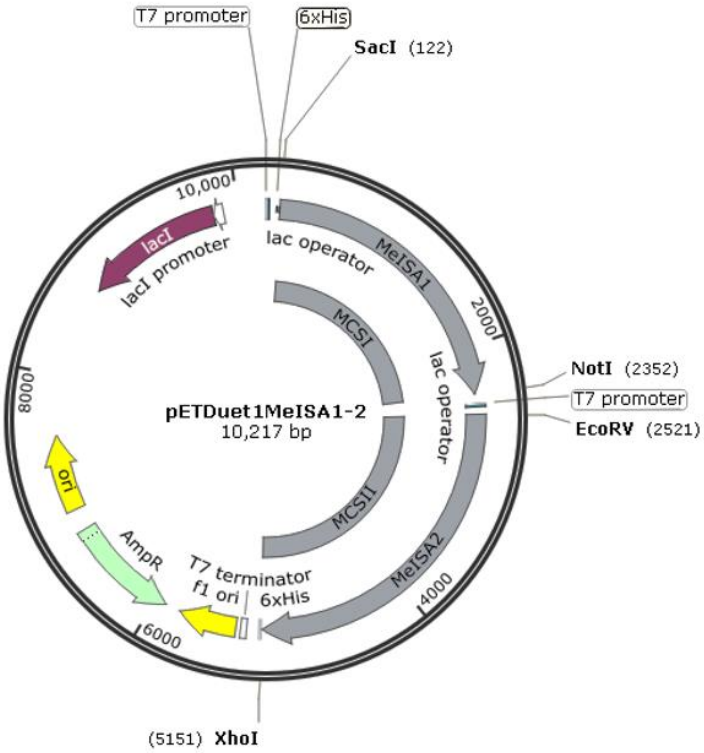

Figure 17 Illustration of pETDuet1MeISA1-2 by using SnapGene server. The MeISA1 and MeISA2 were ligated into MCS I and MCS II of a pETDuet1, respectively.

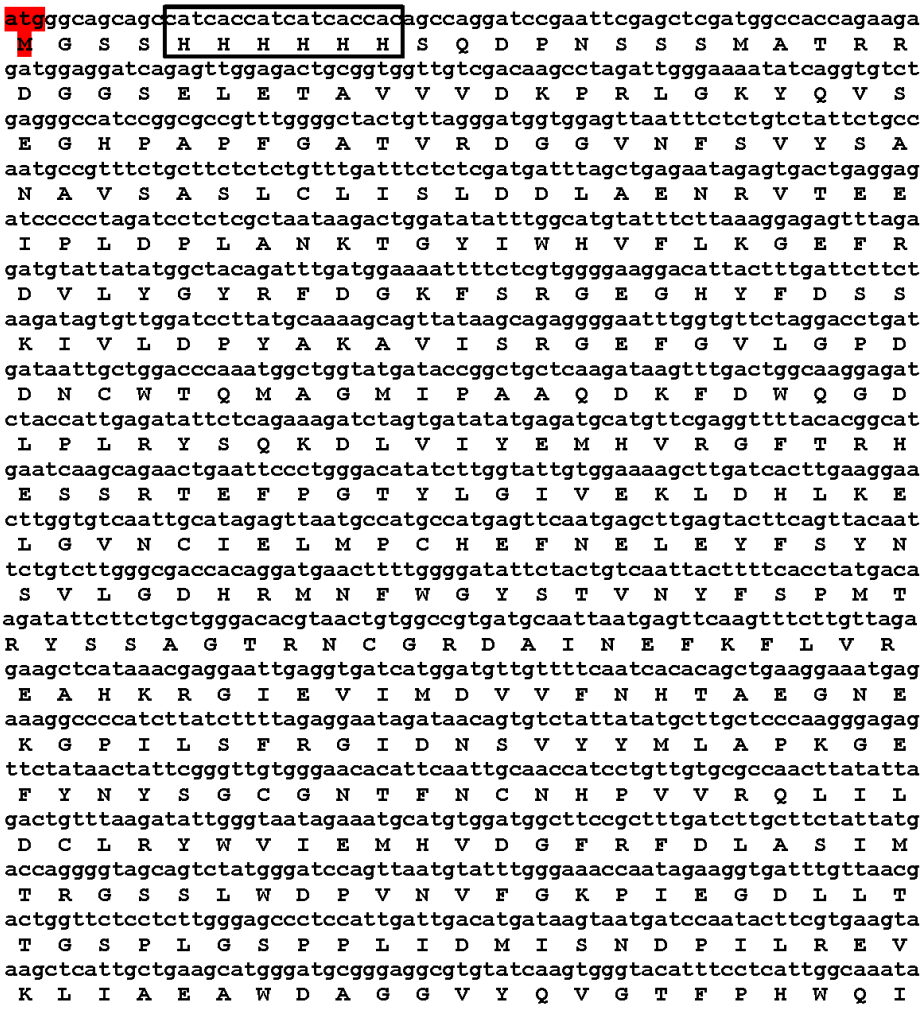

Figure 18 The ORF of rMe*ISA1* (2,292 bp) in pETDuet1MeISA1-2. The ATG start and TAA stop codons were highlighted. Deduced amino acids were shown below the corresponding nucleotide sequences. The 6x His residues at N-terminus were boxed.

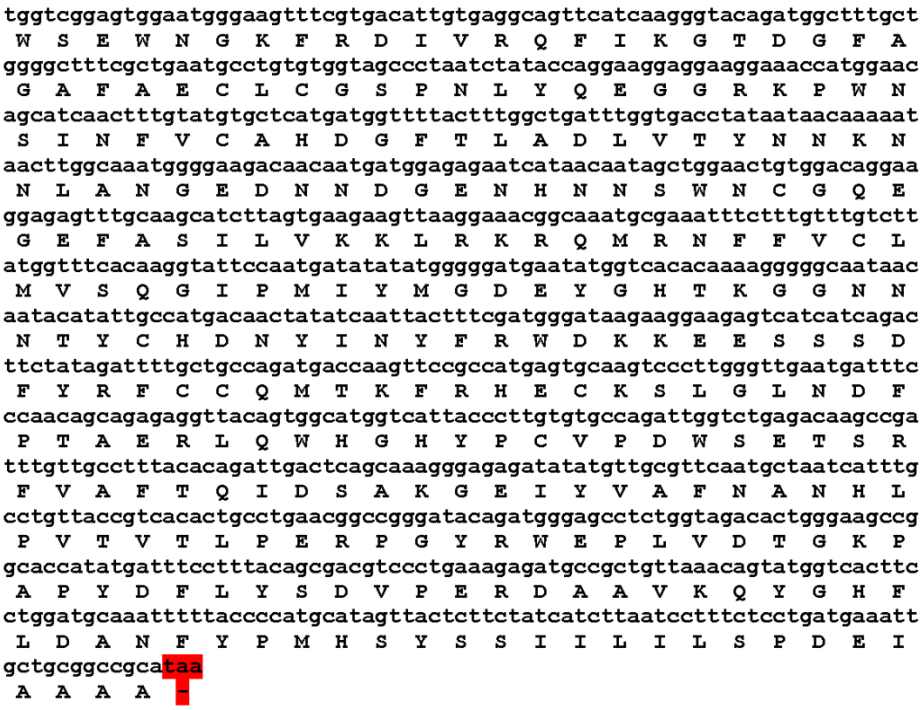

Figure 18 (continued)

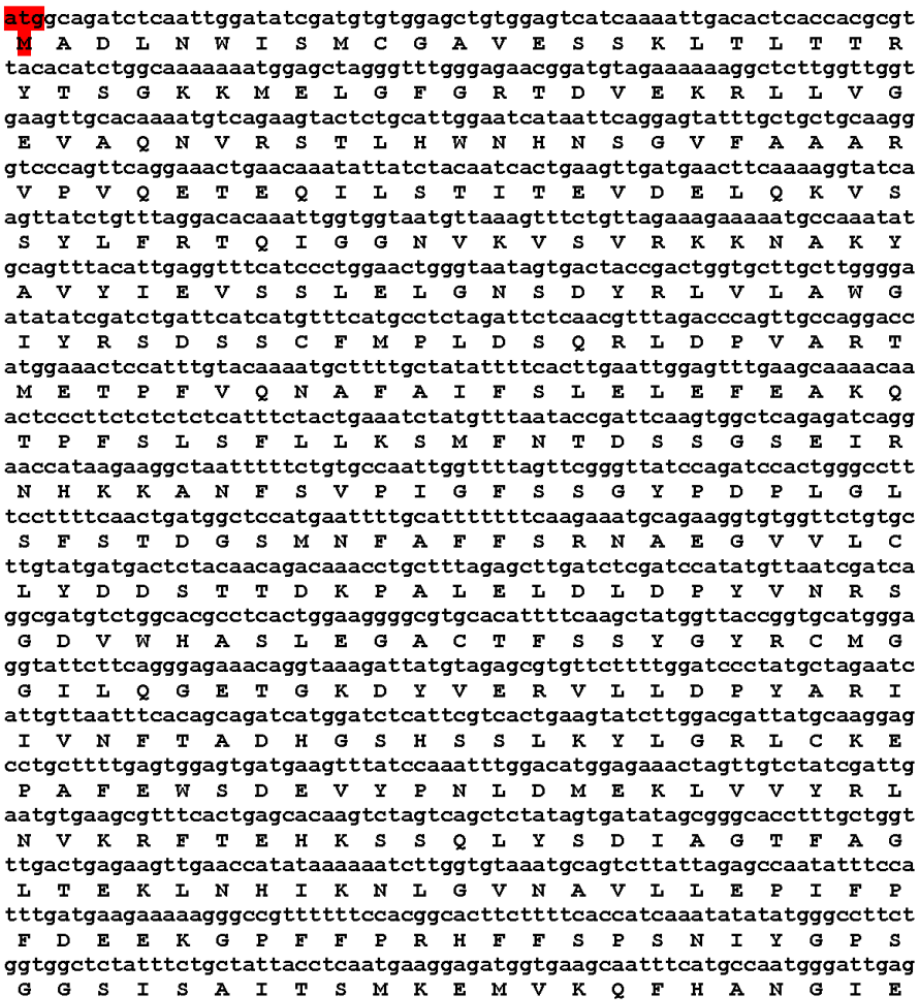

Figure 19 The ORF of rMe*ISA2* in pETDuet1MeISA1-2 consisted of 2,649 bp. The ATG start and TAA stop codons were highlighted. Deduced amino acids were shown below the corresponding nucleotide sequences. The 6x His residues at C-terminus were boxed.

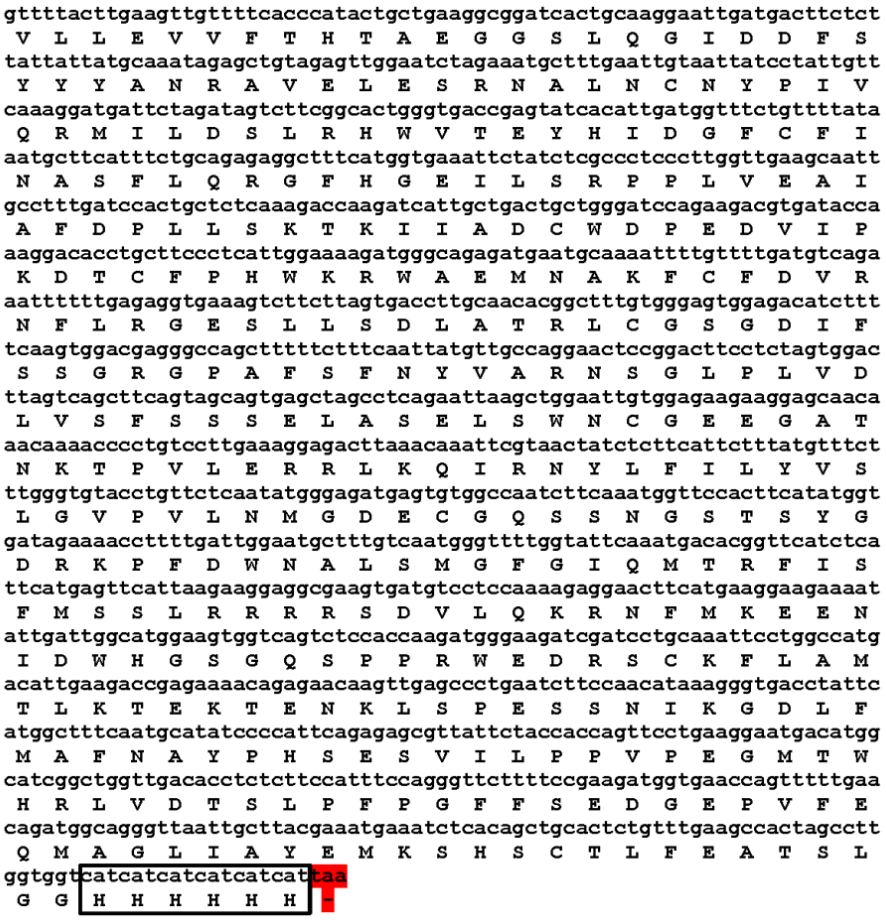

Figure 19 (continued)

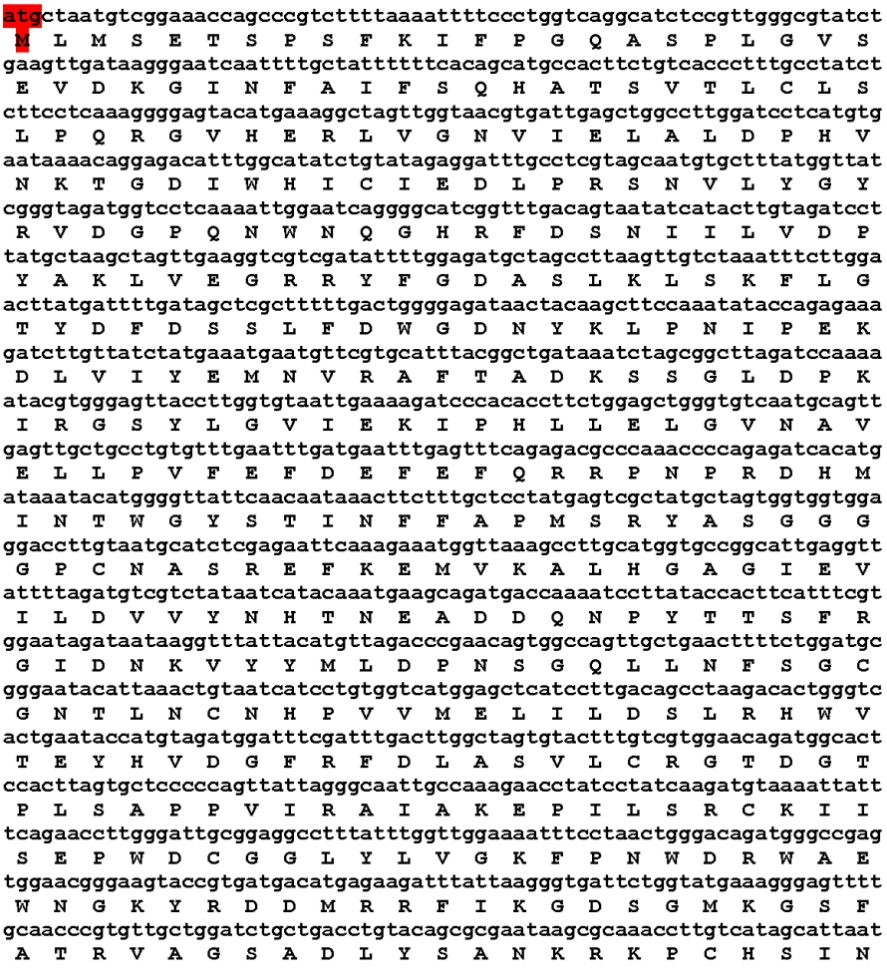

Figure 20 The ORF of rMe*ISA3* in pET21bMeISA3 consists of 2,127 bp. The ATG start and TGA stop codons were highlighted. Deduced amino acids were shown below the corresponding nucleotide sequences. The 6x His residues at C-terminus were boxed.

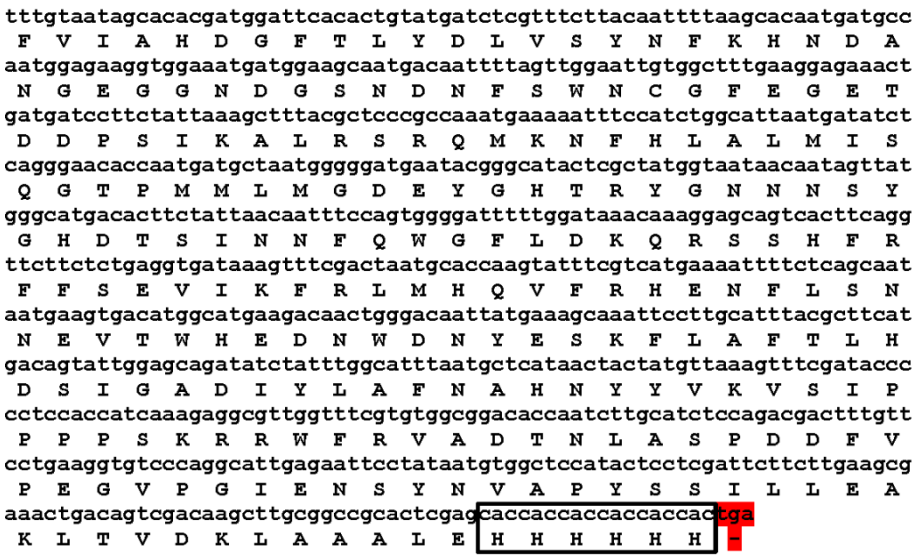

Figure 20 (continued)

The deduced amino acids of all three cassava isoamylases (MeISAs) were compared to those of the *Pseudomonas amyloderamosa* (PaISA) and plants; *Solanum tuberosum* (StISAs) and *Arabidopsis thaliana* (AtISAs) as shown in Table 6 by using ClustalW2 and FUGUE for multiple sequence alignment (Fig. 21). Four conserved domains which were present in all members of glycoside hydrolase family 13 (GH13) were boxed. In addition, eight of conserved residues of GH13 family, which were located in active site, consisting of Asp318, Val320, His323, Arg399, Asp401, Glu461, His535, and Asp536 in PaISA were indicated by black stars, only two of these residues, Val320 and His323, were absolutely conserved in all isoamylase isoforms. Importantly, all three catalytic residues of isoamylase 2 (corresponded to Asp401, Glu461 and Asp536 of PaISA) marked by arrowheads were substituted. Phylogenetic tree was also constructed from the alignment of amino acid sequences of PaISA and three isoamylase isoforms of plants in NCBI database (as shown in Fig. 22). The percent identities among isoamylases of various plant species were also compared and the matrix was created by using Clustal2.1 as shown in Figure 23. The areas of high identity values from the comparison of similar isoform were shown in the frames.

Table 6: Isoamylase isoforms from different sources used for protein sequences. The alignment was performed using ClustalW2 and FUGUE.

Accession number	Abbreviation	Amino acid residue	Source
1BF2_A	PaISA	776	*Pseudomonas amyloderamosa*
-	MeISA1	794	Cassava (*Manihot esculenta* Crantz)
-	MeISA2	883	
-	MeISA3	781	
NP_001274937.1	StISA1	793	Potato (*Solanum tuberosum*)
NP_001274804.1	StISA2	878	
NP_001275220.1	StISA3	766	
NP_181522.1	AtISA1	783	Arabidopsis (*Arabidopsis thaliana*)
NP_171830.1	AtISA2	882	
NP_192641.2	AtISA3	764	

Figure 21 The Protein Sequences Alignment of Three Isoamylases from cassava and other Plants with the Isoamylase from Pseudomonas amyloderamosa. The alighnment was performed using CLUSTALW and FUGUE. Regions of alpha and beta-strand were indicated as (a) and (b) under the sequence alignment, respectively. Beta and loop regions were shown above the alignment. The four conserved domains were boxed. The eight conserved residues were marked by stars which three of these residues indicated by arrowheads were responsible for the catalytic residues of all members of Glycoside Hydrolase family 13 (GH13).

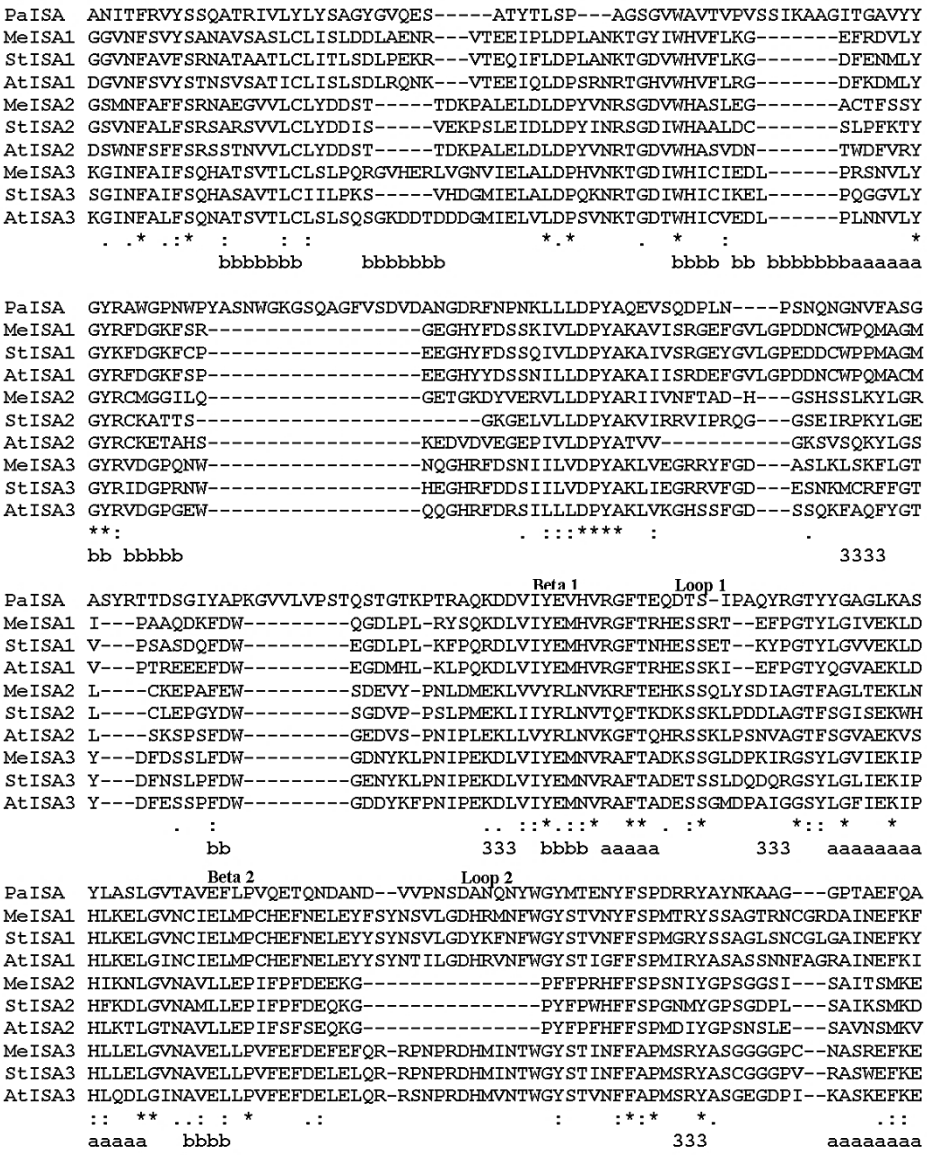

Figure 21 (continued)

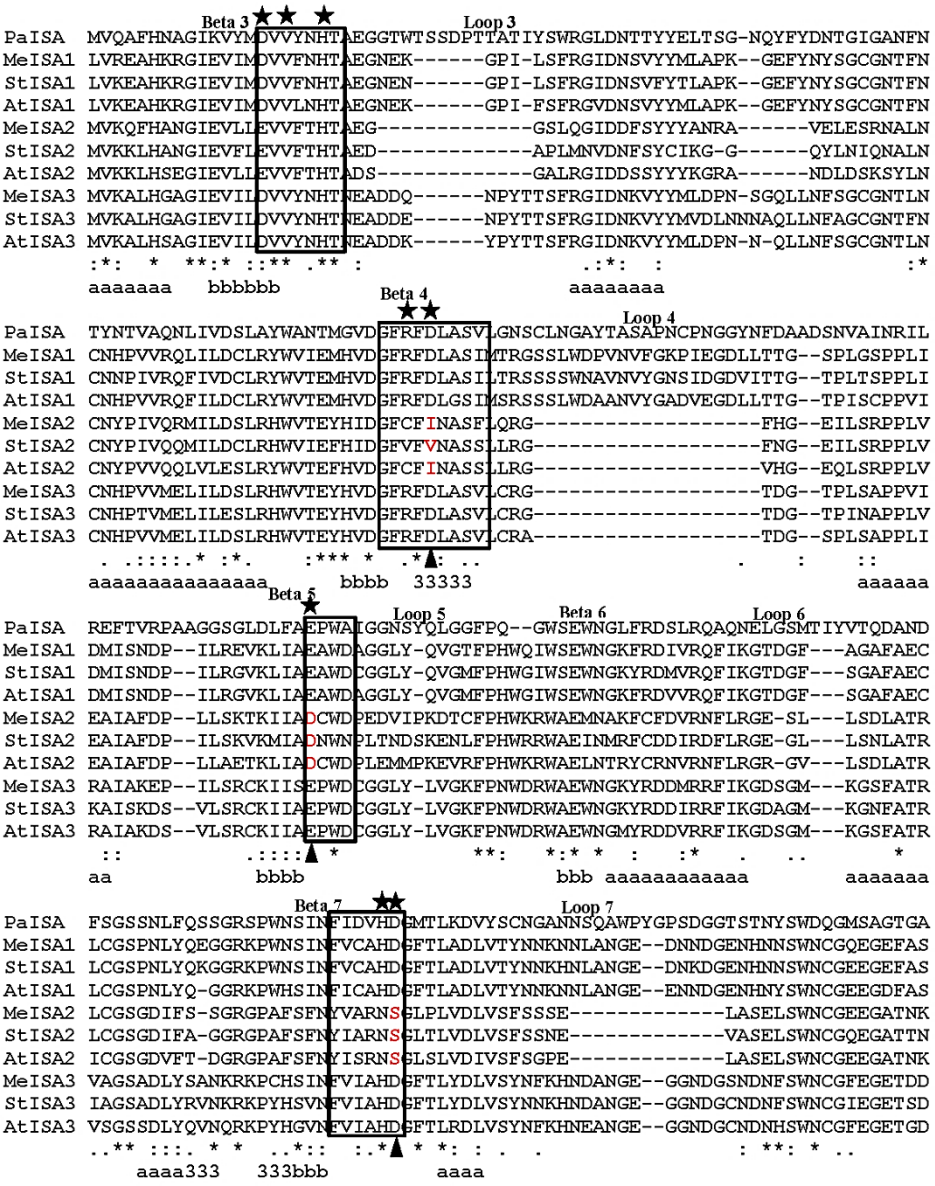

Figure 21 (continued)

Figure 21 (continued)

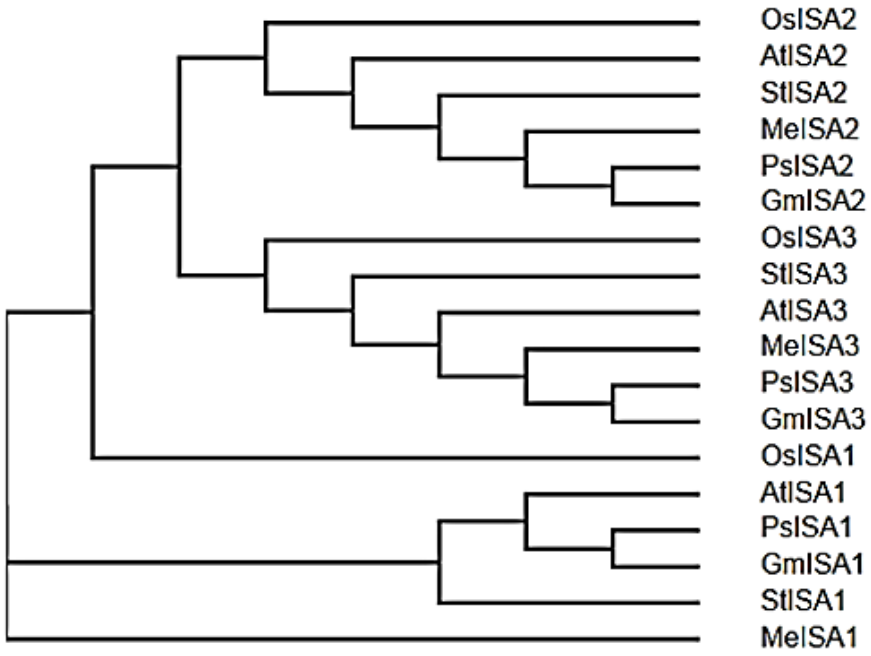

Figure 22 The Neighbour-joining tree constructed from the comparison of deduced amino acid sequences of 3 isoamylase isoforms from different sources. The protein sequences were from *P. amyloderamosa* (PaISA), *Arabisopsis thaliana* (AtISA), *Glycine max* (GmISA), *Pisum sativum* (PsISA), *Solanum tuberosum* (StISA) and *Manihot esculenta* Crantz (MeISA). Details of these isoamylases reported in NCBI database were shown in Appendix C.

1: OsISA2	100.00	49.48	50.72	51.81	48.97	52.59	33.38	31.40	33.77	34.01	32.27	32.81	35.14	34.15	34.39	34.14	35.20	34.23
2: AtISA2	49.48	100.00	53.93	57.31	53.28	55.99	31.34	31.56	32.43	31.39	31.05	31.02	33.52	33.19	34.38	34.17	35.36	35.10
3: StISA2	50.72	53.93	100.00	60.05	52.66	56.39	33.05	33.09	33.24	33.62	33.57	33.24	33.89	34.78	34.96	35.68	35.46	34.69
4: MeISA2	51.81	57.31	60.05	100.00	59.98	61.93	33.10	31.90	33.95	32.20	32.58	32.58	35.00	35.21	36.07	36.29	37.65	36.28
5: PsISA2	48.97	53.28	52.66	59.98	100.00	70.72	32.78	31.81	33.38	33.05	32.44	31.88	34.12	33.90	34.75	34.44	36.43	35.03
6: GmISA2	52.59	55.99	56.39	61.93	70.72	100.00	32.87	31.90	33.19	32.86	31.96	32.11	35.79	35.17	34.66	34.54	36.78	35.64
7: OsISA1	33.38	31.34	33.05	33.10	32.78	32.87	100.00	68.35	70.81	73.15	69.06	71.26	46.30	45.55	45.42	45.92	47.27	45.86
8: AtISA1	31.40	31.56	33.09	31.90	31.81	31.90	68.35	100.00	73.36	73.90	73.45	74.39	44.55	46.66	46.24	46.70	46.12	45.27
9: StISA1	33.77	32.43	33.24	33.95	33.38	33.19	70.81	73.36	100.00	76.44	73.82	75.38	46.04	46.10	46.69	47.08	47.71	46.40
10: MeISA1	34.01	31.39	33.62	32.20	33.05	32.86	73.15	73.90	76.44	100.00	73.89	76.82	47.07	45.53	46.55	46.56	48.11	46.28
11: PsISA1	32.27	31.05	33.57	32.58	32.44	31.96	69.06	73.45	73.82	73.89	100.00	82.91	45.37	45.88	46.76	46.61	47.06	45.73
12: GmISA1	32.81	31.02	33.24	32.58	31.88	32.11	71.26	74.39	75.38	76.82	82.91	100.00	45.58	45.40	45.84	46.15	47.11	44.82
13: OsISA3	35.14	33.52	33.89	35.00	34.12	35.79	46.30	44.55	46.04	47.07	45.37	45.58	100.00	69.03	69.31	69.23	69.93	68.44
14: StISA3	34.15	33.19	34.78	35.21	33.90	35.17	45.55	46.66	46.10	45.53	45.88	45.40	69.03	100.00	70.74	73.48	74.28	72.52
15: AtISA3	34.39	34.38	34.96	36.07	34.75	34.66	45.42	46.24	46.69	46.55	46.76	45.84	69.31	70.74	100.00	76.32	74.83	72.99
16: MeISA3	34.14	34.17	35.68	36.29	34.44	34.54	45.92	46.70	47.08	46.56	46.61	46.15	69.23	73.48	76.32	100.00	78.72	77.68
17: PsISA3	35.20	35.36	35.46	37.65	36.43	36.78	47.27	46.12	47.71	48.11	47.06	47.11	69.93	74.28	74.83	78.72	100.00	85.29
18: GmISA3	34.23	35.10	34.69	36.28	35.03	35.64	45.86	45.27	46.40	46.28	45.73	44.82	68.44	72.52	72.99	77.68	85.29	100.00

Figure 23 Percent Identity Matrix created by Clustal2.1 from the alignment of deduced amino acid sequences of plants isoamylases (see Appendix C)

3.2 Expression of recombinant Me*ISA* genes (rMe*ISA* genes), production of recombinant isoamylases (rMeISAs) in *E. coli* SoluBL21 (DE3) and purification

3.2.1 Co-expression of rMe*ISA1* and rMe*ISA2*

The *E. coli* SoluBL21 (DE3) cells harbouring pETDuet1MeISA1-2 was grown in LB broth containing ampicillin for overnight as starter culture. The starter was cultured in new fresh ampicillin-containing LB broth and cultured and induced with IPTG at various final concentrations of 0.1, 0.5, 1, 5 and 10 mM followed the procedure in section 2.9.1. The his-tagged rMeISA1 was apparently produced under induction with 1 and 5 mM detected on western blot membrane (data not shown). So, the concentration of 2.5 mM of IPTG was selected for large scale protein production. However, only rMeISA1 could be detected from the overnight culture when the cell culture was grown under the same condition as described above at different time points. Both rMeISA1 and rMeISA2 were most abundantly detected by the immunoblot and high level of debranching activity was detected at induction time between 4 to 5 hours (Fig. 24 and 25, respectively). The protein was therefore purified for characterisation from 4 - 5 hours culture and the pooled activity fractions was analysed on SDS-PAGE by silver staining (Fig. 26A).

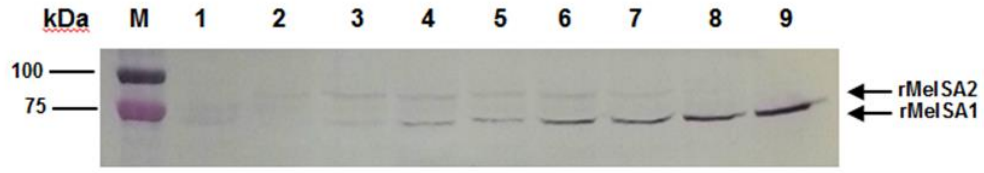

Figure 24 Western blot analysis after SDS-PAGE of soluble rMeISA1 and rMeISA2 produced at various IPTG induction times after induction

Lane M: Prestained protein marker

Lane 1: Non-induced culture

Lane 2: 1 h induction period

Lane 3: 2 h induction period

Lane 4: 3 h induction period

Lane 5: 4 h induction period

Lane 6: 5 h induction period

Lane 7: 6 h induction period

Lane 8: 7 h induction period

Lane 9: 20 h induction period

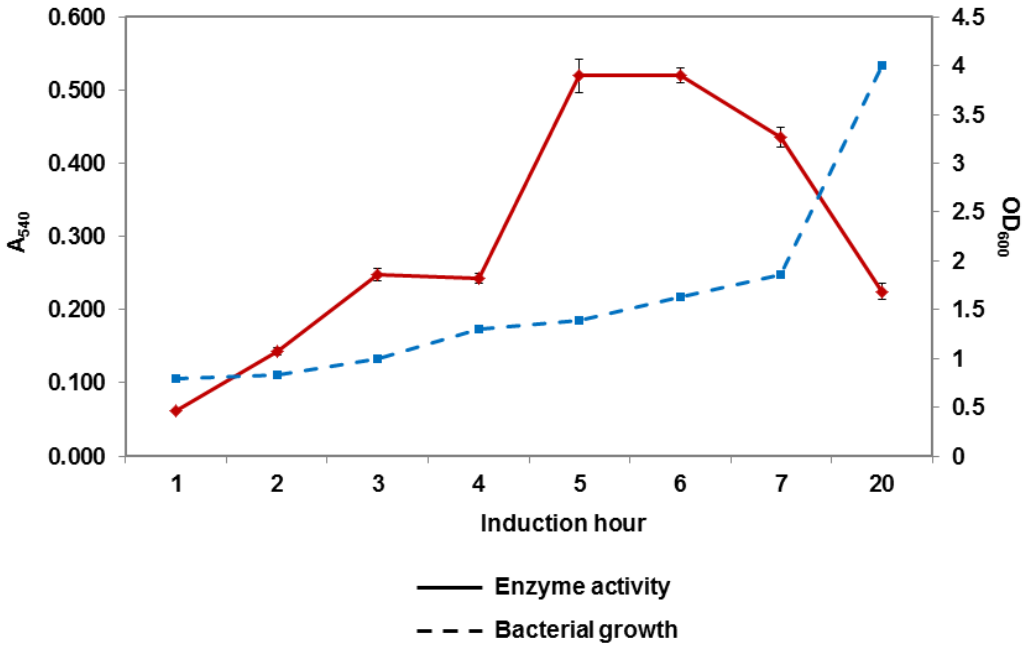

Figure 25 Growth curve of the cell culture (OD_{600}) and debranching activity of crude extracts (A_{540}) at various induction times

Experiments were run in triplicate

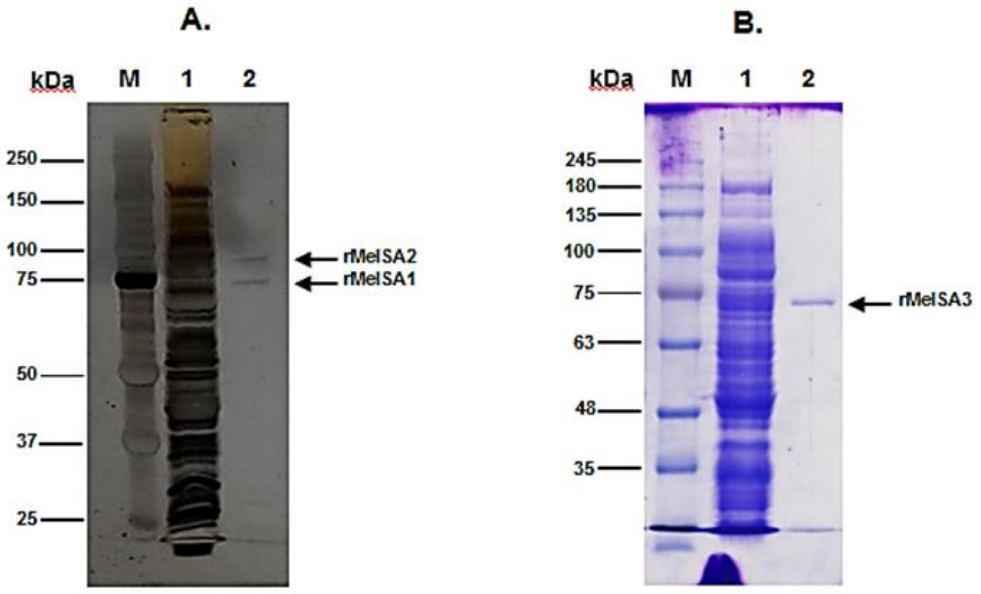

Figure 26 SDS-PAGE analysis of Histrap^{TM}-purified rMeISAs

A. Silver staining

Lane M: Precision Plus Protein^{TM} Standards

Lane 1: Crude extract

Lane 2: Purified rMeISA1/rMeISA2

B. Coomassie staining

Lane M: TriColor Broad Protein Ladder

Lane 1: Crude extract

Lane 2: Purified rMeISA3

In addition, the comparison of activity of single rMeISA1 and rMeISA2 were also studied. Single purified proteins were obtained from fraction 1st and 20th h post induction in which only single rMeISA2 and rMeISA1 were expressed. The purified rMeISAs from 1st, 4-5th and 20th h after induction were analysed on SDS-PAGE by silver staining. The debranching activity was also measured in these fractions and the purified fraction of each indicated time point was chosen (marked by frame in Fig. 27A, B and C). The purified rMeISA1/rMeISA2 from 4 - 5th h obviously showed the highest activity however the purified rMeISA1 and rMeISA2 seemed to lack debranching activity (Fig. 28).

3.2.2 Expression of r*MeISA3*

The *E. coli* SoluBL21 (DE3) cells harbouring pET21bMeISA3 was grown and induced with IPTG following the same procedure for r*MeISA1* and r*MeISA2*. Relatively high amount of rMeISA3 and the highest activity were detected under induction with 0.4 mM of IPTG at 16 °C (as shown in box in Fig. 29 and 30, respectively). Purification of rMeISA3 was thus performed on the culture grown overnight at 16 °C induced by 0.4 mM IPTG. The intracellular enzyme was purified and the pooled activity fractions was analysed by Coomassie staining of SDS-PAGE (Fig. 26B).

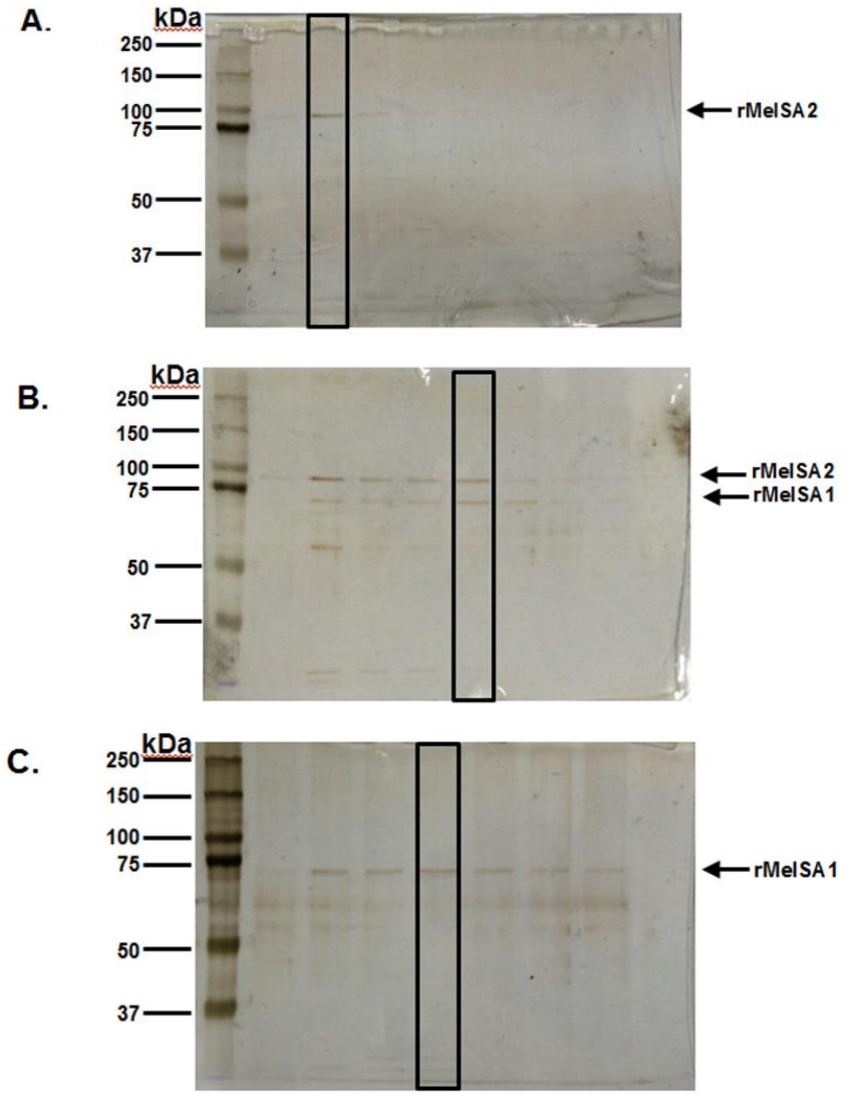

Figure 27 Silver staining of SDS-PAGE of Histrap^{TM}-purified rMeISAs from 1, 4 - 5 and 20 h of induction period

A. Crude extract of 1 h after induction

B. Crude extract of 4 - 5 h after induction

C. Crude extract of 20 h after induction

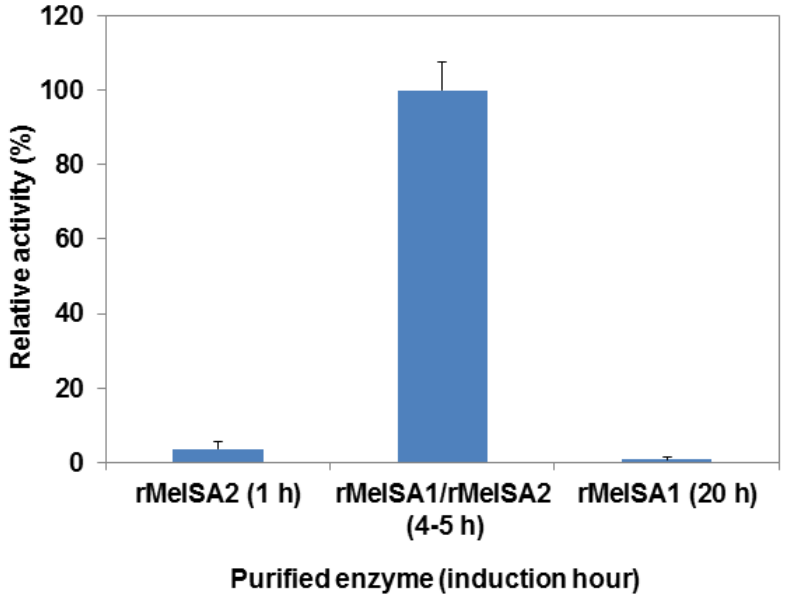

Figure 28 Comparison of debranching activities of purified rMeISA1 and rMeISA2 with that of purified rMeISA1/rMeISA2

Experiments were run in triplicate

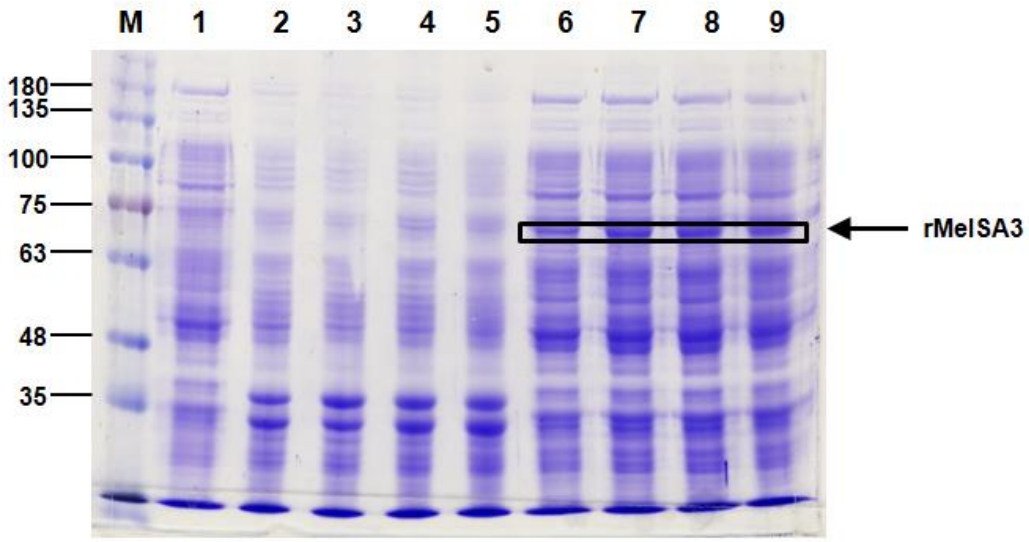

Figure 29 Coomassie staining of SDS-PAGE of crude proteins of *E. coli* SoluBL21 (DE3) harbouring pET21bMeISA3 induced by various IPTG concentrations at 16 °C for overnight

Lane M: TriColor Broad Protein Ladder

Lane 1: Non-induced culture

Lane 2: insoluble proteins induced by 0.2 mM IPTG

Lane 3: insoluble proteins induced by 0.4 mM IPTG

Lane 4: insoluble proteins induced by 0.6 mM IPTG

Lane 5: insoluble proteins induced by 0.8 mM IPTG

Lane 6: soluble proteins induced by 0.2 mM IPTG

Lane 7: soluble proteins induced by 0.4 mM IPTG

Lane 8: soluble proteins induced by 0.6 mM IPTG

Lane 9: soluble proteins induced by 0.8 mM IPTG

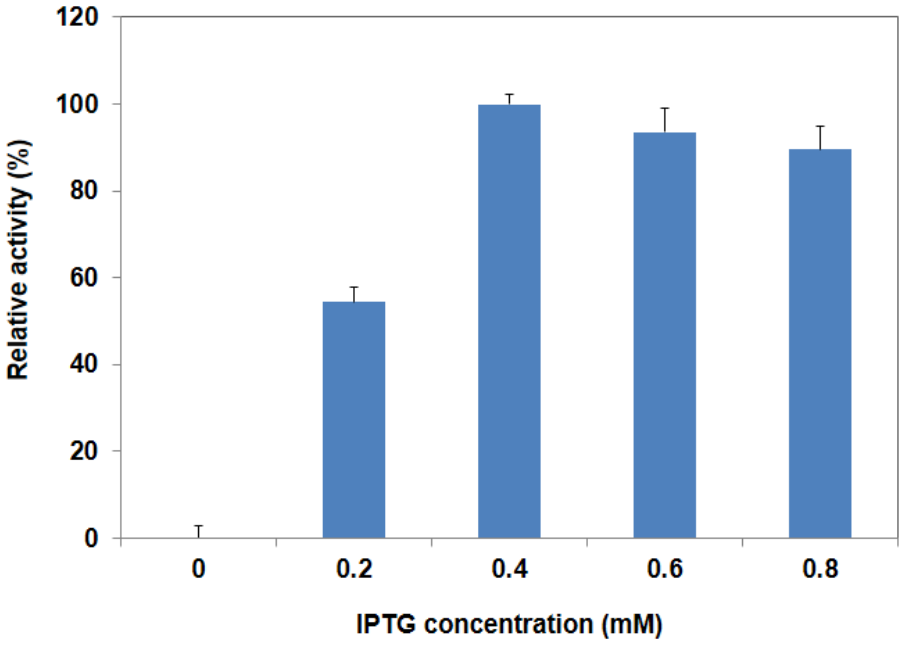

Figure 30 Debranching activity of crude extract of MeISA3 under induction of various IPTG concentrations on β-limit dextrin substrate

Experiments were run in triplicate

3.3 Characterisation of rMeISAs

Optimum pH, optimum temperature, effect of metal ions and some chemicals and substrate specificity for debranching activity of rMeISAs were determined.

3.3.1 Optimum pH

The debranching activity of rMeISA1/rMeISA2 and rMeISA3 were tested at various pH as described in Section 2.11.1.1 and 2.11.2.1, respectively. The relative activity was measured. The pH value which showed the highest activity was set as 100% of relative activity. The results were shown in Fig. 31. The optimum pH of rMeISA1/rMeISa2 and rMeISA3 were at pH 7.0 phosphate buffer and at pH 6.0 acetate buffer, respectively.

3.3.2 Optimum temperature

The reactions were performed at pH 7.0 and pH 6.0 at various temperatures to determine the optimum temperature for debranching activity of rMeISa1/rMeISA2 and rMeISA3, respectively (described in Section 2.11.1.2 and 2.11.2.2). The temperature profiles were shown in Fig. 32, which the highest activity detected at any temperature was designated as 100% of relative activity. Both rMeISA1/rMeISA and rMeISA3 showed similar highest debranching activity at 37 °C.

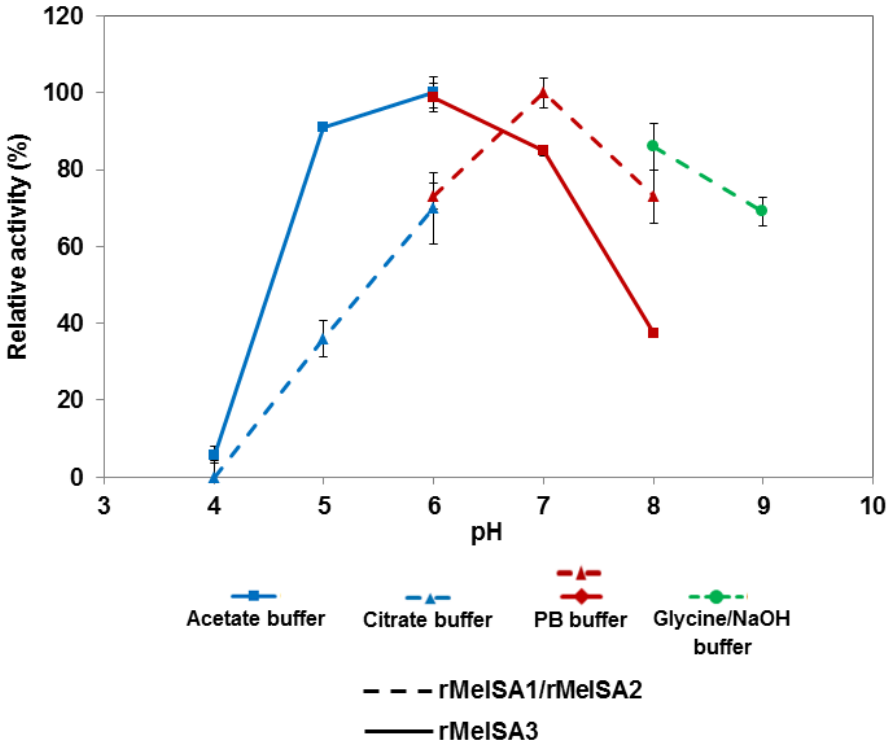

Figure 31 Optimum pH of debranching activities of rMeISA1/rMeISA2 and rMeISA3

Experiments were run in triplicate

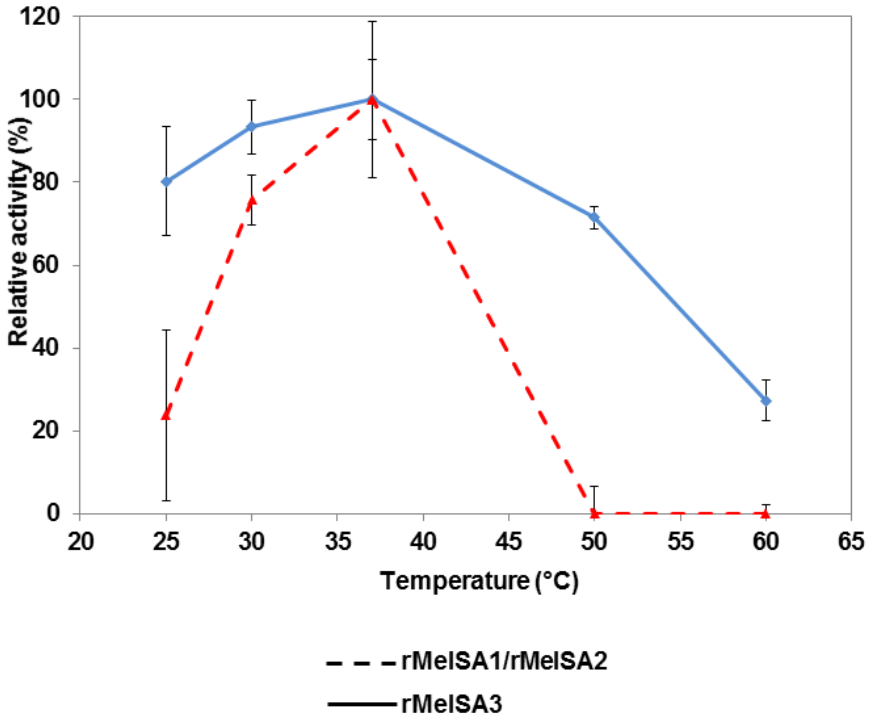

Figure 32 Optimum temperature of debranching activities of rMeISA1/rMeISA2 and rMeISA3

Experiments were run in triplicate

3.3.3 Effect of metal ions and some chemicals

The reactions were carried out under optimum condition of each enzyme as described in Section 2.11.1.3 and 2.11.2.3, with or without 1mM of metal ions or chemicals. The activity of the reaction without adding any ions or chemicals was taken as 100% of relative activity. The results were shown in Fig. 33. The Co^{2+}, Mg^{2+} and Ca^{2+} could enhance the debranching activity of rMeISA1/rMeISA2. For rMeISA3, its enzyme activity could be significantly increased by Mn^{2+} and Co^{2+}, respectively. However, Cu^{2+} was a strong inhibitor for both rMeISA1/rMeISA2 and rMeISa3.

3.3.4 Substrate specificity

The rMeISA1/rMeISA2 and rMeISA3 were incubated with different types of substrates under the optimum condition. The highest activity was specified as 100% of relative activity. The results showed that maize amylopectin was the most suitable substrate for rMeISA1/rMeISA2 while rMeISA3 obviously showed the highest activity on beta-limit dextrin (Fig. 34). Importantly, all these rMeISAs were apparently unable to digest pullulan substrate.

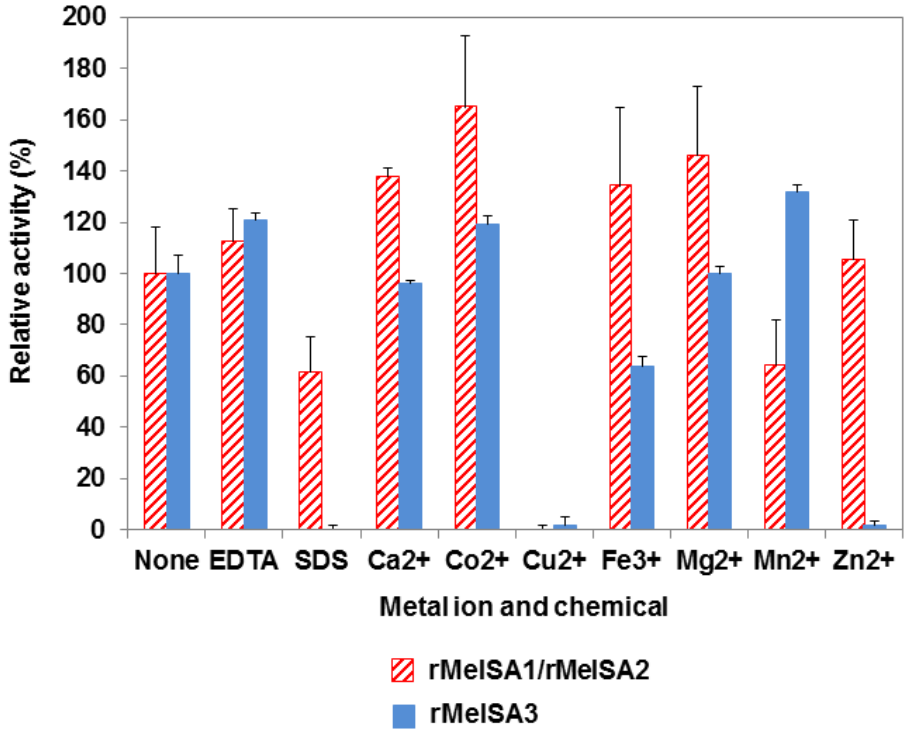

Figure 33 Effect of metal ions and some chemicals on debranching activities of rMeISA1/rMeISA2 and rMeISA3

Experiments were run in triplicate

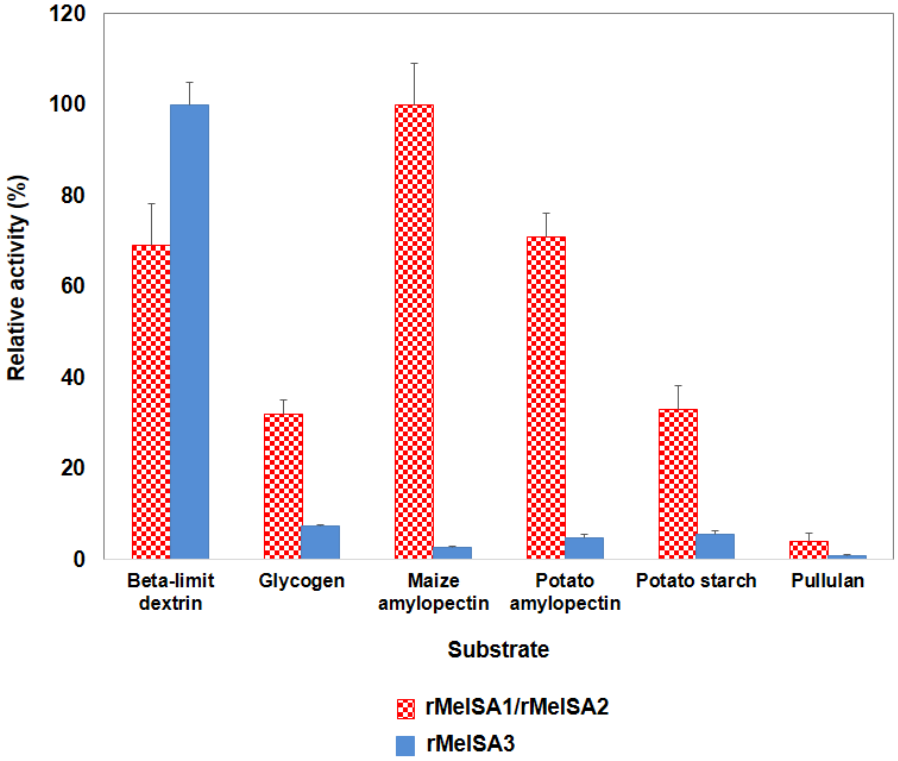

Figure 34 Substrate specificities of debranching activities of rMeISA1/rMeISA2 and rMeISA3

Experiments were run in triplicate

3.3.5 Native-PAGE of purified rMeISA3

The purified rMeISA3 was electrophoresed on 6% (w/v) non-denaturing PAGE containing 0.15% (w/v) beta-limit dextrin. Then, the protein and activity staining were performed as described in Section 2.7.3. Lanes 1 and 2 in Figure 35 showed the protein staining of crude and purified protein, respectively. On the activity staining gel (right panel), clear band of debranching activity present in lanes 3 and 4 of crude and purified rMeISA3 was indicated by arrow.

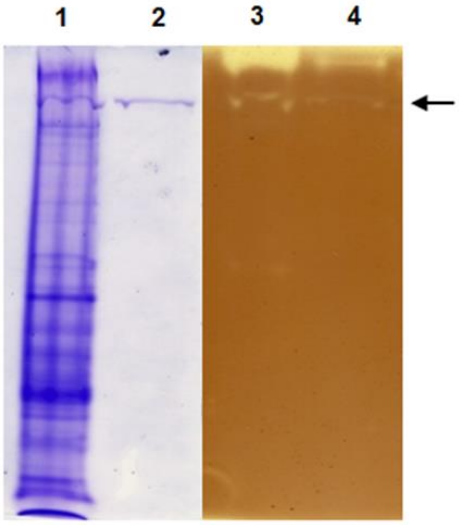

Figure 35 Native-PAGE (6% gel containing 0.15% (w/v) beta-limit dextrin) of Histrap^{TM}-purified rMeISA

Coomassie staining

Lane 1: Crude enzyme (40 µg protein)

Lane 2: Purified rMeISA3 (5 µg protein)

Activity staining

Lane 3: Crude enzyme

Lane 4: Purified rMeISA3

(0.1 Unit of debranching activity was loaded to each well)

3.3.6 Molecular weight determination of rMeISAs

The molecular weights of rMeISAs were theoretically predicted by using Compute PI/Mw (ExPAsy). The molecular weights of deduced amino acid of rMeISA1, rMeISA2 and rMeISA3 were 87, 99 and 80 kDa, respectively. The Histrap^{TM}-purified proteins were analysed on SDS-PAGE (Fig. 26A and B). The protein molecular sizes were calculated from the calibration curve constructed from the R_f values of protein standard markers (shown in Appendix H).

3.3.7 Determination of molecular weight of enzyme complexes and rMeISA1:rMeISA2 ratio in the complexes

Crude extract of 4 - 5 h of induction time was also purified by gel filtration column as described in Section 2.10.2. The sizes of protein complexes with debranching activity were in the range of 260 to 500 kDa calculated from the molecular weight calibration curve of fraction no. 67 to 73 indicated by arrows and numbers of the fraction in the chromatographic profile (Fig. 36). Estimation of the possible combination of rMeISA1: rMeISA2 using the molecular weights predicted from deduced amino acid sequences in section 3.3.6, the possible complexes form were 2:1 (273), 3:1(360), 2:2 (372), 1:3 (384) 1:4 (483) and 4:1 (447). The intensity of the protein bands detected by immunoblot was calculated by Quantity One-4.6.6 program. The ratios of rMeISA1: rMeISA2 in enzyme complexes from the above fractions were in range of 1: 1 to 4: 1 (Fig. 37), with either equal or more intense protein bands of MeISA1.

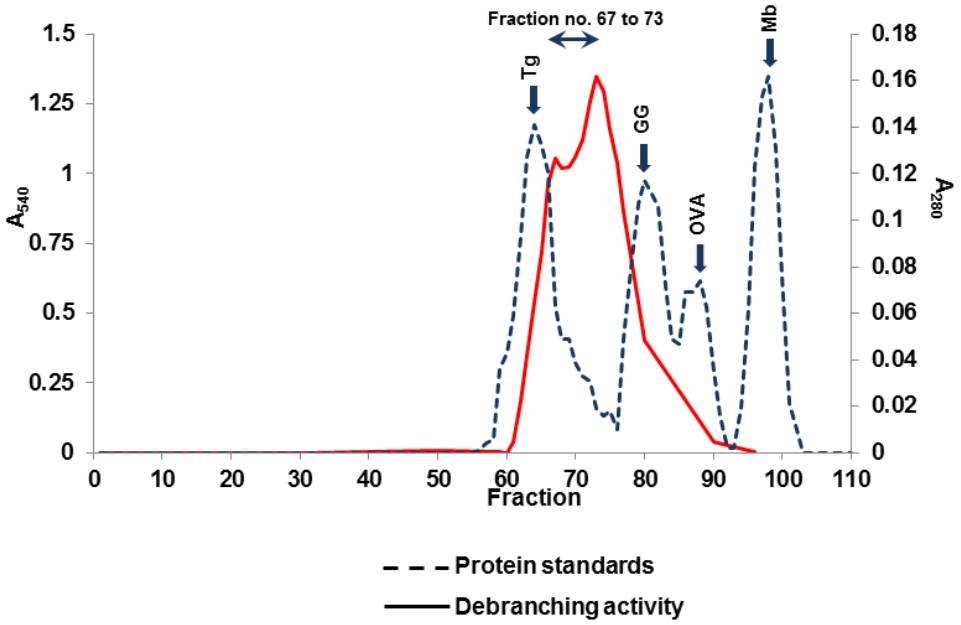

Figure 36 Chromatographic profile of rMeISA1/rMeISA2 from Sephacryl S-300 HR

Standard proteins were:

Tg = Thyroglobulin (bovine) MW = 670,000 Da

GG = γ-globulin (bovine) MW = 158,000 Da

OVA = Ovalbumin (chicken) MW = 44,000 Da

Mb = Myoglobin (horse) MW = 17,000 Da

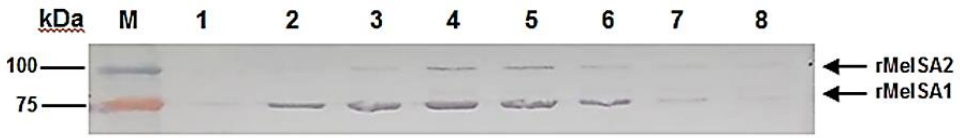

Figure 37 Western blot analysis after SDS-PAGE of partially purified rMeISA1/rMeISA2 by gel filtration column

Lane M: TriColor Broad Protein Ladder

Lane 1: fraction no. 60

Lane 2: fraction no. 62

Lane 3: fraction no. 64

Lane 4: fraction no. 66

Lane 5: fraction no. 68

Lane 6: fraction no. 70

Lane 7: fraction no. 72

Lane 8: fraction no. 74

3.3.8 Chain Length Distribution analysis

3.3.8.1 Products from debranching activities of rMeISA1/rMeISA2 and rMeISA3

Debranching activities of rMeISA1/rMeISA2 and rMeISA3 were tested and the enzymatic reactions were carried out as described in Section 2.11.5.1 and 2.11.5.2, respectively. The CLD of PaISA activity was used as a positive control. Figure 38A and B showed their similar patterns of CLD from the activity of these enzymes. However, under the same reaction condition and the same number of unit of enzyme, rMeISA1/rMeISA2 was about 3 times less active than PaISA. The products contained polysaccharides with DP range of DP 6 to DP 20.

However, debranching activity of rMeISA3 was lower than PaISA under the same reaction condition. Importantly, rMeISA3 was much less active on amylopectin substrate than rMeISA1/rMeISA2.

3.3.9 N- and O-glycosylation prediction of rMeISAs

The glycosylated sites of amino acid sequences of all three MeISA were observed. Three sites specific for N-glycosylation and six of O-glycosylating sites of MeISA1 and MeISA2 were predicted (Fig. 39A and B). For MeISA3, four sites of both N- and O-glycosylation were found (as shown in Fig. 39C).

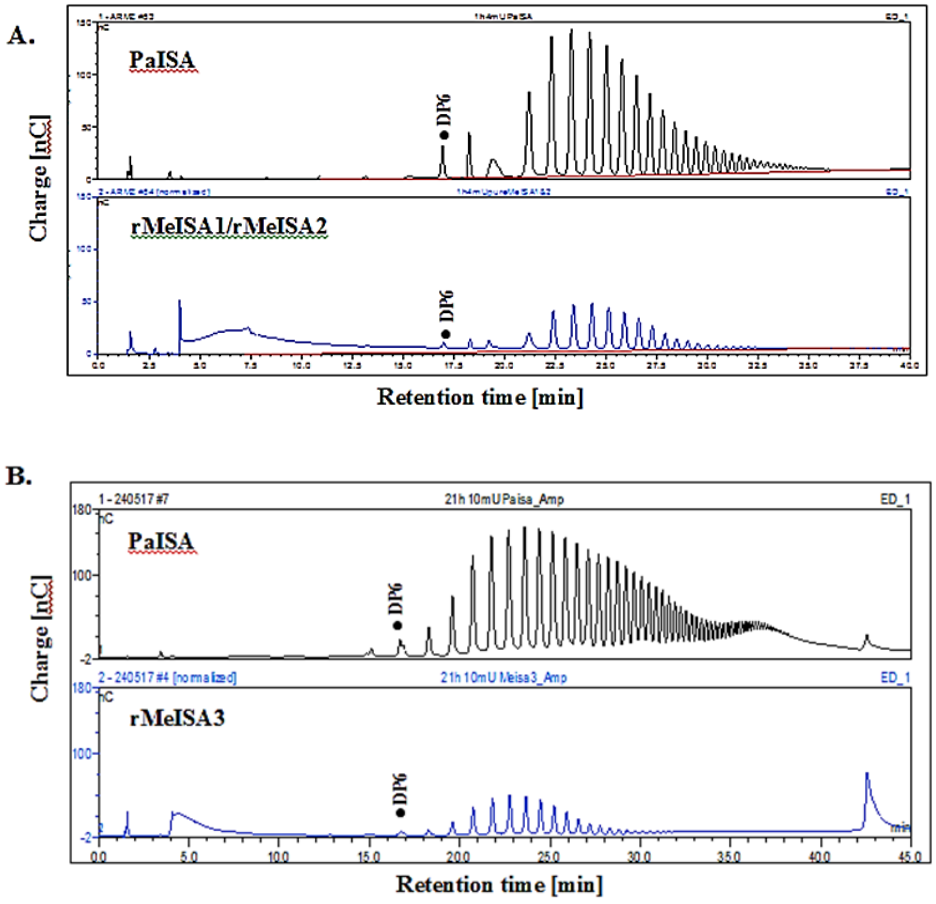

Figure 38 Debranching activity of rMeISAs analysed by chain length distribution (CLD) using HPAEC-PAD. CLD produced by PaISA were used as reference.

A. CLD pattern of debranching activity of 4 mU of rMeISA1/rMeISA2 on amylopectin substrate incubated at 37 °C for 1 h

B. CLD pattern of debranching activity of 10 mU of rMeISA3 on amylopectin substrate incubated at 37 °C for 21 h

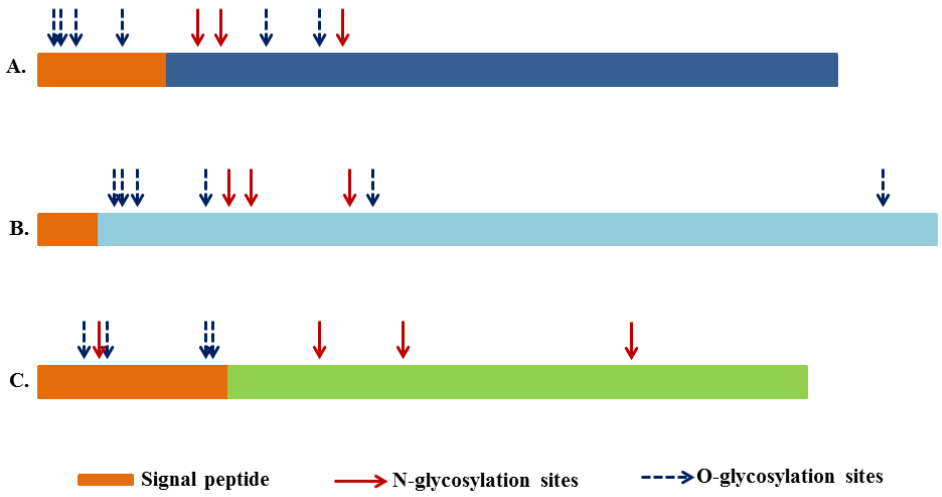

Figure 39 Diagram of N- and O-glycosylating sites prediction by NetNGlyc 1.0 and NetOGlyc 4.0 Servers, respectively in MeISAs

A. Three sites of N-glycosylation and six sites of O-glycosylation in MeISA1

B. Three sites of N-glycosylation and six sites of O-glycosylation in MeISA2

C. Four sites of N-glycosylation and four sites of O-glycosylation in MeISA3

CHAPTER IV

DISCUSSION

Starch debranching enzyme (DBE) is one of the essential enzymes in starch metabolism, both in biosynthesis and degradation. Although the properties of DBE have been studied in many photosynthetic organisms, its definite role in the starch biosynthesis process is still under debated. However, it was proposed to play important role in the determination of the fine structure of starch granule and in the clearance of highly branched polysaccharide (water soluble polysaccharide or phytoglycogen) produced by starch synthase and starch branching enzyme in the starch biosynthetic pathway to reduce the effect of substrate inhibition of these enzymes (Tetlow et al. 2004). Importantly, the information of DBE in cassava, which is one of our major economic crops, is still limited. In this research, we focused on the molecular characterisation of DBE, especially isoamylase-type, in cassava tubers in which starch biosynthesis is prominent. Understanding of its involvement in starch metabolism together with the roles of other starch metabolising enzymes can lead to possible improvement and manipulation of cassava starch production and utilisation.

4.1 Monitoring of debranching activity

Two types of DBE are present in plants and alga; isoamylase-type (EC 3.2.1.68) and pullulanase-type (EC 3.2.1.41) debranching enzymes (Nakamura et al. 1997; Nakamura et al. 1996). Both types of enzymes catalyse the hydrolysis of α-1,6

glucosidic linkages but differ in substrate specificity. Isoamylase-type enzyme catalyses the breaking down of the branch points of amylopectin, beta-limit dextrin and glycogen but not pullulan, whereas pullulanase (also known as limit-dextrinase or R-enzymes) debranches pullulan, amylopectin and limit-dextrins but not glycogen. Interestingly, isoamylase has some advantages over pullulanase, i.e. higher efficiency in cleavage of α-1,6 glucosidic linkages and less product inhibition. However, the information on isoamylases is still limited compared to several studies of pullulanase (Kuroiwa et al. 2005; Reddy et al. 1999). Products of debranching activity were oligosaccharides. Therefore, the activity of isoamylase can be primarily assayed by determining the reducing sugar produced using modified dinitrosalicylic acid (DNS) assay (Miller 1959). Several studies also used this method in their enzymatic assays in maize, potato, *Chlamydomonas* sp. (Dauvillée et al. 2001; Hussain et al. 2003; Rahman et al. 1998). However, substrates of isoamylase can also be utilised by some other carbohydrate hydrolysing enzymes such as α- and β-amylases. The debranching activity of ISA3 can be further confirmed by non-denaturing gel electrophoresis containing 0.15% (w/v) of beta-limit dextrin. The activity band of ISA3 on beta-limit dextrin-containing gel appeared as a colourless band because short, linear glucans produced in gel against brownish background (Dinges et al. 2003; Wattebled et al. 2005; Zeeman et al. 1998). However, some other clear bands were also observed at the top of the gel in both lanes of crude enzyme and purified ISA3 (in lane 3 and 4 of Fig. 35, respectively) which may be caused by immediate debranching of the substrate, beta-limit dextrin, by rMeISA3 during running because the running buffer at the surface area might not be cooled enough. Conversely, activity of ISA1/ISA2 was unable to be detected on Native-gel. This possibly resulted from dissociation of active MeISA1/MeISA2 enzyme

complex during running on the gel. Identification of chain lengths of debranching products by HPAEC-PAD is an important confirmation of debranching activity.

4.2 Cloning of Me*ISA* genes

Previously, Kornsiripanya (2007, unpublished) studied the ISA activity of 3 to 12-month old cassava tubers and found that the activity of MeISA was not changed drastically during developmental stages and reached the highest level in 9-month old. Therefore, cassava tubers of this indicated age were selected and harvested from the National Research Centre of Millet and Corn (Suwan Farm) and then used as source of RNA isolation. The cortex region was used for total RNA extraction because it contains less starch content than parenchyma region. The starch contamination, however, is still a major obstacle. To avoid this problem, the PureLink™ Plant RNA Reagent, which is single-component solution suitable for the isolation of total RNA from a variety of plant tissues especially those rich in polyphenolic compounds or starch, was used. Total RNA with high yields and quality was obtained and used as template for reverse transcription and cDNA was then successfully constructed. Full length sequences of *ISA1* and *ISA2* can be obtained from NCBI and Phytozome databases, and primers for full length Me*ISA1* and Me*ISA2* genes were designed, amplified and sequenced. For *MeISA3*, compared to those of *ISA3* genes in different plant species (e.g., potato and *Arabidopsis*), it seemed about 700 base pairs of 5' region was missing. To get the full length of Me*ISA3* gene, we first attempted to directly deal with the cDNA such as second-strand synthesis and attachment of linkers. Unfortunately, the missing part of the gene could not be obtained. So, the 5'RACE using the SMARTer® RACE 5'/3' Kit was performed. The kit, which is an ideal system for gene racing, provides several

numbers of benefits, i.e., adaptor ligation step was eliminated, very small quantity of either total RNA or mRNA was required as starting material for full length cDNA construction, even of very rare transcripts and large volume of RNA template are allowed. Finally, the full length of putative Me*ISA3* was obtained after subsequent PCR and sequenced.

In plants, isoamylases have different localisations to the starch-producing tissues (Hussain et al. 2003). For instance, in maize endosperm and Arabidopsis leaves, isoamylase activity was detected in the plastid (Doehlert and Knutson 1991; Yu et al. 2001; Zeeman et al. 1998). Furthermore, isoamylase activity in developing pea embryos was mainly found in amyloplasts (Zhu et al. 1998). These evidences suggested that all three cassava ISA genes should carry the sequences encoding signal peptides, which is N-terminally located at the end of nascent protein. The function of signal peptide is to lead the protein to the organelle of destination and then it will be removed. Hence, the deduced amino acid sequences encoding signal peptides of all MeISAs were predicted by ChloroP1.1 algorithm which would be excluded before amplification of the mature genes.

The alignment of the predicted peptide sequences of the three MeISAs of cassava with PaISA from *Pseudomonas amyloderamosa*, StISA from potato and AtISA from *Arabidopsis* showed all four conserved domains of enzymes in Glycoside Hydrolase family13 (GH13). In addition, eight of highly conserved residues which present in all members of GH13 family and located in active site, consisting of Asp318, Val320, His323, Arg399, Asp401, Glu461, His535, and Asp536 in PaISA were also observed indicated by eight of stars in Fig. 21. However, in ISA2, only Val320 and His323 are absolutely conserved. The replacement of the remaining residues (D318E,

R399C, D401I in AtISA2 and MeISA2 or D401V in StISA2, E461D, H535N and D536S) significantly affects the acid-base catalysis. Noticeably, substitution of the two catalytic residues (out of three residues) with non-polar and polar group (V/I and S, respectively) significantly affects the properties of proton transfer between donors and acceptors during the enzymatic catalysis (Hussain and Martin 2009; Koshland 1953; Sinnott 1990). Furthermore, from three important residues that are considered to play a role in substrate binding, Ser404, Val405 and Trp463 in PaISA, only Ser404 and Trp463 were conserved in all ISAs. These three residues were present in other isoamylases although they were not absolutely conserved in all GH13 enzymes. These results suggested that ISA2 might completely lack catalytic activity however it should still be able to bind substrates. Surprisingly, although most ISA2 showed no hydrolytic activity (Facon et al. 2013; Hussain et al. 2003; Hussain and Martin 2009; Kubo et al. 1999), it has been evolutionarily conserved and present in all plant species and was usually associated multimeric complex with ISA1. ISA2 probably plays essential role in enhancing the isoamylase activity probably in substrate binding since it has two important residues, S404 and W463 (PaISA numbering, Fig. 21) and Carbohydrate Binding Module 48 (CBM48), often found in GH family 13 (Katsuya et al. 1998; Sim et al. 2014; Woo et al. 2008), participating in substrate binding. On the other hand, MacGregor (1993) suggested that the different length of the loops between β-sheets and α-helices affected the substrate binding specificity of GH13 enzymes. Abe et al. (1999) revealed that distances between the catalytic residues, which covered loops 4 to 6, were essential for substrate specificity of *Flavobacterium odoratum* KU isoamylase as studied by mutagenesis. In ISA2 and ISA3, the length of loop 4 is significantly shorter than that of ISA1, whereas their loop 5 and 6 lengths were in similar size (Fig. 21). This

suggested that ISA2 and ISA3 would prefer a glucan substrate with relatively short chain lengths like beta-limit dextrin. On the contrary, ISA1 was suggested to have higher susceptibility to longer chain substrates such as amylopectin. This observation correlated with the results of substrate specificity shown in Fig. 34.

The phylogenetic tree construction (Fig. 22) showed all three isoforms of cassava isoamylases were grouped with related isoforms previously reported based on their high percent identity and similarity as shown in the framed areas in Fig. 23.

4.3 Expression and purification of rMe*ISA* genes

4.3.1 Coexpression of rMe*ISA1* and rMe*ISA2* in *E. coli* SoluBL21 (DE3)

Me*ISA1* and Me*ISA2* genes were first separately cloned and expressed using a pET21b vector in *E. coli* T7 expressing strains, only very small amount of rMeISA1 could be detected by immunoblot without detectable debranching activity (data not shown). Previous studies revealed the presence of multimeric isoamylase isoform1 and 2 which led to enhancement of hydrolysis ability of ISA1 and the increasing stability of ISA2 in dicots such as potato and *Arabidopsis* (Hussain et al. 2003; Ishizaki et al. 1983). So, Me*ISA1* and Me*ISA2* genes were cloned together into a pETDuet1 vector and transformed into *E. coli* SoluBL21 (DE3). A pETDuet1, a two-promoter vector, was used to get over undesirable results from co-expression such as apparently lower amount of the second protein in bicistronic vector system or dominancy of copy number of one vector over the other in the dual-vector system (Johnston et al. 2000; Kim et al. 2004). Continuous monitoring of protein and enzyme activity over 20 hours IPTG induction time showed early appearance of protein bands corresponded to rMeISA2 from the first hour with gradual rise in band intensity up to 4 - 6 hours before

disappearing. rMeISA1 protein band appeared at about the second hour of incubation co-incidental with detectable enzyme activity. Appearance of both rMeISA1 and rMeISA2 were observed at incubation times 2 - 20 hours with maximum ISA activity observed at 4 - 5 hours and gradually dropped. The rise and fall of ISA activity were observed in conjunction with the increase in gel intensity of MeISA1 and decline of MeISA2 (Fig. 24 and 25). Then, crude extracts of 1st, 4 - 5th and 20th h post induction were successfully purified by Histrap^{TM} column. The purified rMeISA1/rMeISA2 from 4 - 5th h obviously showed the highest debranching activity while the purified rMeISA1 and rMeISA2 showed no activity. This indicated that rMeISA2 was necessarily required for catalytic activity of rMeISA1 although rMeISA2 is inactive by itself. Moreover, *in vitro* mixing of each single purified rMeISA1 and rMeISA2 at different ratios of rMeISA1: rMeISA2 at 1:3 to 3:1, no debranching activity can be observed (data not shown). This implicated that expression of MeISA1 was stimulated in some way by the presence of MeISA2 and the enzyme activity observed when both isoforms present together did not result from simple association and the coexpression is the key of its debranching activity.

4.3.2 Expression of rMe*ISA3* in *E. coli* SoluBL21 (DE3)

Me*ISA3* was cloned into a pET21b and expressed in the *E. coli* SoluBL21 (DE3) as was used in coexpression of Me*ISA1* and Me*ISA2* as described in section 2.9.1. Comparing to the expression system of Me*ISA1* and Me*ISA2*, in terms of the same of promoter type and *E. coli* expressing strain, Me*ISA3* can be induced by much lower concentration of IPTG than that of Me*ISA1* and Me*ISA2*, about 6 times. Moreover, rMeISA3 was produced in soluble form with much higher level than rMeISA1 and

rMeISA2 which could to be visualised easily by Coomassie staining of SDS-PAGE whereas rMeISA1 and rMeISA2 were detectable on SDS-PAGE by Silver staining (Fig. 26). The higher level of stability of rMeISA3 than that of rMeISA1/rMeISA2 complex either before or after purification by Histrap^{TM} column was also observed. This might result from the instability of rMeISA2, which was crucial for activity of rMeISA1 in the functional enzyme complex. Small sizes protein bands in the purified sample at few hours after purification were visible on SDS-PAGE which was probably the degradation products of rMeISA2 (data not shown).

Crude extract of rMeISA3 from the overnight culture was partially purified by gel filtration column (as described in section 2.10.2 for rMeISA1 and rMeISA2). The eluted fractions with debranching activity were observed around the size corresponded to its monomer (data not shown). This suggested that functional rMeISA3 is in monomeric form. There was no report on the presence of homomultimeric form of ISA3 in plants.

4.4 Characterisation of rMeISAs

4.4.1 Optimum pH and temperature

The pooled activity fractions of Histrap^{TM}-purified rMeISA1/rMeISA2 was incubated with 0.75% (w/v) of amylopectin substrate at various pHs and ISA activity was assayed. rMeISA1/rMeISA2 enzyme complex was most active in phosphate buffer pH 7.0. The activity was decreased about 20% at pH 6.0, 8.0 and 9.0. However, rMeISA1/rMeISA2 seemed to be more stable in slightly alkaline condition than in acidic condition because its activity was dramatically decreased about 60% at pH 5.0 and completely lost at pH 4.0 (Fig. 31). Debranching activity of the purified rMeISA3

was assayed by incubating with 0.75% (w/v) of beta-limit dextrin substrate at different pH values. The highest activity was detected at pH 6.0 citrate or acetate buffers. Its activity was slightly dropped around 20% at pH range 5 - 7 but completely lost at pH 4.0 similar to rMeISA1/rMeISA2. Nonetheless, acetate buffer was chosen for further activity assays of rMeISA3 since citrate buffer harbours chelating property which possibly affects the study of effect of metal ion on debranching activity. These results were similar to optimum pHs of ISA, which were around pH 5.5 - 7.5, reported in other plants such as potato and maize (Doehlert and Knutson 1991; Ishizaki et al. 1983; Rahman et al. 1998).

Then, optimum temperatures of rMeISAs were determined. rMeISA1/rMeISA2 was incubated with 0.75% (w/v) of amylopectin substrate in phosphate buffer pH 7.0 at various temperatures. rMeISA1/rMeISA2 showed the highest activity at 37 ºC but its activity was completely lost at over 50 ºC. The optimum temperature for debranching activity of rMeISA3 was analysed. rMeISA3 was incubated with 0.75% (w/v) of beta-limit dextrin in acetate buffer pH 6.0. rMeISA3 showed the highest activity at 37 ºC same as rMeISA1/rMeISA2 but rMeISA3 was highly active in wide range of temperatures ranging from 25 - 50 ºC (Fig. 32). Optimum temperatures of ISA reported in other plants were in the range of 30 - 37 ºC (Hussain et al. 2003; Rahman et al. 1998).

4.4.2 Effect of metal ions and some chemicals on debranching activity .

Metal ions showed diverse effect on activities of enzymes. The metal ions and chemicals which were commonly found to affect enzyme activity were used in activity assay of all rMeISAs. In our work, Co^{2+}, Mg^{2+} and Ca^{2+} could potentially activate debranching activity of rMeISA1/rMeISA2, whereas its activity was completely lost in

the presence of Cu^{2+}. On the other hand, Mn^{2+} and Co^{2+} were potent activator for rMeISA3 but Cu^{2+} and Zn^{2+} were strong inhibitor. (Iwaki and Fuwa 1981) reported that at concentration of 1 mM of Cu^{2+}, Zn^{2+}, Ag^{2+} and Cd^{2+} acted as inhibitors for rice endosperm debranching enzyme. However, the cations were not essentially required for activity of *SU1* (sugary1 gene) in maize (Rahman et al. 1998). Furthermore, debranching activities of both rMeISA1/rMeISA2 and rMeISA3 were slightly increased in the presence of 1 mM EDTA in the reaction. This probably resulted from chelation of some metal ions possibly contaminated in the reaction such as Ni^{2+} from Histrap^{TM} column although the effect of Ni^{2+} was not tested. Moreover, effect of SDS (0.04% (w/v)) on enzyme activity was also determined. About 50% of activity of rMeISA1/rMeISA2 was lost while no debranching activity of rMeISA3 was observed. This implicated that SDS probably led to structurally changing of protein structure of rMeISA1/rMeISA2 and especially rMeISA3. (Barela and Darnall 1974) revealed that SDS cause loss in β-sheet with concomitant increase of α-helix and random coil in glyceraldehyde-3-phosphate dehydrogenase. Obviously, all three catalytic residues and important residues involving in substrate binding were located in beta 4, 5 and 7 regions shown in the primary sequence alignment of ISAs (Fig. 21), suggesting that both hydrolytic activity and substrate binding ability were interfered.

4.4.3 Substrate specificity

rMeISA1/rMeISA2 and rMeISA3 were incubated with 0.75% (w/v) of various types of substrate under their optimum conditions as mentioned above. rMeISA1/rMeISA2 showed the highest activity on maize amylopectin followed by potato amylopectin suggesting that structure of amylopectin was more appropriate for

interaction with the enzyme complex than other polysaccharides. However, glycogen was rarely to be digested because it was more extensively branched and compact than amylopectin. Optimal activity of rMeISA3 was apparently detected when beta-limit dextrin was used as substrate, supported by the peptide sequence analysis (Fig. 21 and Section 4.2). ISA3 was suggested to be most preferably active on glucan substrate with short chain lengths. Importantly, they could hardly hydrolyse pullulan, confirming their belonging to the isoamylase-type debranching enzyme.

4.4.4 Molecular weight determination of rMeISAs

Purification of the crude enzyme from 4 - 5 hours culture of recombinant cells was performed on Histrap^{TM} column eluted with imidazole. The pooled activity fraction was analysed by Silver stain of the SDS gel electrophoresis showing 2 protein bands with molecular weights of 87 and 99 kDa, corresponding to the deduced molecular weight of rMeISA1 and rMeISA2 respectively (Fig. 26A). rMeISA3 was also purified by Histrap^{TM} column and the single band with the size around 80 kDa was detected on SDS-PAGE by Coomassie staining (Fig. 26B), also similar to the size estimated from deduced amino acids.

4.4.5 Determination of molecular weight and rMeISA1:rMeISA2 ratio of enzyme complexes

To determine the heteromeric complexes between rMeISA1 and rMeISA2, crude extract of 4 - 5 h culture after induction was subjected to gel filtration chromatography on Sephacryl S-300 HR column. Enzyme activity was present in fractions 67 to 73, molecular weight of around 260 to 500 kDa (Fig. 36). Quantitation

of band intensity of his-tagged protein bands from fractions 60 - 74 immunoblotted on the membrane showed estimation of rMeISA1: rMeISA2 from 1:1 to 4:1 (Fig. 37). These results were supported by previous reports on enhanced enzyme activity when these two proteins associated. Wattebled et al. (2005) showed that these two isoforms of isoamylase are both crucial from the results of single mutation of At*ISA1* and At*ISA2* gene *in vivo* that represented the equal effect on amylopectin synthesis in *Arabidopsis*. In opposition to monocot plants and algae, there are three ISA complexes detected on nondenaturing PAGE consisting of one complex of homomeric ISA1 and two complexes of ISA1/ISA2 heteromers such as in maize (Facon et al. 2013; Fujita et al. 1999; Fujita et al. 2003; Kubo et al. 2010; Kubo et al. 1999) and *Chlamydomonas reinhardtii* (Dauvillée et al. 2001). Nevertheless, ISA1 was proposed to be more greatly important than ISA2. For example, Kubo and colleagues (2010) revealed that ISA1-null line caused the missing of all three complexes impacting on amylopectin biosynthesis by obviously increasing of degree of polymerization (DP) 5 to 12 chains while DP long chains were decreased compared to the wild type and significantly decreasing of starch content which displayed as flattened and distorted granules, whereas near-normal starch characteristics was observed in ISA2-null. This suggested that ISA1-null line showed more severe effects on amylopectin biosynthesis.

4.4.6 Chain Length Distribution analysis

Debranching products of rMeISA1/rMeISA2 were analysed on HPAEC-PAD compared to products from PaISA as a positive control (Fig. 38A). The patterns of chain length distribution of both enzymes were similar in the range of DP 6 to DP 20. However, under the same reaction condition and equal enzyme activity,

rMeISA1/rMeISA2 was 3 times less active than PaISA. At the same condition, rMeISA3 did not showed detectable products. When incubation time of rMeISA3 was increased from 1 to 21 hours, some products were observable with similar chain length distribution to those of rMeISA1/rMeISA2 and PaISA because amylopectin was not a preferable substrate for rMeISA3 (Fig. 38B).

4.4.7 Prediction of N- and O-glycosylations in rMeISAs

As these proteins were originally derived from eukaryotic organism, the prediction of glycosylation was performed. Glycosylation is the process of covalent attachment of a carbohydrate to a target biomolecule such as proteins and lipids. The modification provides various functions (Drickamer 2006). For example, some proteins folded correctly after they were glycosylated (Shental-Bechor and Levy 2008; Xu and Ng 2015). In addition, proteins could be more stable after containing oligosaccharides linked to asparagine residues. All three MeISAs were predicted to contain some sites for N- and O-glycosylations (Fig. 39). However, soluble rMeISA proteins could be produced and their debranching activities expressed in *E. coli* system, suggesting that the glycosylation, which is a post-translational process, was not absolutely required for enzyme activity. However, the glycosylation may affect the protein stability and solubility.

There have not been reports on cassava debranching enzymes. Although isoamylases have been reported in many plants and bacteria. This is the first report on molecular characterisation of three cassava isoamylases consisting of Me*ISA1*, Me*ISA2* and Me*ISA3*; co-expression of Me*ISA1* and Me*ISA2* and a unique pattern of its expression in recombinant form, and expression of Me*ISA3*. Unlike other biomolecules

such as nucleic acid and protein, carbohydrate is much more complicated in terms of its components and structure since it is a non-template coding molecule. Starch granule formation depends on the action of several enzymes including isoamylases. Although the real mechanism of isoamylases in starch synthesis is still unclear, our findings together with other reports suggested that ISA1 and ISA2 are important carbohydrate-metabolising enzymes playing a key role in mature amylopectin formation in starch biosynthesis although they were found to exist differently depending on sources. While, ISA3 showed the highest activity on beta-limit dextrin which is the major product of β-amylolysis in starch granules degradation therefore it is considered to be an important enzyme in starch degradation. The results from our works together with other previous studies on starch-metabolising enzymes would be a powerful tool of more clearly understanding of starch metabolism in cassava tubers for improvement of starch quantity and quality in the future such as by genetic modification.

CHAPTER V

CONCLUSIONS

1. Total RNA was isolated from cortex region of 9-month old cassava tubers cultivar KU50 and used as template for cDNA synthesis.
2. Full lengths of Me*ISA1* and Me*ISA2* were amplified by using the gene specific primers designed from Phytozome database, whereas full length of Me*ISA3* was obtained by 5' RACE using SMARTer 3'/5' RACE kit.
3. The mature Me*ISA1* and Me*ISA2* genes without their signal peptides were amplified and cloned into MCSI and MCSII of a pETDuet1 expression vector (pETDuet1MeISA1-2) for co-expression in *E. coli* SoluBL21 (DE3).
4. Crude extracts from recombinant cultures of MeISA1 and MeISA2 at 1^{st}, 4 - 5^{th} and 20^{th} h post induction were purified by Histrap^{TM} column eluted with imidazole, resulting in purified rMeISA2, rMeISA1/rMeISA2 and rMeISA1, respectively.
5. The maximum debranching activity was observed from the purified rMeISA1/rMeISA2. No debranching activity can be detected from the single purified rMeISA1 and rMeISA2 or in *in vitro* mixture of these two isoforms.
6. The molecular weights of rMeISA1 and rMeISA2 were determined to be 87 kDa and 99 kDa, respectively as analysed on SDS-PAGE.
7. Several rMeISA1/rMeISA2 complexes with debranching activity were determined to be in the range of 259 to 496 kDa by gel filtration on Sephacryl S-300 HR, with estimation of possible combination of rMeISA1: rMeISA2 at 1:1 to 4:1.

8. Mature Me*ISA3* gene excluding its signal peptide was cloned into a pET21b vector (pET21bMeISA3). Its molecular weight on SDS-PAGE was 80 kDa.
9. The optimum pH of rMeISA1/rMeISA2 was 7.0 while rMeISA3's was 6.0. The optimum temperatures of both rMeISA1/rMeISA2 and rMeISA3 were 37 ºC.
10. Debranching activity of rMeISA1/rMeISA2 was activated by Co^{2+}, Mg^{2+} and Ca^{2+}, whereas debranching activity of rMeISA3 was enhanced by Mn^{2+} and Co^{2+}. Cu^{2+} strongly inhibited all three rMeISAs. SDS led to 40% and 100% decreasing of activities of rMeISA1/rMeISA2 and rMeISA3, respectively.
11. rMeISA1/rMeISA2 was highly active on amylopectin substrate but rMeISA3 was most active on beta-limit dextrin. No activity on pullulan could be observed in both rMeISA1/rMeISA2 and rMeISA3.
12. The patterns of chain length distribution of rMeISA1/rMeISA2 and rMeISA3 were similar to that of PaISA but their activities were much lower, especially rMeISA3.
13. N- and O-glycosylations were detected in all MeISAs predicted by NetNGlyc 1.0 and NetOGlyc 4.0 servers.
14. Our finding, especially according to substrate specificity, demonstrated that ISA1/ISA2 are involved in starch synthesis via formation of mature amylopectin, while ISA3 is a key enzyme in starch degradation.

REFERENCES

Allem AC (1994) the origin of *Manihot esculenta* crantz (Euphorbiaceae). Genetic Resources and Crop Evolution 41:133-150

Baba T, Kimura K, Mizuno K, Etoh H, Ishida Y, Shida O, Arai Y (1991) Sequence conservation of the catalytic regions of anylolytic enzymes in maize branching enzyme-I. Biochemical and Biophysical Research Communications 181:87-94

Baguma Y (2004) Regulation of starch synthesis in cassava. Dissertation, Swedish University of Agricultural Sciences

Baguma Y et al. (2003) Expression patterns of the gene encoding starch branching enzyme II in the storage roots of cassava (*Manihot esculenta* Crantz). Plant Science 164:833-839

Ball S et al. (1996) From glycogen to amylopectin: A model for the biogenesis of the plant starch granule. Cell 86:349-352

Ball SG, Morell MK (2003) From bacterial glycogen to starch: Understanding the biogenesis of the plant starch granule. Annual Review of Plant Biology 54:207-233

Ballicora MA, Laughlin MJ, Fu Y, Okita TW, Barry GF, Preiss J (1995) Adenosine 5 [prime]-diphosphate-glucose pyrophosphorylase from potato tuber (significance of the N-terminus of the small subunit for catalytic properties and heat stability). Plant Physiology 109:245-251

Barela TD, Darnall DW (1974) Practical aspects of calculating protein secondary structure from circular dichroism spectra. Biochemistry 13:1694-1700

Beck E (1985) The degradation of transitory starch granules in chloroplasts

BeMiller JN, Whistler RL (2009) Starch: chemistry and technology. 3rd eds Academic Press, Amsterdam

Bertoft E, Piyachomkwan K, Chatakanonda P, Sriroth K (2008) Internal unit chain composition in amylopectins. Carbohydrate Polymers 74:527-543

Bhattacharyya MK, Smith AM, Ellis TN, Hedley C, Martin C (1990) The wrinkled-seed character of pea described by Mendel is caused by a transposon-like insertion in a gene encoding starch-branching enzyme. Cell 60:115-122

Blauth SL, Kim K-N, Klucinec J, Shannon JC, Thompson D, Guiltinan M (2002) Identification of Mutator insertional mutants of starch-branching enzyme 1 (sbe1) in Zea mays. Plant Molecular Biology 48:287-297

Blennow A, Engelsen SB (2010) Helix-breaking news: Fighting crystalline starch energy deposits in the cell. Trends in Plant Science 15:236-240

Bollag D, Rozycki M, Edelstein S (1996) Protein methods. 2nd eds Viley-Liss Press, USA

Bradbury JH, Holloway WD (1988) Chemistry of tropical root crops: Significance for nutrition and agriculture in the Pacific. Ramsay Ware Printing, Melhourne

Buléon A, Colonna P, Planchot V, Ball S (1998) Starch granules: Structure and biosynthesis. International Journal of Biological Macromolecules 23:85-112

Burton RA et al. (1995) Starch branching enzymes belonging to distinct enzyme families are differentially expressed during pea embryo development. The Plant Journal 7:3-15

Bustos R et al. (2004) Starch granule initiation is controlled by a heteromultimeric isoamylase in potato tubers. Proceedings of the National Academy of Sciences 101:2215-2220

Cao H, Imparl-Radosevich J, Guan H, Keeling PL, James MG, Myers AM (1999) Identification of the soluble starch synthase activities of maize endosperm. Plant Physiology 120:205-216

Catley B, Whelan W (1971) Observations on the structure of pullulan. Archives of Biochemistry and Biophysics 143:138-142

Colleoni C et al. (1999) Biochemical characterization of the *Chlamydomonas reinhardtii* α-1, 4 glucanotransferase supports a direct function in amylopectin biosynthesis. Plant Physiology 120:1005-1014

Craig J et al. (1998) Mutations in the gene encoding starch synthase II profoundly alter amylopectin structure in pea embryos. The Plant Cell 10:413-426

Critchley JH, Zeeman SC, Takaha T, Smith AM, Smith SM (2001) A critical role for disproportionating enzyme in starch breakdown is revealed by a knock-out mutation in Arabidopsis. The Plant Journal 26:89-100

Cross JM, Clancy M, Shaw JR, Greene TW, Schmidt RR, Okita TW, Hannah LC (2004) Both subunits of ADP-glucose pyrophosphorylase are regulatory. Plant Physiology 135:137-144

Dauvillée D et al. (2001) Biochemical characterization of wild-type and mutant isoamylases of *Chlamydomonas reinhardtii* supports a function of the multimeric enzyme organization in amylopectin maturation. Plant Physiology 125:1723-1731

Denyer K, Dunlap F, Thorbjornsen T, Keeling P, Smith AM (1996) The major form of ADP-glucose pyrophosphorylase in maize endosperm is extra-plastidial. Plant Physiology 112:779-785

Denyer K, Foster J, Smith AM (1995) The contributions of adenosine 5′-diphosphoglucose pyrophosphorylase and starch-branching enzyme to the control of starch synthesis in developing pea embryos. Planta 197:57-62

Denyer K, Johnson P, Zeeman S, Smith AM (2001) The control of amylose synthesis. Journal of Plant Physiology 158:479-487

Dinges JR, Colleoni C, James MG, Myers AM (2003) Mutational analysis of the pullulanase-type debranching enzyme of maize indicates multiple functions in starch metabolism. The Plant Cell 15:666-680

Doehlert DC, Knutson CA (1991) Two classes of starch debranching enzymes from developing maize kernels. Journal of Plant Physiology 138:566-572

Doehlert DC, Kuo TM, Juvik JA, Beers EP, Duke SH (1993) Characteristics of carbohydrate metabolism in sweet corn (sugary-1) endosperms. Journal of the American Society for Horticultural Science 118:661-666

Drickamer K (2006) Introduction to glycobiology. Oxford University Press, Oxford

Edner C et al. (2007) Glucan, water dikinase activity stimulates breakdown of starch granules by plastidial β-amylases. Plant Physiology 145:17-28

Edwards A et al. (1999) A combined reduction in activity of starch synthases II and III of potato has novel effects on the starch of tubers. The Plant Journal 17:251-261

Edwards A, Vincken J-P, Suurs LC, Visser RG, Zeeman S, Smith A, Martin C (2002) Discrete forms of amylose are synthesized by isoforms of GBSSI in pea. The Plant Cell 14:1767-1785

Facon M et al. (2013) Distinct functional properties of isoamylase-type starch debranching enzymes in monocot and dicot leaves. Plant Physiology 163:1363-1375

Fargette D, Fauquet C, Grenier E, Thresh J (1990) The spread of African cassava mosaic virus into and within cassava fields. Journal of Phytopathology 130:289-302

Favier J (1977) Nutritive value of two African staple foods: Cassava and sorghum nutritive value of two

Fazekas E, Szabó K, Kandra L, Gyémánt G (2013) Unexpected mode of action of sweet potato β-amylase on maltooligomer substrates. Biochimica et Biophysica Acta (BBA)-Proteins and Proteomics 1834:1976-1981

Fettke J, Fernie A, Steup M (2012) Transitory starch and its degradation in higher plant cells. Essential Reviews in Experimental Biol 5:309-372

Fontaine T et al. (1993) Toward an understanding of the biogenesis of the starch granule. Evidence that *Chlamydomonas* soluble starch synthase II controls the synthesis of intermediate size glucans of amylopectin. Journal of Biological Chemistry 268:16223-16230

Fujita N, Kubo A, Francisco PB, Nakakita M, Harada K, Minaka N, Nakamura Y (1999) Purification, characterization, and cDNA structure of isoamylase from developing endosperm of rice. Planta 208:283-293

Fujita N et al. (2003) Antisense inhibition of isoamylase alters the structure of amylopectin and the physicochemical properties of starch in rice endosperm. Plant and Cell Physiology 44:607-618

Gao M, Fisher DK, Kim K-N, Shannon JC, Guiltinan MJ (1997) Independent genetic control of maize starch-branching enzymes IIa and IIb (isolation and characterization of a Sbe2a cDNA). Plant Physiology 114:69-78

Gao M, Wanat J, Stinard PS, James MG, Myers AM (1998) Characterization of dull1, a maize gene coding for a novel starch synthase. The Plant Cell 10:399-412

Ghosh B, Ray R (2010) Saccharification of raw native starches by extracellular isoamylase of *Rhizopus oryzae*. Biotechnology 9:224-228

Giroux MJ, Shaw J, Barry G, Cobb BG, Greene T, Okita T, Hannah LC (1996) A single mutation that increases maize seed weight. Proceedings of the National Academy of Sciences 93:5824-5829

Gómez-Casati DF, Iglesias AA (2002) ADP-glucose pyrophosphorylase from wheat endosperm. Purification and characterization of an enzyme with novel regulatory properties. Planta 214:428-434

Green MM, Blankenhorn G, Hart H (1975) Which starch fraction is water-soluble, amylose or amylopectin?. Journal of Chemical Education 52:729-730

Guan HP, Preiss J (1993) Differentiation of the properties of the branching isozymes from maize (*Zea mays*). Plant Physiology 102:1269-1273

Hannah L, Nelson O (1976) Characterization of ADP-glucose pyrophosphorylase from shrunken-2 and brittle-2 mutants of maize. Biochemical Genetics 14:547-560

Hejazi M et al. (2008) Glucan, water dikinase phosphorylates crystalline maltodextrins and thereby initiates solubilization. The Plant Journal 55:323-334

Hickman BE, Janaswamy S, Yao Y (2009) Autoclave and β-amylolysis lead to reduced *in vitro* digestibility of starch. Journal of Agricultural and Food Chemistry 57:7005-7012

Hovenkamp-Hermelink J et al. (1987) Isolation of an amylose-free starch mutant of the potato (*Solanum tuberosum* L.). Theoretical and Applied Genetics 75:217-221

Hussain H et al. (2003) Three isoforms of isoamylase contribute different catalytic properties for the debranching of potato glucans. The Plant Cell 15:133-149

Hussain H, Martin C (2009) Comparative analysis of primary and secondary structure for pea isoamylase isoforms predicts different catalytic properties against glucan substrates. Starch-Stärke 61:570-577

Hwang S-K, Salamone PR, Okita TW (2005) Allosteric regulation of the higher plant ADP-glucose pyrophosphorylase is a product of synergy between the two subunits. FEBS letters 579:983-990

Imparl-Radosevich JM, Nichols DJ, Li P, McKean AL, Keeling PL, Guan H (1999) Analysis of purified maize starch synthases IIa and IIb: SS isoforms can be distinguished based on their kinetic properties. Archives of Biochemistry and Biophysics 362:131-138

Ishikawa N, Ishihara J, Itoh M (1994) Artificial induction and characterization of amylose-free mutants of barley. Barley Genetics Newsletter

Ishizaki Y, Taniguchi H, Maruyama Y, Nakamura M (1983) Debranching enzymes of potato tubers (*Solanum tuberosum* L.). Purification and some properties of potato isoamylase. Agricultural and Biological Chemistry 47:771-779

Iwaki K, Fuwa H (1981) Purification and some properties of debranching enzyme of germinating rice endosperm. Agricultural and Biological Chemistry 45:2683-2688

James MG, Robertson DS, Myers AM (1995) Characterization of the maize gene sugary1, a determinant of starch composition in kernels. The Plant Cell 7:417-429

Jespersen HM, Ann MacGregor E, Henrissat B, Sierks MR, Svensson B (1993) Starch- and glycogen-debranching and branching enzymes: Prediction of structural features of the catalytic (β/α) 8-barrel domain and evolutionary relationship to other amylolytic enzymes. Journal of Protein Chemistry 12:791-805

Jobling SA et al. (1999) A minor form of starch branching enzyme in potato (*Solanum tuberosum* L.) tubers has a major effect on starch structure: Cloning and characterisation of multiple forms of SBE A. The Plant Journal 18:163-171

Johnson PE et al. (2003) A low-starch barley mutant, Risø 16, lacking the cytosolic small subunit of ADP-glucose pyrophosphorylase, reveals the importance of the cytosolic isoform and the identity of the plastidial small subunit. Plant Physiology 131:684-696

Johnston K, Clements A, Venkataramani RN, Trievel RC, Marmorstein R (2000) Coexpression of proteins in bacteria using T7-based expression plasmids: Expression of heteromeric cell-cycle and transcriptional regulatory complexes. Protein Expression and Purification 20:435-443

Jos J (1969) Cytological aspects of cassava. Cassava Production Technologies:10-14

Kainuma K (1988) Structure and chemistry of the starch granule. The Biochemistry of Plants 14:141-180

Kalinga DN, Waduge R, Liu Q, Yada RY, Bertoft E, Seetharaman K (2013) On the differences in the granular architecture and starch structure between pericarp and endosperm wheat starches. Starch-Stärke 65:791-800

Katsuya Y, Mezaki Y, Kubota M, Matsuura Y (1998) Three-dimensional structure of *Pseudomonas* isoamylase at 2.2 Å resolution. Journal of Molecular Biology 281:885-897

Kawasaki T, Hayashida N, Baba T, Shinozaki K, Shimada H (1993) The gene encoding a calcium-dependent protein kinase located near the sbe1 gene encoding starch branching enzyme I is specifically expressed in developing rice seeds. Gene 129:183-189

Keeling PL, Myers AM (2010) Biochemistry and genetics of starch synthesis. Annual Review of Food Science and Technology 1:271-303

Kim J-S et al. (1999) Crystal structure of a maltogenic amylase provides insights into a catalytic versatility. Journal of Biological Chemistry 274:26279-26286

Kim KJ, Kim HE, Lee KH, Han W, Yi MJ, Jeong J, Oh BH (2004) Two-promoter vector is highly efficient for overproduction of protein complexes. Protein science 13:1698-1703

Koshland DE (1953) Stereochemistry and the mechanism of enzymatic reactions. Biological Reviews 28:416-436

Kötting O et al. (2009) Starch-excess 4 is a laforin-like phosphoglucan phosphatase required for starch degradation in *Arabidopsis thaliana*. The Plant Cell Online 21:334-346

Kubo A et al. (2010) Functions of heteromeric and homomeric isoamylase-type starch-debranching enzymes in developing maize endosperm. Plant Physiology 153:956-969

Kubo A, Fujita N, Harada K, Matsuda T, Satoh H, Nakamura Y (1999) The starch-debranching enzymes isoamylase and pullulanase are both involved in amylopectin biosynthesis in rice endosperm. Plant Physiology 121:399-410

Kuroiwa T, Shoda H, Ichikawa S, Sato S, Mukataka S (2005) Immobilization and stabilization of pullulanase from *Klebsiella pneumoniae* by a multipoint attachment method using activated agar gel supports. Process Biochemistry 40:2637-2642

Leathers TD (2003) Biotechnological production and applications of pullulan. Applied Microbiology and Biotechnology 62:468-473

Leloir LF, de Fekete MAR, Cardini CE (1961) Starch and oligosaccharide synthesis from uridine diphosphate glucose. Journal of Biological Chemistry 236:636-641

Lin T-P, Preiss J (1988) Characterization of D-enzyme (4-α-glucanotransferase) in *Arabidopsis* leaf. Plant Physiology 86:260-265

Lloyd JR, Landschutze V, Kossmann J (1999) Simultaneous antisense inhibition of two starch-synthase isoforms in potato tubers leads to accumulation of grossly modified amylopectin. Biochemical Journal 338:515-521

Lorberth R, Ritte G, Willmitzer L, Kossmann J (1998) Inhibition of a starch-granule–bound protein leads to modified starch and repression of cold sweetening. Nature Biotechnology 16:473-477

Manners D, Rowe KL (1969) Studies on carbohydrate-metabolising enzymes: Part XXI. The α-glucosidase and D-enyme activity of extracts of carrots and tomatoes. Carbohydrate Research 9:441-450

McGuffin M, Tucker A., Leung A. Y., Kartesz J. T. (2000) Herbs of commerce. American Herbal Products Association, 2nd eds.

Mikami B, Degano M, Hehre EJ, Sacchettini JC (1994) Crystal structures of soybean. beta-amylase reacted with beta-maltose and maltal: Active site components and their apparent roles in catalysis. Biochemistry 33:7779-7787

Miller G (1959) Modified DNS method for reducing sugars. Analytical Chemistry 31:426-428

Mizuno K et al. (1993) Alteration of the structural properties of starch components by the lack of an isoform of starch branching enzyme in rice seeds. Journal of Biological Chemistry 268:19084-19091

Morell MK, Blennow A, Kosar-Hashemi B, Samuel MS (1997) Differential expression and properties of starch branching enzyme isoforms in developing wheat endosperm. Plant Physiology 113:201-208

Mouille G, Maddelein M-L, Libessart N, Talaga P, Decq A, Delrue B, Ball S (1996) Preamylopectin processing: A mandatory step for starch biosynthesis in plants. The Plant Cell 8:1353-1366

Müller-Röber BT, Koßmann J, Hannah LC, Willmitzer L, Sonnewald U (1990) One of two different ADP-glucose pyrophosphorylase genes from potato responds strongly to elevated levels of sucrose. Molecular and General Genetics 224:136-146

Munyikwa T, Langeveld S, Salehuzzaman S, Jacobsen E, Visser R (1997) Cassava starch biosynthesis: New avenues for modifying starch quantity and quality. Euphytica 96:65-75

Murata T, Sugiyama T, Akazawa T (1965) Enzymic mechanism of starch synthesis in glutinous rice grains. Biochemical and Biophysical Research Communications 18:371-376

Mutisya J et al. (2003) Starch branching enzymes in sorghum (*Sorghum bicolor*) and barley (*Hordeum vulgare*): Comparative analyses of enzyme structure and gene expression. Journal of Plant Physiology 160:921-930

Myers AM, Morell MK, James MG, Ball SG (2000) Recent progress toward understanding biosynthesis of the amylopectin crystal. Plant Physiology 122:989-998

Nair RB, Båga M, Scoles GJ, Kartha KK, Chibbar RN (1997) Isolation, characterization and expression analysis of a starch branching enzyme II cDNA from wheat. Plant Science 122:153-163

Nakamura T, Vrinten P, Hayakawa K, Ikeda J (1998) Characterization of a granule-bound starch synthase isoform found in the pericarp of wheat. Plant Physiology 118:451-459

Nakamura T, Yamamori M, Hirano H, Hidaka S, Nagamine T (1995) Production of waxy (amylose-free) wheats. Molecular and General Genetics 248:253-259

Nakamura Y, Kubo A, Shimamune T, Matsuda T, Harada K, Satoh H (1997) Correlation between activities of starch debranching enzyme and α-polyglucan structure in endosperms of sugary-1 mutants of rice. The Plant Journal 12:143-153

Nakamura Y, Umemoto T, Ogata N, Kuboki Y, Yano M, Sasaki T (1996) Starch debranching enzyme (R-enzyme or pullulanase) from developing rice endosperm: Purification, cDNA and chromosomal localization of the gene. Planta 199:209-218

Okita TW (1992) Is there an alternative pathway for starch synthesis?. Plant Physiology 100:560-564

Okita TW, Greenberg E, Kuhn DN, Preiss J (1979) Subcellular localization of the starch degradative and biosynthetic enzymes of spinach leaves. Plant Physiology 64:187-192

Olsen KM, Schaal BA (2001) Microsatellite variation in cassava (*Manihot esculenta*, Euphorbiaceae) and its wild relatives: Further evidence for a southern Amazonian origin of domestication. American Journal of Botany 88:131-142

Peat S, Whelan W, Rees W (1956). The enzymic synthesis and degradation of starch. Part XX. The disproportionating enzyme (D-enzyme) of the potato. Journal of the Chemical Society (Resumed) 10:44-53

Qian M, Nahoum V, Bonicel J, Bischoff H, Henrissat B, Payan F (2001) Enzyme-catalyzed condensation reaction in a mammalian α-amylase. High-resolution structural analysis of an enzyme-inhibitor complex. Biochemistry 40:7700-7709

Rahman A, Wong K-s, Jane J-l, Myers AM, James MG (1998) Characterization of SU1 isoamylase, a determinant of storage starch structure in maize. Plant Physiology 117:425-435

Reddy RM, Reddy PG, Seenayya G (1999) Enhanced production of thermostable β-amylase and pullulanase in the presence of surfactants by *Clostridium* thermosulfurogenes SV2. Process Biochemistry 34:87-92

Ritte G, Heydenreich M, Mahlow S, Haebel S, Kötting O, Steup M (2006) Phosphorylation of C6-and C3-positions of glucosyl residues in starch is catalysed by distinct dikinases. FEBS letters 580:4872-4876

Rogers DJ, Appan SG (1973) *Manihot* and *Manihotoides* (Euphorbiaceae): A computer assisted study. Flora Neotropica. Hafner Press, New York

Salamone PR, Kavakli IH, Slattery CJ, Okita TW (2002) Directed molecular evolution of ADP-glucose pyrophosphorylase. Proceedings of the National Academy of Sciences 99:1070-1075

Salehuzzaman S, Jacobsen E, Visser R (1992) Cloning, partial sequencing and expression of a cDNA coding for branching enzyme in cassava. Plant Molecular Biology 20:809-819

Sambrook J, Fritsch EF, Maniatis T (1989) Molecular cloning: A laboratory manual. 2nd eds Cold Spring Harbor Laboratory Press, New York

Satoh H et al. (2003) Starch-branching enzyme I-deficient mutation specifically affects the structure and properties of starch in rice endosperm. Plant Physiology 133:1111-1121

Scheidig A, Fröhlich A, Schulze S, Lloyd JR, Kossmann J (2002) Downregulation of a chloroplast-targeted β-amylase leads to a starch-excess phenotype in leaves. The Plant Journal 30:581-591

Schwall GP et al. (2000) Production of very-high-amylose potato starch by inhibition of SBE A and B. Nature Biotechnology 18:551-554

Seo B-s, Kim S, Scott MP, Singletary GW, Wong K-s, James MG, Myers AM (2002) Functional interactions between heterologously expressed starch-branching enzymes of maize and the glycogen synthases of Brewer's yeast. Plant Physiology 128:1189-1199

Shental-Bechor D, Levy Y (2008) Effect of glycosylation on protein folding: A close look at thermodynamic stabilization. Proceedings of the National Academy of Sciences 105:8256-8261

Sim L, Beeren SR, Findinier J, Dauvillée D, Ball SG, Henriksen A, Palcic MM (2014) Crystal structure of the *Chlamydomonas* starch debranching enzyme isoamylase ISA1 reveals insights into the mechanism of branch trimming and complex assembly. Journal of Biological Chemistry 289:22991-23003

Singh S, Choi S-B, Modi MK, Okita TW (2002) Isolation and characterization of cDNA clones encoding ADP-glucose pyrophosphorylase (AGPase) large and small subunits from chickpea (*Cicer arietinum* L.). Phytochemistry 59:261-268

Sinnott ML (1990) Catalytic mechanism of enzymic glycosyl transfer. Chemical Reviews 90:1171-1202

Smith-White BJ, Preiss J (1992) Comparison of proteins of ADP-glucose pyrophosphorylase from diverse sources. Journal of Molecular Evolution 34:449-464

Smith A, Martin C (1993) Starch biosynthesis and the potential for its manipulation. Biosynthesis and Manipulation of Plant Products. Springer, Netherlands

Smith AM (2012) Starch in the *Arabidopsis* plant. Starch-Stärke 64:421-434

Smith AM, Denyer K, Martin CR (1995) What controls the amount and structure of starch in storage organs?. Plant Physiology 107:673

Srichuwong S, Sunarti TC, Mishima T, Isono N, Hisamatsu M (2005) Starches from different botanical sources II: Contribution of starch structure to swelling and pasting properties. Carbohydrate Polymers 62:25-34

Steup M, Robenek H, Melkonian M (1983) *In-vitro* degradation of starch granules isolated from spinach chloroplasts. Planta 158:428-436

Sun C, Sathish P, Ahlandsberg S, Jansson C (1998) The two genes encoding starch-branching enzymes IIa and IIb are differentially expressed in barley. Plant Physiology 118:37-49

Svensson B (1994) Protein engineering in the α-amylase family: Catalytic mechanism, substrate specificity, and stability. Plant Molecular Biology 25:141-157

Tabata S, Hizukuri S, Nagata K (1978) Action of sweet-potato beta-amylase on phosphodextrin of potato starch. Carbohydrate Research 67:189-195

Takaha T, Critchley J, Okada S, Smith SM (1998) Normal starch content and composition in tubers of antisense potato plants lacking D-enzyme (4-α-glucanotransferase). Planta 205:445-451

Takeda Y, Hizukuri S (1981) Re-examination of the action of sweet-potato beta-amylase on phosphorylated (1→ 4)-χ-d-glucan. Carbohydrate Research 89:174-178

Takeda Y, Hizukuri S (1982) Location of phosphate groups in potato amylopectin. Carbohydrate Research 102:321-327

Tantanarat K, O'Neill EC, Rejzek M, Field RA, Limpaseni T (2014) Expression and characterization of 4-α-glucanotransferase genes from *Manihot esculenta* Crantz and *Arabidopsis thaliana* and their use for the production of cycloamyloses. Process Biochemistry 49:84-89

Tester RF, Karkalas J, Qi X (2004) Starch-composition, fine structure and architecture. Journal of Cereal Science 39:151-165

Tetlow IJ, Morell MK, Emes MJ (2004) Recent developments in understanding the regulation of starch metabolism in higher plants. Journal of Experimental Botany 55:2131-2145

Thorbjørnsen T, Villand P, Denyer K, Olsen OA, Smith AM (1996) Distinct isoforms of ADP-glucose pyrophosphorylase occur inside and outside the amyloplasts in barley endosperm. The Plant Journal 10:243-250

Tonukari NJ (2004) Cassava and the future of starch. Electronic Journal of Biotechnology 7:5-8

Topping DL, Clifton PM (2001) Short-chain fatty acids and human colonic function: Roles of resistant starch and nonstarch polysaccharides. Physiological Reviews 81:1031-1064

Vermeylen R, Goderis B, Delcour JA (2006) An X-ray study of hydrothermally treated potato starch. Carbohydrate Polymers 64:364-375

Visser R, Somhorst I, Kuipers G, Ruys N, Feenstra WJ, Jacobsen E (1991) Inhibition of the expression of the gene for granule-bound starch synthase in potato by antisense constructs. Molecular and General Genetics 225:289-296

Vrinten PL, Nakamura T (2000) Wheat granule-bound starch synthase I and II are encoded by separate genes that are expressed in different tissues. Plant Physiology 122:255-264

Wattebled F et al. (2005) Mutants of *Arabidopsis* lacking a chloroplastic isoamylase accumulate phytoglycogen and an abnormal form of amylopectin. Plant Physiology 138:184-195

Weatherwax P (1922) A rare carbohydrate in waxy maize. Genetics 7:568-572

Woo E-J, Lee S, Cha H, Park J-T, Yoon S-M, Song H-N, Park K-H (2008) Structural insight into the bifunctional mechanism of the glycogen-debranching enzyme TreX from the archaeon *Sulfolobus solfataricus*. Journal of Biological Chemistry 283:28641-28648

Woot-Tsuen W, Busson F, Jardin C (1968) Food composition table for use in Africa. FAO Corporate Document Repository. Rome, Italy.

Xu C, Ng DT (2015) Glycosylation-directed quality control of protein folding. Nature Reviews Molecular Cell Biology 16:742-752

Yaiyen S (2009) Expression of strach branching enzyme genes cloned from cassava *Manihot esculenta* crantz and immunological monitoring of the enzymes. Dissertation, Chulalongkorn University

Yu T-S et al. (2001) The Arabidopsis sex1 mutant is defective in the R1 protein, a general regulator of starch degradation in plants, and not in the chloroplast hexose transporter. The Plant Cell 13:1907-1918

Zeeman SC, Smith SM, Smith AM (2007) The diurnal metabolism of leaf starch. Biochemical Journal 401:13-28

Zeeman SC, Umemoto T, Lue W-L, Au-Yeung P, Martin C, Smith AM, Chen J (1998) A mutant of *Arabidopsis* lacking a chloroplastic isoamylase accumulates both starch and phytoglycogen. The Plant Cell 10:1699-1711

Zhang H, Jin Z (2011) Preparation of resistant starch by hydrolysis of maize starch with pullulanase. Carbohydrate Polymers 83:865-867

Zhu Z-P, Hylton CM, Rössner U, Smith AM (1998) Characterization of starch-debranching enzymes in pea embryos. Plant Physiology 118:581-590

จุฬาลงกรณ์มหาวิทยาลัย
Chulalongkorn University

APPENDICES

APPENDIX A

Preparation of polyacrylamide gel electrophoresis

1. Stock reagents

1 M Tris-HCl pH 6.8

Tris (hydroxymethyl)-aminomethane 12.1 g

Adjust pH to 6.8 with conc. HCl and adjust volume to 100 ml with distilled water

1 M Tris-HCl pH 8.8

Tris (hydroxymethyl)-aminomethane 12.1 g

Adjust pH to 8.8 with conc. HCl and adjust volume to 100 ml with distilled water

10% (w/v) SDS solution

SDS 10 g

Add distilled water to the final volume of 100 ml

10% Ammonium persulfate ($(NH_4)_2S_2O_8$)

Ammonium persulfate 1 g

Add distilled water to the final volume of 10 ml

2. Non-denaturing PAGE

6% Separating gel, 10ml

40% Acrylamide solution	1.5 ml
1 M Tris-HCl pH 8.8	3.75 ml
1.5% (w/v) amylopectin/ 1.5% (w/v) beta-limit dextrin	1 ml
Distilled water	3.65 ml
10% $(NH_4)_2S_2O_8$	100 µl
TEMED	13 µl

5% Stacking gel, 4 ml

40% Acrylamide solution	0.5 ml
1 M Tris-HCl pH 6.8	0.5 ml
Distilled water	3 ml
10% $(NH_4)_2S_2O_8$	50 µl
TEMED	13 µl

5X Sample buffer

1 M Tris-HCl pH 6.8	3.1 ml
Glycerol	5.0 ml
1% Bromophenol blue	0.5 ml
Distilled water	1.4 ml

One part of sample was mixed with four parts of protein sample.

10X Electrophoresis buffer pH 8.3, 1 litre

Tris (hydroxymethyl)-aminomethane	30 g
Glycine	144 g

Adjust pH to 8.3 and adjust volume to 1 litre with distilled water,

One part of electrophoresis buffer was mixed with nine parts of distilled water.

3. SDS-PAGE

8% Separating gel, 10 ml

40% Acrylamide solution	2 ml
1 M Tris-HCl pH 8.8	3.75 ml
Distilled water	4.05 ml
10% SDS solution	100 µl
10% $(NH_4)_2S_2O_8$	100 µl
TEMED	13 µl

5% Stacking gel, 5 ml

40% Acrylamide solution	625 µl
1 M Tris-HCl pH 6.8	625 µl
Distilled water	3.65 ml
10% SDS solution	50 µl
10% $(NH_4)_2S_2O_8$	50 µl
TEMED	13 µl

5X Sample buffer, 10 ml

1 M Tris-HCl pH 6.8	0.6 ml
50% Glycerol	5 ml
2-Mercaptoethanol	0.5 ml
10% SDS solution	2 ml
1% Bromophenol blue	1 ml
Distilled water	0.9 ml

One part of sample was mixed with four parts of protein sample.

10X Electrophoresis buffer, 1 litre

Tris (hydroxymethyl)-aminomethane	30 g
Glycine	144 g
SDS	10 g

Adjust volume with distilled water to 1 litre (No pH adjustment is required, final pH should be 8.3), One part of electrophoresis buffer was dissolved in nine parts of distilled water.

APPENDIX B

Preparation of Western blot reagents

Stock reagents

10X Tris Buffer Saline (TBS) pH 7.6, 1 litre

Tris (hydroxymethyl)-aminomethane	60.5 g
NaCl	87.6 g

Adjust to pH 7.6 and adjust to final volume of 1 litre

One part of TBS buffer was mixed with nine parts of distilled water.

10X Tris Glycine buffer (TG) pH 8.3, 1 litre

Tris (hydroxymethyl)-aminomethane	30 g
Glycine	144 g

(Final pH should be 8.3)

One part of electrophoresis buffer was mixed with nine parts of distilled water.

Alkaline phosphatase buffer;

10X $MgCl_2 \cdot H_2O$, 100 ml

$MgCl_2 \cdot H_2O$	1.02 g

Adjust to 100 ml with distilled water

10X NaCl, 100 ml

NaCl	5.84 g

Adjust to 100 ml with distilled water

10X Tris-HCl pH 9.5, 100 ml

Tris (hydroxymethyl)-aminomethane	12.11 g

Adjust pH to 9.5 with conc. HCl and adjust volume to 100 ml with distilled water

Alkaline phosphatase substrates;

50 mg/ml NBT

NBT	50 mg
70% dimethylformamide	1 ml

Stored at -20 °C

50 mg/ml BCIP

BCIP	50 mg
100% dimethylformamide	1 ml

Stored at -20 °C

APPENDIX C

Lists of isoamylase isoforms in different sources

Accession number	Abbreviation	Amino acid residue	Source
1BF2_A	PaISA	776	*Pseudomonas amyloderamosa*
-	MeISA1	794	Cassava (*Manihot esculenta* Crantz)
-	MeISA2	883	
-	MeISA3	781	
NP_001274937.1	StISA1	793	Potato (*Solanum tuberosum*)
NP_001274804.1	StISA2	878	
NP_001275220.1	StISA3	766	
NP_181522.1	AtISA1	783	Arabidopsis (*Arabidopsis thaliana*)
NP_171830.1	AtISA2	882	
NP_192641.2	AtISA3	764	
XP_003532455.2	GmISA1	798	Soybeaan (*Glycine max*)
XP_003554240.1	GmISA2	865	
XP_006578313.1	GmISA3	783	
AAZ81835.1	PsISA1	791	Pea (*Pisum sativum*)
AAZ81836.1	PsISA2	857	
AAZ81837.1	PsISA3	736	
AII21931.**1**	OsISA1	803	Rice (*Oryza sativa*)
XP_015637296.1	OsISA2	800	
XP_015612255.1	OsISA3	782	

APPENDIX D

Protein staining solution

1. Coomassie staining

Coomassie stain solution, 1 litre

Coomassie Blue R-250	1 g
Methanol	450 ml
Gracial acetic acid	100 ml
Adjust volume to 1 litre with distilled water	

Destaining solution, 1 litre

Methanol	100 ml
Gracial acetic acid	100 ml
Adjust volume to 1 litre with distilled water	

2. Silver staining

Fix solution

Methanol	50 ml
Gracial acetic acid	10 ml
Adjust volume to 100 ml with ultra-pure water	

Solution A

Silver nitrate	4 g
Add distilled water to the final volume of 2 ml	

Solution B

0.36% (w/v) NaOH	10.5 ml
25% ammoniumhydroxide	840 µl
Adjust volume to 50 ml with ultra-pure water	

Solution D

1% (w/v) citric acid	250 µl
30% formaldehyde	31.67 µl
Adjust volume to 50 ml with ultra-pure water	

Stop solution

Gracial acetic acid	1 ml
Adjust volume to 100 ml with ultra-pure water	

APPENDIX E

Preparation of agarose gel electrophoresis buffer

10X Tris Boric EDTA (TBE) buffer, pH 8.3

Tris (hydroxymethyl)-aminomethane	108 g
Boric acid	55 g
EDTA	9.3 g

Adjust pH to 8.3 and adjust volume to 1 litre with distilled water

APPENDIX F

Preparation of buffer solutions

1 M potassium phosphate buffer, pH 7.2

K_2HPO_4	87 g
KH_2PO_4	68 g

Adjust pH to 7.2 and adjust volume to 1 litre with distilled water

Binding buffer, pH 7.2

1M potassium phosphate buffer	25 ml
NaCl	5.8 g
Imidazole	2.7 g

Adjust pH to 7.2 and adjust volume to 1 litre with distilled water

Elution buffer, pH 7.2 (500 mM imidazole)

1M potassium phosphate buffer	25 ml
NaCl	5.8 g
Imidazole	29 g

Adjust pH to 7.2 and adjust volume to 1 litre with distilled water

Gel filtration buffer, pH 7.2

1M potassium phosphate buffer	25 ml
NaCl	2.9 g

Adjust pH to 7.2 and adjust volume to 1 litre with distilled water

APPENDIX G

Iodine solution

Iodine solution

1% Potassium iodide; 0.1% Iodine

Potassium iodide	1 g
Iodine	0.1 g

Adjust to final volume of 100 ml with distilled water

APPENDIX H

Calibration curves

1. Calibration curve of protein concentration (Bradford method)

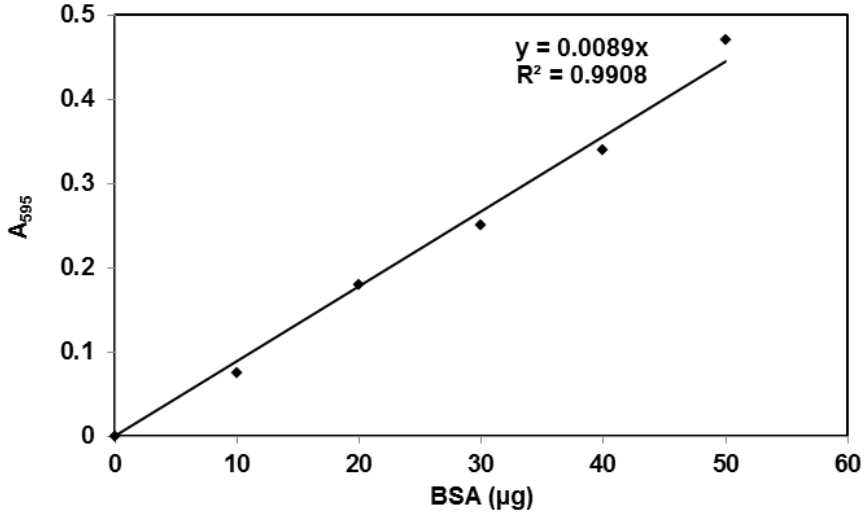

2. Calibration curve of glucose (Modified DNS method)

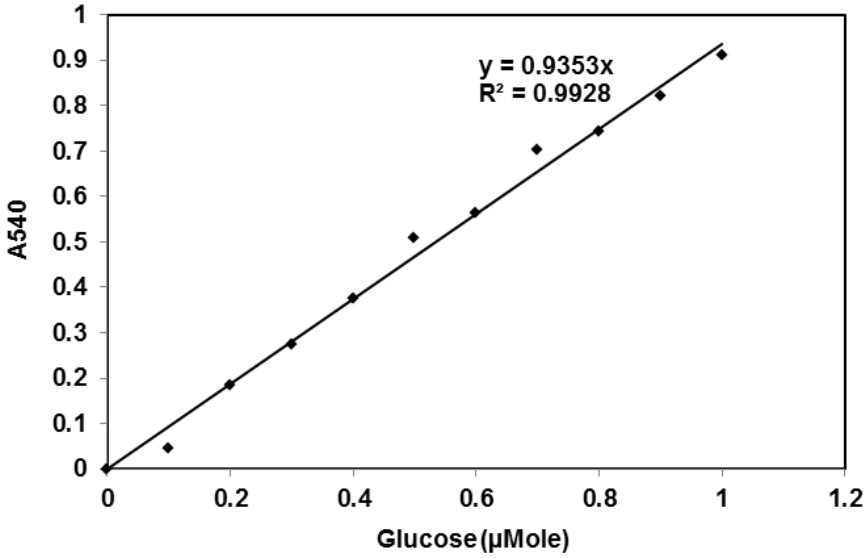

3. Calibration curve of protein standard markers

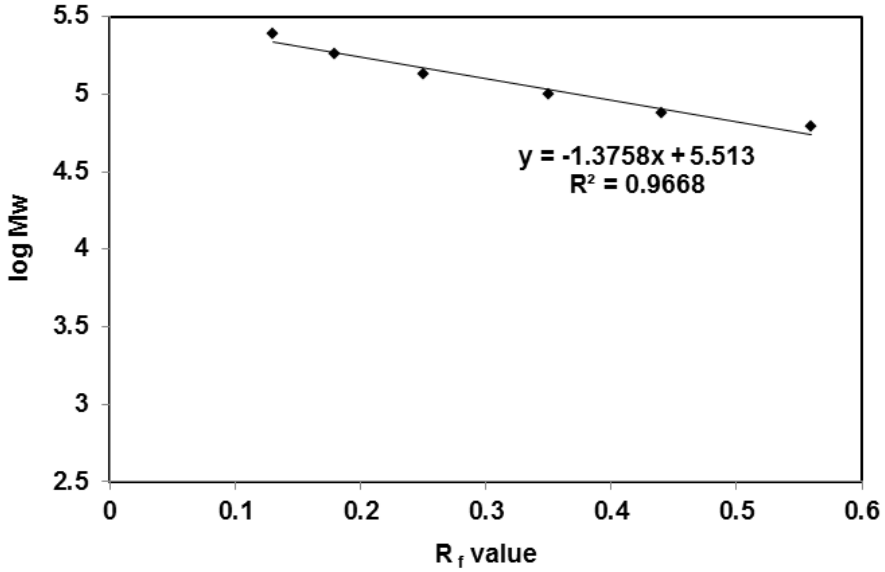

APPENDIX I

Vector maps

1. pJET1.2/blunt cloning vector

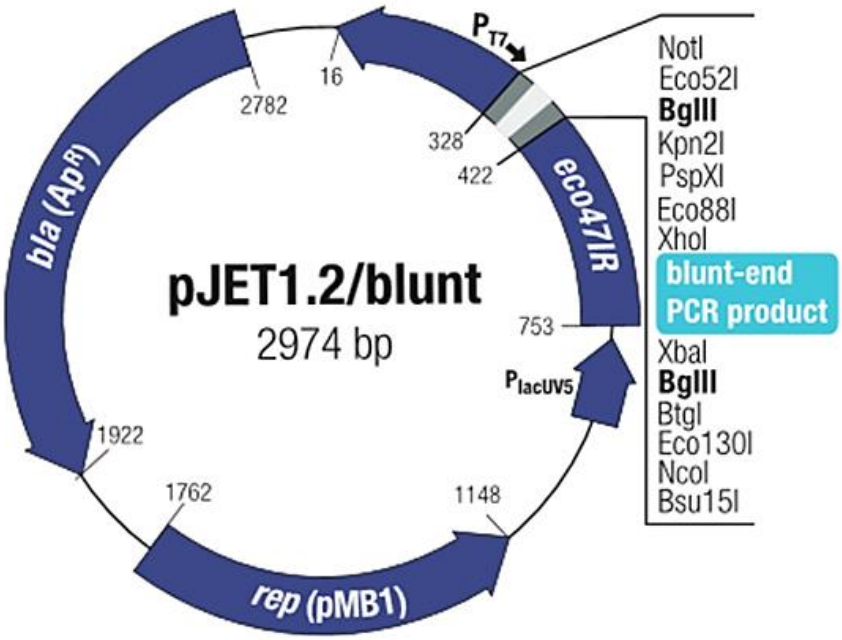

2. pETDuet1 expression vector

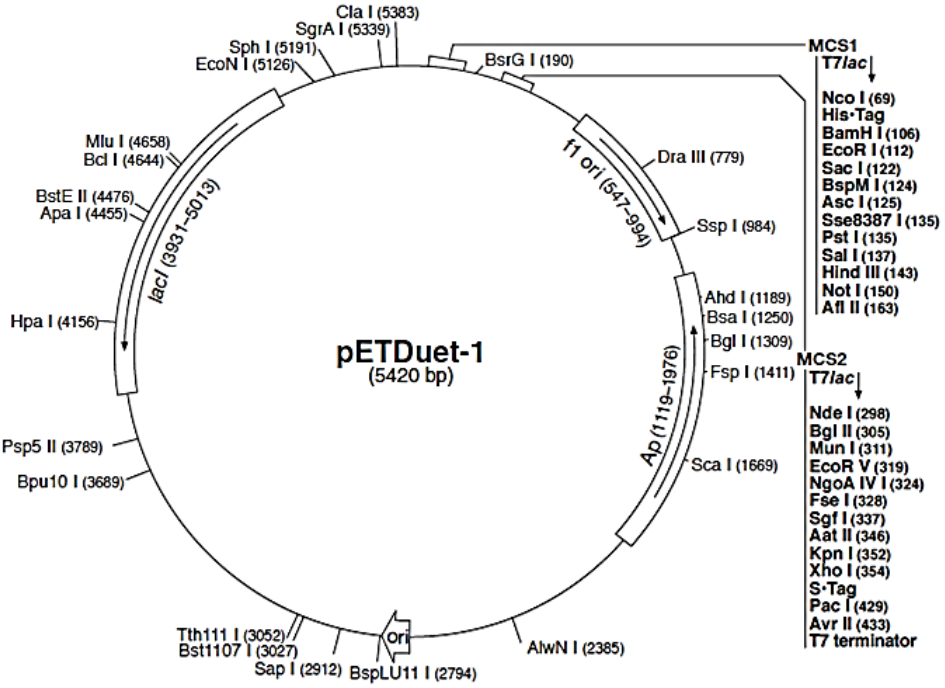

3. pETDuet1MeISA1-2 plasmid

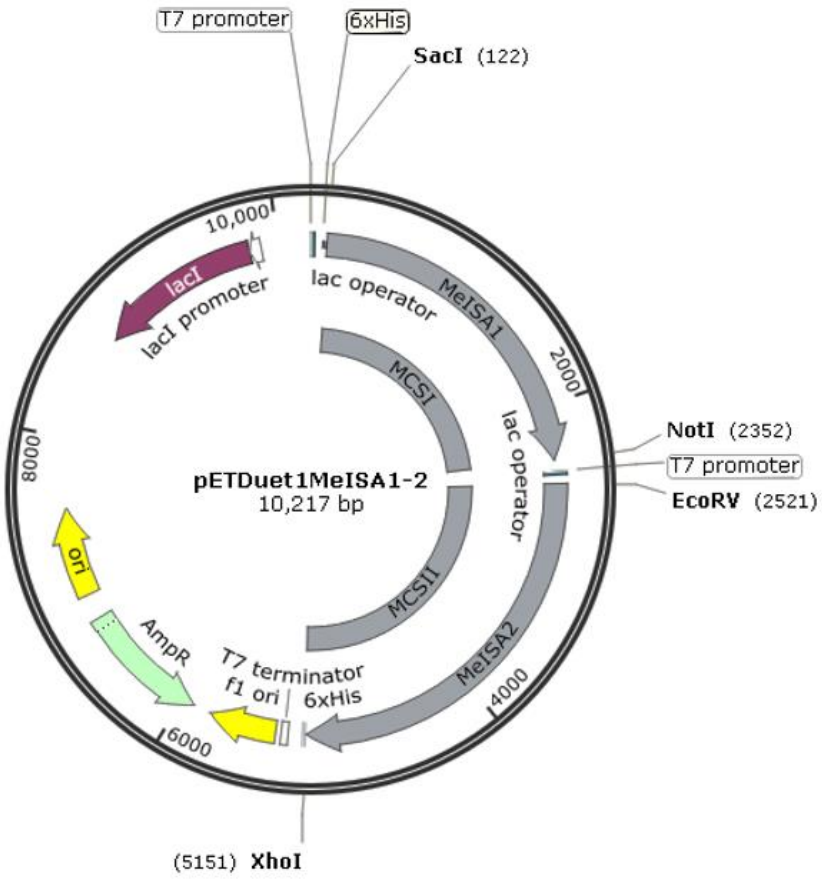

4. pET21b expression vector

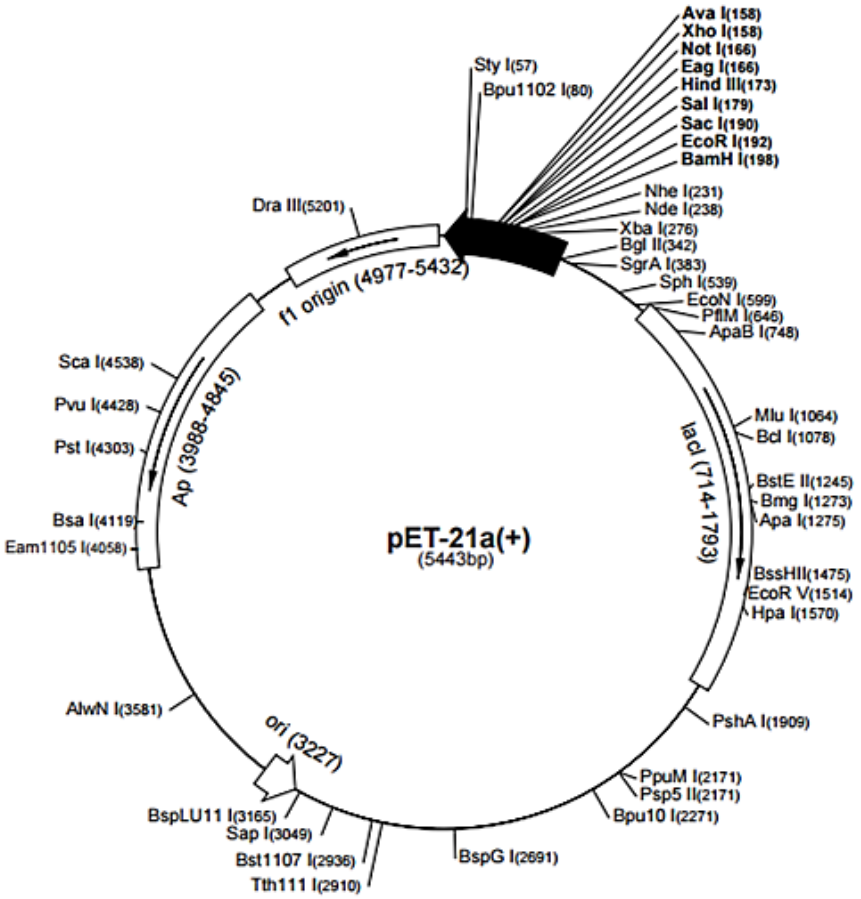

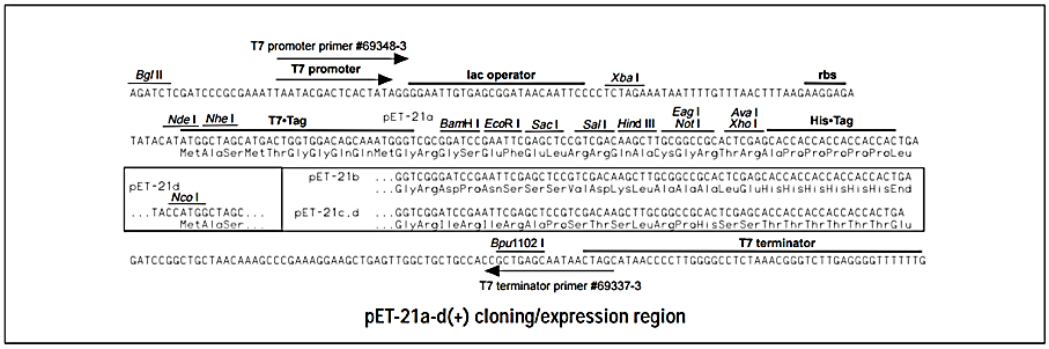

pET-21a-d(+) cloning/expression region

VITA

Ms. Pawinee Panpetch was born on 15 May, 1985. She finished secondary school from Bodindecha (Sing Singhaseni) school. She graduated with the degree of Bachelor of Science from the Department of Microbiology at Chulalongkorn University in 2007 (2nd-class honours). She has studied for the degree of Doctor of Philosophy of Science at the program of Biochemistry and Molecular Biology, Faculty of Science, Chulalongkorn University since 2011.